

**DESIGN AND CONSTRUCTION OF A BRAIN MAGNETIC  
SIGNAL GENERATION PHANTOM FOR SOURCE  
RECONSTRUCTION STUDY**

by

Feng-yu Liu  
B.A.Sc., Simon Fraser University, 2008

THESIS SUBMITTED IN PARTIAL FULFILLMENT OF  
THE REQUIREMENTS FOR THE DEGREE OF

MASTER OF APPLIED SCIENCE

In the  
School of Engineering Science  
Faculty of Applied Science

© Feng-yu Liu 2011

SIMON FRASER UNIVERSITY

Fall 2011

All rights reserved. However, in accordance with the *Copyright Act of Canada*, this work may be reproduced, without authorization, under the conditions for *Fair Dealing*. Therefore, limited reproduction of this work for the purposes of private study, research, criticism, review and news reporting is likely to be in accordance with the law, particularly if cited appropriately.

# APPROVAL

**Name:** Feng-yu Liu  
**Degree:** Master of Applied Science  
**Title of Thesis:** Design and Construction of a Brain Magnetic Signal Generation Phantom for Source Reconstruction Study

**Examining Committee:**

**Chair:** Michael Sjoerdsma, Lecturer  
School of Engineering Science

---

**Dr. Ash M. Parameswaran, P. Eng**  
Senior Supervisor  
Professor, School of Engineering Science

---

**Dr. Mirza Faisal Beg, P. Eng**  
Supervisor  
Associate Professor, School of Engineering Science

---

**Dr. Andrew Rawicz, P. Eng**  
Internal Examiner  
Professor, School of Engineering Science

**Date Defended/Approved:** November 24, 2011



SIMON FRASER UNIVERSITY  
LIBRARY

## Declaration of Partial Copyright Licence

The author, whose copyright is declared on the title page of this work, has granted to Simon Fraser University the right to lend this thesis, project or extended essay to users of the Simon Fraser University Library, and to make partial or single copies only for such users or in response to a request from the library of any other university, or other educational institution, on its own behalf or for one of its users.

The author has further granted permission to Simon Fraser University to keep or make a digital copy for use in its circulating collection (currently available to the public at the "Institutional Repository" link of the SFU Library website <[www.lib.sfu.ca](http://www.lib.sfu.ca)> at: <<http://ir.lib.sfu.ca/handle/1892/112>>) and, without changing the content, to translate the thesis/project or extended essays, if technically possible, to any medium or format for the purpose of preservation of the digital work.

The author has further agreed that permission for multiple copying of this work for scholarly purposes may be granted by either the author or the Dean of Graduate Studies.

It is understood that copying or publication of this work for financial gain shall not be allowed without the author's written permission.

Permission for public performance, or limited permission for private scholarly use, of any multimedia materials forming part of this work, may have been granted by the author. This information may be found on the separately catalogued multimedia material and in the signed Partial Copyright Licence.

While licensing SFU to permit the above uses, the author retains copyright in the thesis, project or extended essays, including the right to change the work for subsequent purposes, including editing and publishing the work in whole or in part, and licensing other parties, as the author may desire.

The original Partial Copyright Licence attesting to these terms, and signed by this author, may be found in the original bound copy of this work, retained in the Simon Fraser University Archive.

Simon Fraser University Library  
Burnaby, BC, Canada

## **ABSTRACT**

Magnetoencephalography (MEG) is a powerful tool in measuring magnetic fields associated with human brain activities, provided that a reliable inverse analysis method is available for mapping the recorded magnetic field patterns to active regions of neurons in the brain. The present study aims to develop a method of physically generate magnetic field patterns of which the MEG data can be used for developing a novel dipole localization technique. The mechanism of generating specific magnetic field patterns consists of coils attached to individual signal-generating circuits controlled by a central unit linked to a computer through a standard USB port. This study explored various coil designs that generated the simulated-brain magnetic dipoles. The use of triangular coils, as opposed to magnetic dipoles generated by helical coils, was also studied.

The use of triangular coils was observed to have limitations in modelling true dipoles. The inverse analysis technique developed in association with this study showed high consistency in mapping the location and directionality of the source dipoles.

**Keywords:** Magnetoencephalography; Magnetic fields; Inverse analysis; Dipole localization; Triangular coil; Current dipole; Signal-generating circuit; Mapping

## **DEDICATION**

I would like to dedicate this thesis to my family, without whose support I could never have a chance to accomplish anything so far, especially to my passed grandfather. His friendliness and kindness towards people around him have always been my guidance towards life.

## **ACKNOWLEDGEMENTS**

I would like to specially acknowledge Teresa Cheung, the MEG laboratory manager in DSRF Burnaby and Dr. Yoshinao Kishimoto, without whom this project could never have been proceeded. I want to thank Teresa's kind assistance on MEG measurement and Yoshinao's dedicated contribution on inverse analysis portion of the project and provision of valuable knowledge.

Many thanks also go to Dr. Ash M. Parameswaran, my senior supervisor, for his continuing support and guidance on my research, both academically and personally. Thank you to Dr. Mirza Faisal Beg and Dr. Andrew Rawicz for providing feedback to the work and sparing time for the defence. Thank you to Mike Sjoerdsma for chairing the defence and his provision of inspirational thinking throughout my study. Thank you to all my lab mates in microelectronics lab for their frequent encouragement and provision of ideas. At last but not the least, I thank the staffs at DSRF Burnaby for their generosity in granting me access to the MEG lab.

# TABLE OF CONTENTS

<b>Approval.....</b>	<b>ii</b>
<b>Abstract.....</b>	<b>iii</b>
<b>Dedication.....</b>	<b>iv</b>
<b>Acknowledgements .....</b>	<b>v</b>
<b>Table of Contents.....</b>	<b>vi</b>
<b>List of Figures .....</b>	<b>viii</b>
<b>List of Tables .....</b>	<b>xi</b>
<b>List of Abbreviations .....</b>	<b>xii</b>
<b>1: Introduction .....</b>	<b>1</b>
1.1 Basics of Brain Neurons .....	1
1.2 Methods of Measuring Brain Activity.....	3
1.3 Inverse Problem.....	4
1.4 Objectives .....	7
1.5 Thesis Outline .....	9
<b>2: Theory and Approach.....</b>	<b>10</b>
2.1 Magnetoencephalography .....	10
2.2 Inverse Analysis.....	13
<b>3: Progression of the Project.....</b>	<b>15</b>
3.1 Previous Implementation .....	15
3.2 Modified Design .....	16
3.3 Further Improvement in Design .....	23
<b>4: Design of HardWare.....</b>	<b>24</b>
4.1 Signal Emitting Mechanism.....	24
4.2 Control Electronics.....	25
4.3 Signal Filtering .....	27
<b>5: Design of Algorithm.....</b>	<b>32</b>
5.1 Overall Design Structure.....	32
5.2 Graphic User Interface.....	34
5.3 Signal Generating Algorithm .....	36
5.4 Frequency Calibration.....	42

5.5 Embedded Control and Communication .....	44
<b>6: Measurement and Analysis.....</b>	<b>50</b>
6.1 Experiment and Method .....	50
6.2 MEG Measurement using Helical Coils .....	53
6.3 Simulated Magnetic Field Pattern of a Triangular Coil.....	55
6.4 MEG Measurement using Triangular Coils .....	61
<b>7: Conclusion and Future Work.....</b>	<b>69</b>
7.1 Conclusion .....	69
7.2 Future Work .....	69
<b>Appendices .....</b>	<b>71</b>
Appendix A: Schematic Drawings .....	72
Appendix A1: Schematic of standalone waveform-generating unit in previous implementation .....	72
Appendix A2: Schematic drawing of waveform-generating unit developed for this thesis work.....	73
Appendix A3: Schematic drawing of the MUX/DeMUX circuit .....	74
Appendix B: Matlab Code for Waveform-composing GUI .....	75
Appendix C: C++ Code for Interactive Host GUI.....	85
Appendix D: C++ Code for AT90USB1287 Microcontroller Firmware.....	102
Appendix E: Assembly Code for Programming ATMega32 Microcontroller.....	108
Appendix F: Simulated Magnetic Field Patterns .....	121
I. Z-component with triangular coils of 5-mm base length and various leg lengths.....	121
II. Y-component with triangular coils of 5-mm base length and various leg lengths.....	122
III. Z-component with equilateral triangular coils of various side lengths.....	123
Appendix G: Inverse Analysis Results .....	124
<b>Reference List .....</b>	<b>126</b>



## LIST OF FIGURES

Figure 1.1: Procedures of studying brain neuronal activities and the emitted magnetic fields.....	5
Figure 1.2: Study of inverse analysis methods by replacing the human subject with a magnetic-field-emitting device.....	8
Figure 2.1: Sensing mechanism of (a) axial gradiometer and (b) Planar gradiometer.....	11
Figure 2.2: (a) SQUID sensors and a liquid helium Dewar and (b) MEG signal processing electronics at Burnaby DSRF.....	13
Figure 2.3: Procedures of inverse analysis on measured MEG data.....	14
Figure 3.1: (a) "Wet phantom" consisting of a pair of electrodes at the end of a twisted wire pair immersed in electrolyte and (b) illustration of flow of ions completes the current loop inside a wet phantom.....	15
Figure 3.2: Hardware configuration of the previously implemented magnetic-signal-generating electronics.....	17
Figure 3.3: Control algorithm of the magnetic-signal-emitting electronics (previous implementation).....	18
Figure 3.4: (a) Helical coils mounted on a plastic base. (b) Test coils placed in the SQUID measurement cavity inside a magnetically shielded room.....	20
Figure 3.5: Magnetic flux density recorded at MEG channels when (a) a rectangular waveform and (b) a sinusoidal waveform was used as the source signal.....	21
Figure 3.6: Spatial magnetic flux density distribution when (a) 2 helical coils (b) 4 helical coils were energized simultaneously.....	21
Figure 3.7: (a) Magnetic flux density distribution after truncated singular value decomposition (TSVD) was applied. (b) Localized dipoles after cluster analysis was applied to the TSVD result and after down simplex method (DSM) was applied to the cluster analysis result.....	22
Figure 4.1: Modified design of the overall simulated-brainwave-generating electronics.....	26
Figure 4.2: Dataflow among components in a signal generating unit.....	27
Figure 4.3: Unfiltered sinusoidal signal at the output ( $V_{pk-pk} = 3.2$ V, period = 81 ms).....	28
Figure 4.4: Resulting cutoff frequency in comparison with the input cutoff frequency of the implementation.....	30

Figure 4.5: (a) Magnitude response and (b) phase shift of the output filter. ....	30
Figure 4.6: (a) Unfiltered and (b) filtered signals at the output ( $V_{pk-pk} = 2.78$ V, period = 9.7 ms).....	31
Figure 4.7: Frequency spectra of (a) unfiltered and (b) filtered signals. ....	31
Figure 5.1: Overall representation of data exchange between interconnected control algorithm blocks .....	33
Figure 5.2: Graphic user interface for composing the output signal waveform (programmed in Matlab). ....	35
Figure 5.3: Real-time interactive graphic user interface dialog on host PC. ....	35
Figure 5.4: Control algorithm of the Matlab GUI on host PC. ....	37
Figure 5.5: Implementation of the signal generating algorithm of SGU. ....	38
Figure 5.6: Representation of a sinusoidal signal (a) 3 times and (b) 10 times of the coexisting fundamental frequency, both with 32 quantization coefficients.....	40
Figure 5.7: A sinusoidal signal composed of different numbers of quantization coefficients.....	40
Figure 5.8: Frequency spectra of an unfiltered sinusoidal signal of 100Hz fundamental frequency formed with (a) 32, (b) 64, (c) 128, and (d) 256 quantization coefficients .....	41
Figure 5.9: Relationship between resulting frequency of the output sinusoidal signal and the input value of frequency for different number of quantization coefficients before frequency calibration. ....	43
Figure 5.10: Relationship between resulting frequency of the output sinusoidal signal and the input value of frequency after frequency calibration. ....	44
Figure 5.11: Data structure of the stored parameters for each individual channel on host PC. ....	46
Figure 5.12: Structure of the packets sent from host PC to CCU during each data transfer.....	46
Figure 5.13: Command-decoding algorithm on each SGU. ....	47
Figure 5.14: Communication states of data point forwarding from CCU to SGU.....	49
Figure 6.1: (a) A helical coil (3 loops) and (b) an isosceles triangular coil fixed on a wooden stick. The distance between two adjacent marked lines on the stick is 1 cm. ....	50
Figure 6.2: (a) Front view, (b) left-side view, and (c) right-side view of coil placements on a plastic skull covered with a layer of rubber sheet mounted on a plastic base.....	51
Figure 6.3: Final assembled magnetic-field-emitting circuit.....	52
Figure 6.4: Polhemus FASTRAK® 3D Digitizer used for localizing points in 3D space, including a transmitter and a receiver fixed around the test skull	

during the experiment and a stylus used for physically locating the coils on the skull. ....	53
Figure 6.5: Relative locations of the helical coils on the head surface. ....	53
Figure 6.6: Frequency spectra of (a) all coils at 13 Hz, maximum current and (b) all coils at 13 Hz, minimum current. ....	54
Figure 6.7: Frequency spectra of (a) coil 4 at 50 Hz, the rest at 13 Hz, half current and (b) coil 4 at 50 Hz, coil 7 at 90 Hz, the rest at 13 Hz, half current.....	55
Figure 6.8: Example triangular coil model constructed in COMSOL.....	56
Figure 6.9: Simulated space in COMSOL, consisting of a cube of 10-cm side length.....	57
Figure 6.10: (a) Z-component on xy-plane ( $z = 5$ cm), (b) y-component on zx-plane ( $y = 5$ cm), and (c) x-component on yz-plane ( $x = 5$ cm) of the magnetic field generated by the simulated triangular coils. ....	58
Figure 6.11: Max z-component magnetic flux density in the xy-plane at $z = 5$ cm from origin of isosceles triangular coils. ....	59
Figure 6.12: Y-component magnetic flux density in the zx-plane at $y = 5$ cm ( $x = 0, z = 0$ ) from origin of isosceles triangular coils.....	60
Figure 6.13: Max magnetic flux density in the plane perpendicular to the axial component at 5 cm from origin of equilateral triangular coils. ....	61
Figure 6.14: Relative locations of the triangular coils on the head surface. ....	62
Figure 6.15: Spatial distribution of sensors around the measured space, for a total of 151 channels, each having an inner and an outer sensors. ....	63
Figure 6.16: Spatial magnetic flux density distribution of test cases 1, 2, 5, 11 at time equal to 1.1 seconds after the start of recording (Unit: $\mu$ T).....	64
Figure 6.17: AC component of the recorded magnetic flux densities on all channels for test cases 1, 2, 7, 8, 10, and 11. ....	65
Figure 6.18: Left – Resulting magnetic flux density distribution after TSVD; middle – Resulting dipole locations after data clustering; right – Adjusted dipole locations after downhill simplex computation of test cases 5, 8, and 9. ....	67

## LIST OF TABLES

Table 6.1: Measured base and side lengths of different types of triangular coils used in the experiment. ....	62
Table 6.2: Coils energized in different test cases in the experiment. ....	63
Table 6.3: Resulting dipole moments for the dipole associated with each coil across different test cases from the inverse analysis and their correlation. ....	68

## **LIST OF ABBREVIATIONS**

<b>MEG</b>	Magnetoencephalography
<b>PET</b>	Positron emission tomography
<b>fMRI</b>	Functional magnetic resonance imaging
<b>DAC</b>	Digital to analog converter
<b>EEG</b>	Electroencephalography
<b>ECD</b>	Equivalent current dipole model
<b>SQUID</b>	Superconducting quantum interference device
<b>AICC</b>	Akaike information criterion for small sample sizes
<b>TSVD</b>	Truncated singular value decomposition
<b>CCU</b>	Central control unit
<b>SGU</b>	Signal generating unit
<b>GUI</b>	Graphic user interface

# 1: INTRODUCTION

## 1.1 Basics of Brain Neurons

The human brain, the most critical part of the central nervous system, contains mostly interneurons, which integrate and analyze signals sent from sensory neurons and send signals to the motor neurons to perform response in accordance to the environmental stimuli [1, 2]. The highly evolved ability of information integration and interpretation by the human brain is reflected by the highly complex interconnection among interneurons in the brain. Neurons are composed of three major structures: the dendrite, the cell body, and the axons. The neuron cell membrane is impermeable to charged particles. In the resting state, the inside of a neuron cell contains a higher concentration of  $K^+$  and a lower concentration of  $Na^+$  compared to the extracellular environment, and the bilayer structure of the cell membrane contributes to maintaining the ion gradients caused by the difference in charged particle concentrations. The  $Na^+$  and  $K^+$  gradients maintained across the membrane are mainly responsible for the activation of a neuron. Upon receiving signals from other neurons by the dendrites, the axon of a neuron transmits signals to other neurons. The stimulus received by a neuron causes transmembrane proteins called ion channels to open up and thus increases the permeability of the membrane. The propagation of a nerve pulse within a neuron results as  $Na^+$  and  $K^+$  ions are passed in and out of the neuron down their concentration gradients through gated ion channels

located on the cell membrane. After each activation process, the resting potential of the neuron is restored by the cell actively pumping these charged particles across the membrane against their concentration gradients. The membrane potential of a neuron that is constantly stimulated by the signal from a sensory receptor consists of a pulse train of action potentials. The frequency of the pulse trains is dependent upon the magnitude of the stimulus the sensory receptor is exposed to. The stronger the external stimulus, the shorter the time interval between adjacent action potential pulses is on the neuron.

Any cognitive and thinking process or environmental stimulation may trigger the change of membrane potential in certain neurons [3]. Through this membrane depolarization-repolarization process, an action potential is created once the magnitude of membrane potential reaches a particular threshold value and the electrical signal is passed down the axon of the neuron. The relay of signals between two adjacent neurons is achieved by the release of neurotransmitters across the gap junction between the transmitting axon of a neuron and the receiving dendrite of the next neuron. The combination of the action potential and neurotransmitters results in the relay of signals across the nervous system. The current and its corresponding magnetic field generated by the flow of charged particles when neurons are active in the human brain form the basis of the present study.

## 1.2 Methods of Measuring Brain Activity

Research on human cognitive behaviours and their corresponding regions of neurons activated in the brain finds its application in various fields of study, including psychology, cognitive science, and clinical science. Moreover, the correlation between given cognitive processes and the resulting brainwave patterns is also subject to intense study. Various methods have been developed for the detection of neuronal activities in human brains. Commonly employed methods include positron emission tomography (PET), functional magnetic resonance imaging (fMRI), electroencephalography (EEG), magnetoencephalography (MEG), and etc.. Both PET and fMRI provide good spatial resolution but relatively poor temporal resolution compared to EEG and MEG, on the order of seconds or more. PET and fMRI are capable of generating high-resolution 3D images [4, 5]. However, as opposed to EEG and MEG, the present technology limits PET and fMRI for continuous recording of neuronal activity over a substantial period of time. EEG and MEG are capable of resolving temporal precision on the order of milliseconds. Furthermore, PET requires the test subject to be pre-treated with radioactive tracer molecules, which would increase the risk of damaging bio-tissues. EEG measurement, accomplished by placing electrodes that record electrical potentials at fixed locations on the scalp, is limited by the poor conductivity of the skull. It greatly increases the difficulty to locate the source of neuronal activity. Meanwhile, the magnetic fields not attenuated by the skull and other tissues make MEG a more effective method in spatially localizing the sources in the brain compared to EEG [6]. In addition,



MEG is a completely non-invasive method because the sensors do not make direct contact with the head. MEG, due to its high spatial resolving capability, is often performed in conjunction with EEG due to their complementary measuring capabilities, since the fields detected by these two methods are mutually orthogonal. MEG detects mainly the activities in the cortical fissures. Notably, it is the intracellular post-synaptic potentials on active pyramidal neurons that MEG detects, not the potentials created by the polarization-depolarization process within the neurons [7].

### **1.3 Inverse Problem**

In electromagnetism, when the source that generates a magnetic field is initially known, such as the location, orientation, and current density of a current dipole, the resulting distribution of the magnetic flux density can be easily computed using Biot-Savart law and Maxwell's equations. Such a procedure of determining the magnetic field from a given electrical field is a *forward problem*. However, in the study of biomagnetism, *inverse problems* are often involved, when the information of locations, magnitudes, and numbers of individual dipoles are initially unknown, while only measured distribution of magnetic flux densities is available. Figure 1.1 illustrates the procedures of studying the pattern of magnetic fields generated by brain neuronal activities.

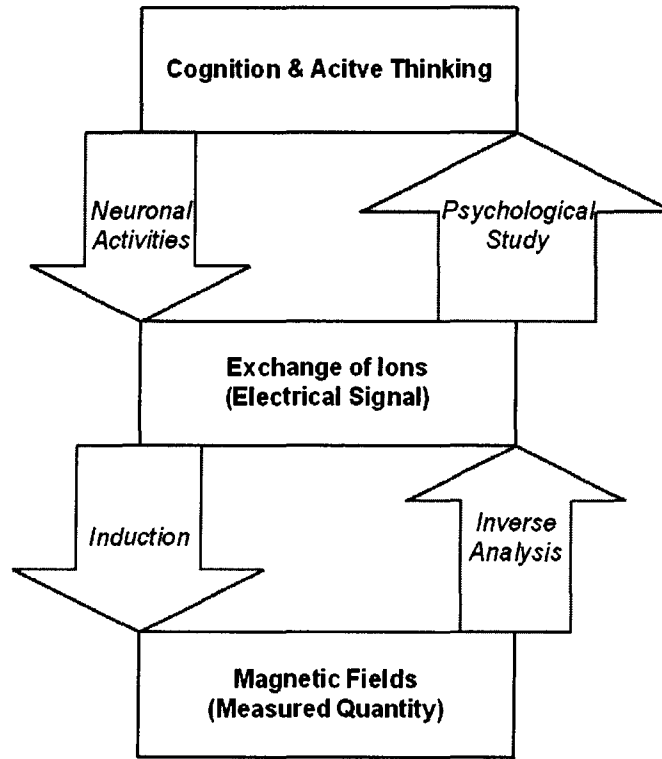


**Figure 1.1: Procedures of studying brain neuronal activities and the emitted magnetic fields.**

In a MEG recording with a human subject, very often the resulting magnetic field distribution can be modelled as the equivalent current dipole (ECD) model [8, 9]. The brain-induced magnetic field that is measured by MEG is [10]:

$$4\pi\bar{H}(r) = \int_v \bar{j}^i \times \nabla \left( \frac{1}{r} \right) dv + \sum_j \int_{S_j} (\sigma_j'' - \sigma_j') \Phi \nabla \left( \frac{1}{r} \right) \times d\bar{S}_j \quad (1)$$

$\bar{j}$  is the impressed current density resulting from neuron cellular bioelectricity, equivalent to the source volume dipole moment density if the ECD model is used. The  $\sigma_j'' - \sigma_j'$  term, being the conductivities of different materials, accounts for any inhomogeneity of the volume conductor. Single-dipole model assumes

synchronous activation of a group of functionally interconnected neurons which are closely located in the cerebral cortex, for a given neuron-triggering event. Nonetheless, when the resulting distribution of magnetic field involves multiple individually activated brain neuron groups or large patches, the single-dipole model would be less suitable in estimating the location of the sources [3, 11]. In such cases, multidipole models should be used to give accurate estimation of the source dipoles. The study of inverse analysis of MEG data is usually combined with EEG and fMRI, since EEG detects all primary current components, while MEG only detects the tangential components. Meanwhile, fMRI or other tomography methods are capable of providing higher spatial resolutions.

Brain activity reconstruction typically involves forward modelling components including the source model, the volume conductor model, and the measurement model, together with the reconstruction algorithm for inverse modelling [12]. Various inverse algorithms including the commonly adapted minimum-norm estimates have been demonstrated to give good source-current localization result and often depend largely on the accuracy of the *a priori* information [13, 14]. Given a set of MEG data recorded, the general approach for localizing the sources of dipoles using inverse analysis is to make an initial assumption about the location and number of individual dipoles based on the data. Then the error between the estimation and the actual measured data needs to be minimized by iterative computation to yield the best approximation of the sources of the measured magnetic field.

## 1.4 Objectives

The study of the inverse problem on the MEG data using human subjects is significantly deterred by the lack of the ground truth about the actual location and orientation of the dipoles. The main problem of using a human subject for MEG data collection is the actual location of source dipoles, which are associated with the neuronal activities in particular regions of the brain. This can only be estimated in conjunction with methods such as fMRI, due to the fact that normal humans do not have voluntary control over the groups of brain neurons to be activated. However, if the magnitude, location, and orientation of the dipole sources are initially known, together with the measured MEG data, the accuracy of a particular inverse analysis technique can be evaluated. Moreover, study using human subjects is more prone of noise due to the movement of the head or limbs and the magnetic fields produced by the heartbeats and pulses.

Constructing realistic brain phantoms have been attempted for assisting the inverse analysis study of EEG and MEG data [15-18]. In the present study, a brain phantom is constructed to replace human subjects, in attempt to serve physical simulation of magnetic field emitted by brain neuronal activities for inverse analysis study, as shown in Figure 1.2. More specifically, such a phantom is to be used for assisting the development of a dipole localization technique by providing control over the pattern of the magnetic fields produced and the orientation and location of each individual dipole. Furthermore, the noise introduced by the simulation circuit can also be characterized and attenuated. Eventually, the objective of the inverse analysis technique development is to

more accurately reconstruct the active regions in the brain from measured MEG data. Such localization tool can be used for future psychological study or clinical diagnosis.

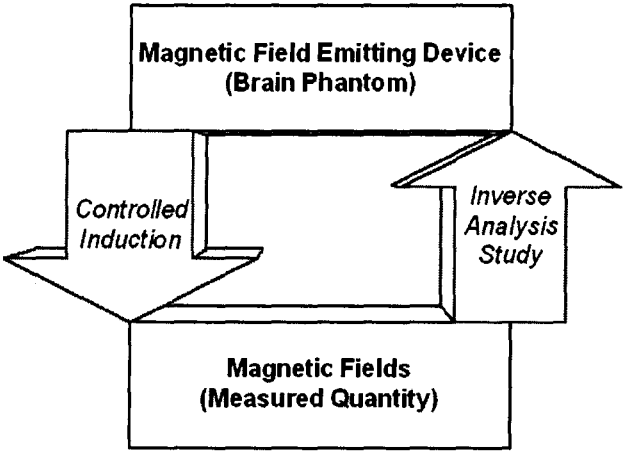


**Figure 1.2: Study of inverse analysis methods by replacing the human subject with a magnetic-field-emitting device.**

## **1.5 Thesis Outline**

The study presented in this thesis focuses on developing a method of physically simulating magnetic fields emitted by the human brain (brain phantom), as well as how the brain phantom can be used for developing a novel inverse analysis method. Chapter 2 provides a brief overview on the principles of magnetoencephalography and its operational mechanism. Chapter 3 covers the progression of the current project and earlier development of the present project. Chapters 4 and 5 provide details of implementation of the current brainwave simulating mechanism in hardware and software aspects, respectively. Chapter 6 outlines experimental procedures of recording magnetic fields generated using the brain phantom developed and results of the inverse analysis technique developed. Finally, a conclusion and future work are outlined in the last chapter.

## **2: THEORY AND APPROACH**

### **2.1 Magnetoencephalography**

Magnetoencephalography measures the biomagnetic signals associated with the movement of charged particles in active brain neurons. The problem mostly encountered in the measurement of human brain signal is the relatively weak magnitude of the signal of interest [4, 19]. The magnetic field produced by brain neuron activities is often orders of magnitude weaker than background magnetic interference, including the earth's magnetic field. The typical urban background noise, which may include the magnetic fields generated by electric power lines and geomagnetic field fluctuations, could be in the order of microteslas, while the magnetic fields generated by human brain activities are in the range of picoteslas. The measurement of human brain signal requires superconducting quantum interference device (SQUID), which has extremely high sensitivity in detecting the magnetic field of the brain [20]. A typical SQUID system consists of a flux transformer connected to the SQUID electronics. The flux transformer is composed of a gradiometer and a SQUID assembly. At the output of the system, the SQUID electronics renders a voltage signal whose magnitude is proportional to the amount of magnetic flux sensed by the gradiometer. The gradiometer, which functions as a sensor in detecting the magnetic field signals, is connected to the input coil of the SQUID assembly. Liquid helium cooling is required for the flux transformer, of which the

implementation is based on the Meissner effect and Josephson effects of superconductors [21]. Usually, the measurement needs to be conducted in a heavily magnetically shielded environment to further attenuate the interference of the background noise. The principle of detection relies on the different homogeneities of magnetic signals from different sources. In a properly magnetically shielded space, while the magnetic field generated by the human brain weakens as the distance from the source increases, the background magnetic signals are mostly homogeneous across the gradiometer antennae [10, 21]. A SQUID gradiometer is designed to detect the brain magnetic field from the discrepancy in magnetic flux densities caused by the distance. Figure 2.1 illustrates the mechanism of magnetic field sensing of the first-order gradiometer.

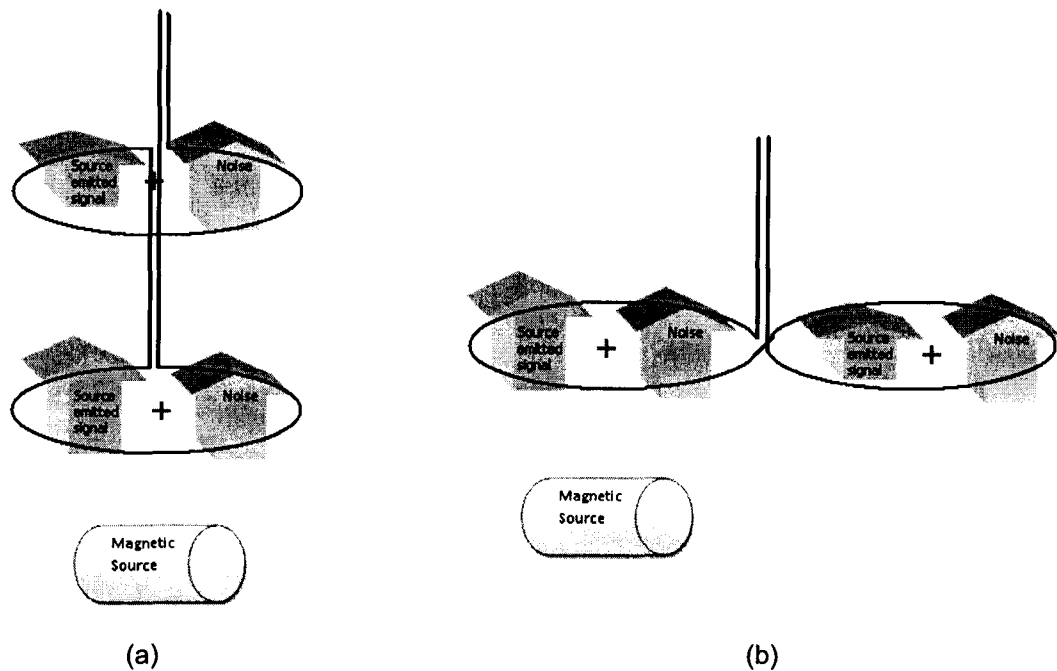


**Figure 2.1: Sensing mechanism of (a) axial gradiometer and (b) Planar gradiometer.**



Located at the Down Syndrome Research Foundation,<sup>1</sup> the MEG system manufactured by CTF System is capable of measuring 151 channels, formed by individual axial gradiometers. These 151 gradiometers are spatially distributed to cover the whole brain cortical system and are capable of sensing magnetic field emitted by most of the regions in the human brain cortex. The MEG system is equipped with two environmental noise reduction methods. Noise reduction can be achieved either by higher-order gradiometer formation or by adaptive filtering or both. Higher-order gradiometer noise cancellation employs hardware mechanism while keeping the filter coefficient static. Adaptive filtering, on the other hand, is implemented via signal processing approach using variable filtering coefficients [22]. The change of the coefficients depends on the environment. As shown in Figure 2.2 below, located in a magnetically shield room, the magnetic signal emitting test subject is fitted inside the cavity surrounded by the gradiometers together with the liquid helium containing Dewar. The signal processing electronics of MEG, meanwhile, is located outside of the room to minimize the noise emitted by the MEG circuits.

---

<sup>1</sup> Down Syndrome Research Foundation is a registered non-profitable charity focusing on both servicing the community and researching Down Syndrome. It is located at 1409 Sperling Avenue, Burnaby, BC V5B 4J8

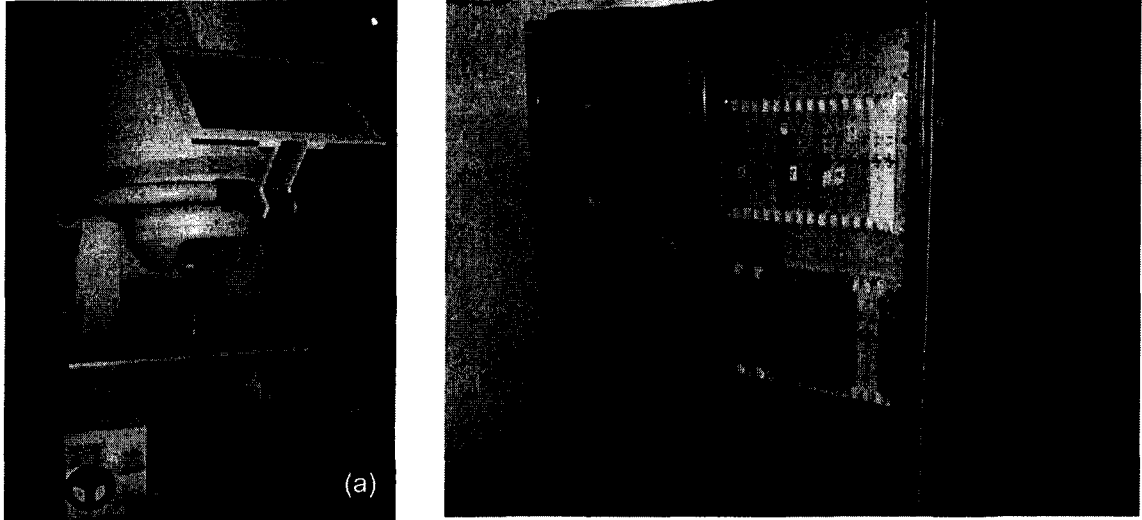


**Figure 2.2: (a) SQUID sensors and a liquid helium Dewar and (b) MEG signal processing electronics at Burnaby DSRF.**

## **2.2 Inverse Analysis**

The novel inverse analysis method for localizing the dipoles in the present study was developed by Kishimoto [23]. As shown in Figure 2.3 below, the method consists of two major phases: extracting phase and grouping phase. In the data extracting phase, in which the magnitude distributions of the dipoles are to be determined, truncated singular value decomposition (TSVD) is applied to the MEG data recorded using Akaike information criterion for small sample sizes (AICC) repeatedly. In the grouping phase, the distributions of the dipoles are grouped by data clustering before downhill simplex computation are applied to these groups of data for optimizing the locations of these dipoles.

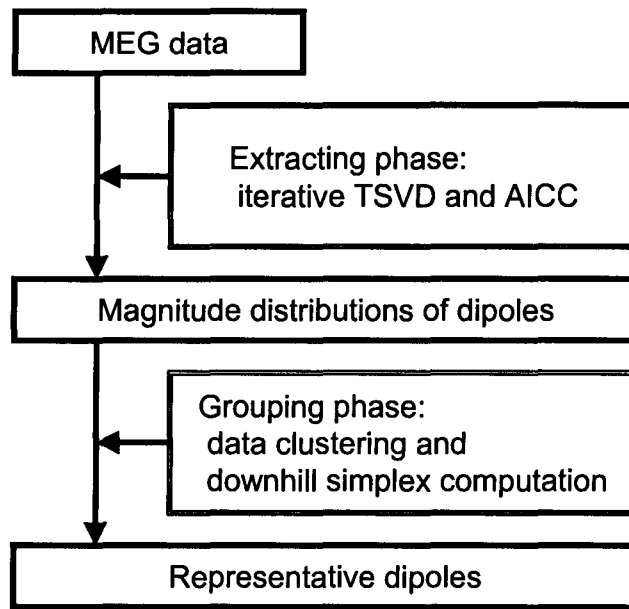


**Figure 2.3: Procedures of inverse analysis on measured MEG data.**

### 3: PROGRESSION OF THE PROJECT

#### 3.1 Previous Implementation

An electrolyte-based electromagnetic signal-emitting device was previously constructed to physically generating magnetic signal. Such a device consisted of a control electronic circuit connected to a symmetrical twisted pair of wires ended as a pair of electrodes immersed in a saline solution, which functioned as the medium for ion exchange, as shown in Figure 3.1. The twisted pair of wires had insulated coating except at the tips which function as the electrodes.

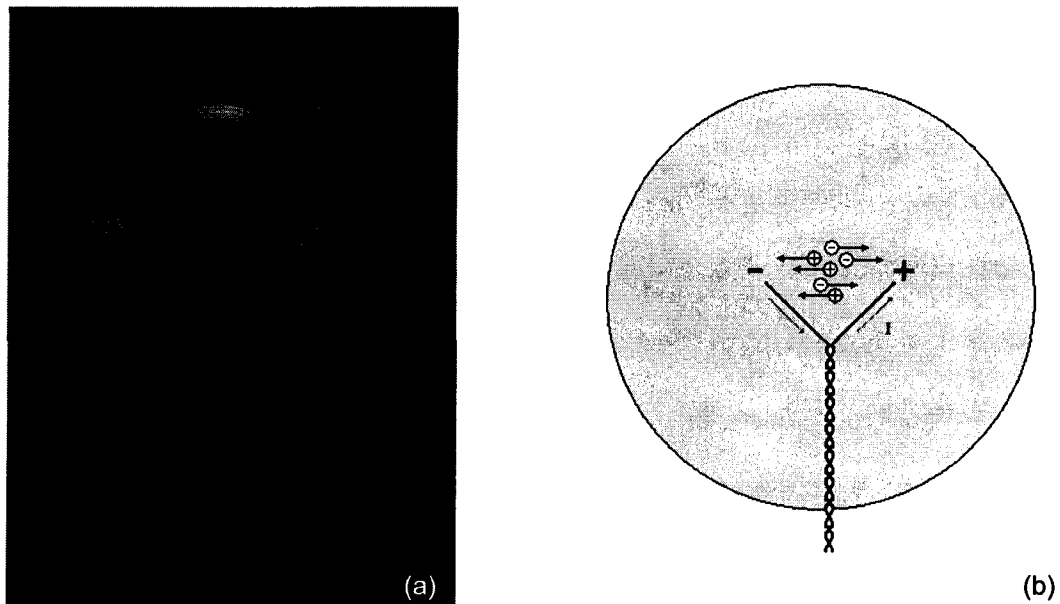


**Figure 3.1: (a) “Wet phantom” consisting of a pair of electrodes at the end of a twisted wire pair immersed in electrolyte and (b) illustration of flow of ions completes the current loop inside a wet phantom.**

The previous version of control electronics was developed by Simon Fraser University research group for generating basic waveforms such as

sinusoidal signals with one frequency component. The control circuit included mainly a microcontroller with two 8-bit digital-to-analog converters (DAC's) attached. One of the two DAC's was used as a reference DAC for fixing the input voltage level of another DAC, the output DAC. While the DAC's lacked memory components and could not be programmed, a microcontroller was required for dictating the output voltage of the output DAC. The microcontroller was programmed with 32 predefined 8-bit coefficients, ranging from 0 to 255 in decimal for composing the output waveform. These 32 coefficients defined the shape of the waveform to be output to the coil. Sequentially, each of these coefficients was transferred one-by-one from the microcontroller to the output DAC, which synchronously generated the corresponding voltage level. The signal generated by the DAC was transmitted to the twisted pair of wires, and the pair of wires, together with the saline solution, formed a closed loop for the current sourced by the DAC chip to flow, as shown in Figure 3.1 above. In this case, the saline was the electrolyte, in which the ion exchange allowed the charges in the wires to be transferred. Due to the symmetrical configuration of the twisted pair, the magnetic field emitted by each wire in the twisted pair was largely cancelled out, and only the ion exchange between the twisted pair in the electrolyte and the current carried by the two arms of electrodes would contribute to a measurable magnetic field.

### **3.2 Modified Design**

The design elaborated above was not without its limitations. First, the electronic design allowed only limited signal generating capability. In addition to

only one set of waveform coefficients that could be defined each time, the microcontroller had to be re-programmed using a development board provided by Atmel®, whenever an alteration of the waveform parameters, such as the amplitude or the frequency, was required. Such programming procedures, involving the un-mounting and mounting of the microcontroller on the development board, tend to be laborious if frequent change of the waveform parameters is needed during the operation of the device. Moreover, the electronic parts are more prone to damage by electrostatic charges when frequent mounting and un-mounting of the microchips are performed.

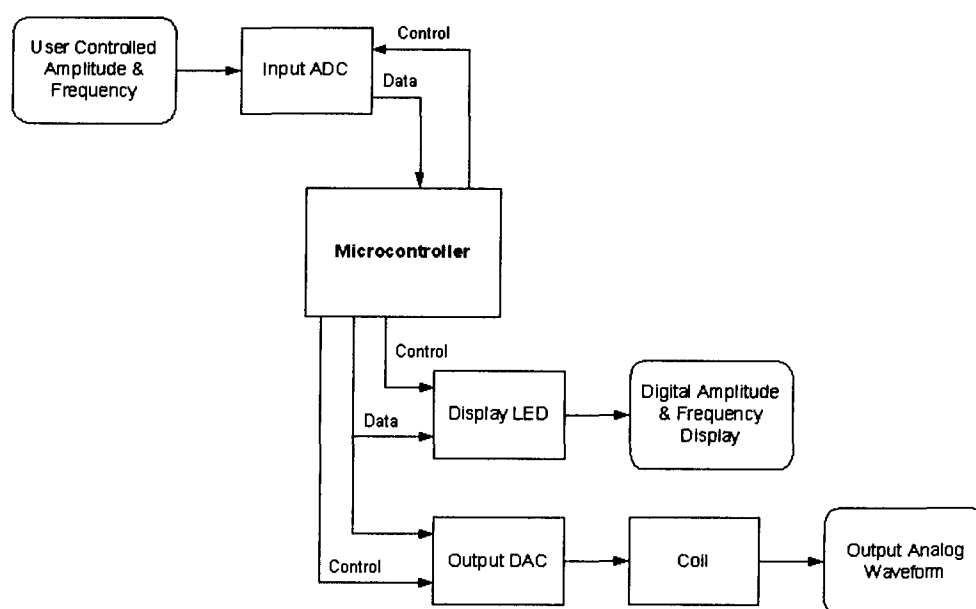


**Figure 3.2: Hardware configuration of the previously implemented magnetic-signal-generating electronics.**

To improve on the issues mentioned above, it was necessary to design control electronics that allowed the waveform parameters to be updated without re-programming the microcontroller [24]. The hardware was constructed using

electronic blocks shown in Figure 3.2. See Appendix A1 for the detailed schematic. To accomplish this, a voltage and amplitude input control elements were integrated to the circuit using analog-to-digital converters (ADC's) and potentiometers. Also the corresponding display elements were implemented using 7-segment LED displays. The microcontroller was programmed to periodically sample and display the input values of these waveform parameters and adjust the DAC's to generate waveforms defined by the specific parameters, following the algorithm shown in Figure 3.3.

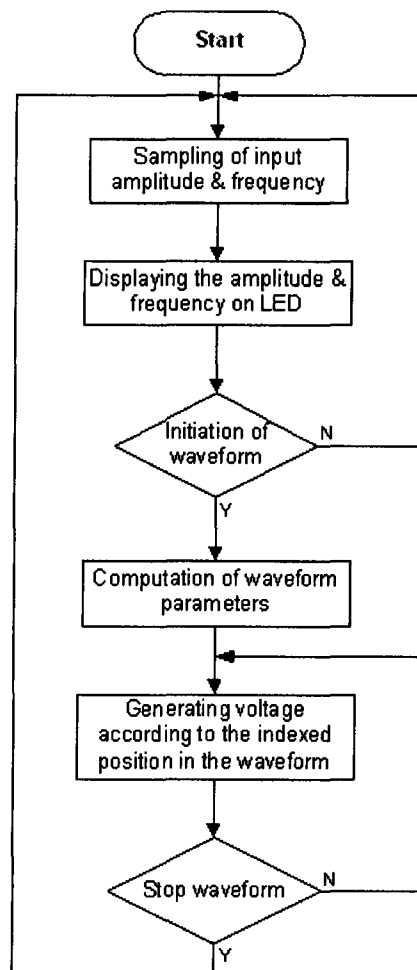


**Figure 3.3: Control algorithm of the magnetic-signal-emitting electronics (previous implementation).**

Furthermore, the use of liquid electrolyte as the conducive medium between the twisted pair of wires, though might more physically resemble the ion exchange occurring in each individual neuron in a human brain, would incur interference, if the number of twisted pairs of wires increases. One problem for using saline water in the construction of a brain phantom is the nonlinearity between the source signal and the measured magnetic field due to the electrical double layer around the electrodes in the saline water [25]. The electrical double layer occurs in the pre-electrolysis process due to the minimum energy required for the electrolysis of the saline molecules to begin. Another problem would arise if the distance between two pairs decreases, as the number of twisted pairs increases, given that they all share the same liquid conducive medium. To form a complete loop of electrical charge flow, the amount of current carried by the pair of wires has to be replaced by the equivalent amount of charges exchanged in the electrolyte at the ends of the twisted pair of wires immersed in the saline. Since the direction of ion flow in the electrolyte is not restricted as the flow of electrons in a conducive wire, the majority to the ions would take the shortest paths between the source and the sink of the electrical charges. When the distance between individual twisted pairs becomes comparable to the distance between the two electrodes of each individual wire pair, as the number of wire pairs increases, interference due to the cross-flow of charges would be expected.

For allowing a larger number of dipoles to be generated simultaneously without cross-interference among individual dipoles, small coils combined with twisted pairs of wires were used, termed “dry phantom”, as opposed to the “wet



phantom” previously described, which has twisted pairs immersed in liquid electrolyte.

In the previous MEG measurement conducted [24, 26], using the brainwave simulating circuit aforementioned to provide signals, helical coils were properly mounted on a plastic base, as shown in Figure 3.4. In this case, each of the coils was positioned at approximately equidistance from the centre of the base. Then the base was positioned inside the measurement cavity of the MEG, located inside a magnetically shielded room.

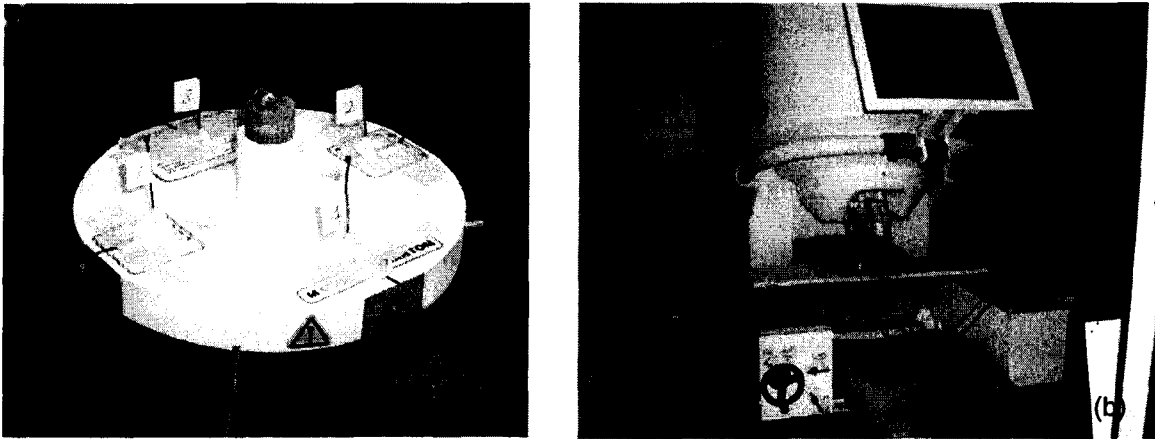


**Figure 3.4: (a) Helical coils mounted on a plastic base. (b) Test coils placed in the SQUID measurement cavity inside a magnetically shielded room.**

The magnetic flux density recorded by multiple gradiometers over a time period is shown in Figure 3.5 using the brain phantom constructed. The observed multiple traces at a given time are due to the superimposition of the recordings by multiple gradiometers. A sinusoidal and a rectangular waveform source signal are shown for example. It can be observed that the magnetic field patterns are consistent with the original source signal waveforms. The amount of current  $i$

carried by an  $N$ -turn helical coil of constant loop area  $A$  governs the magnetic field strength according to the relationship [27]:

$$B(z) = \frac{\mu_0 NiA}{2\pi z^3} \quad (2)$$

and can be adjusted accordingly to fit the range of magnetic field required for the experiment.

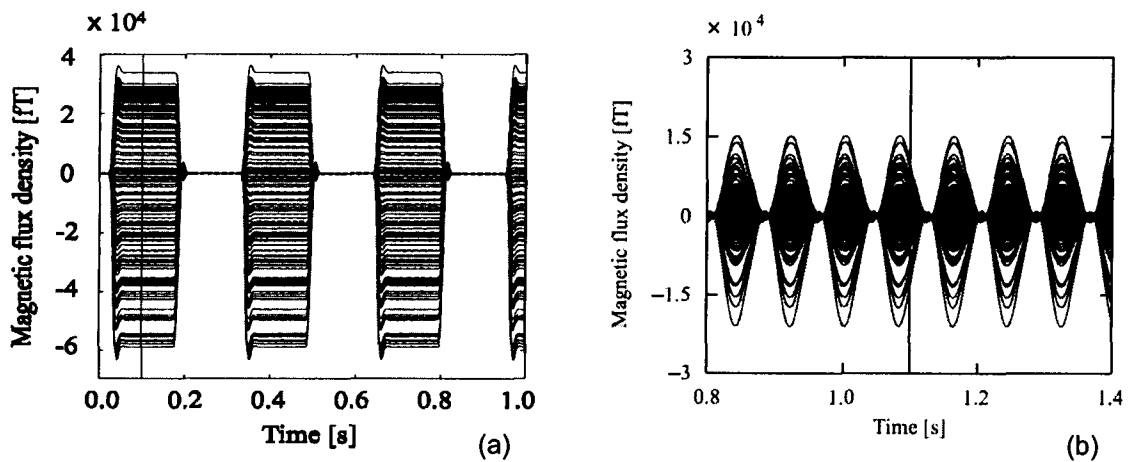


**Figure 3.5: Magnetic flux density recorded at MEG channels when (a) a rectangular waveform and (b) a sinusoidal waveform was used as the source signal.**

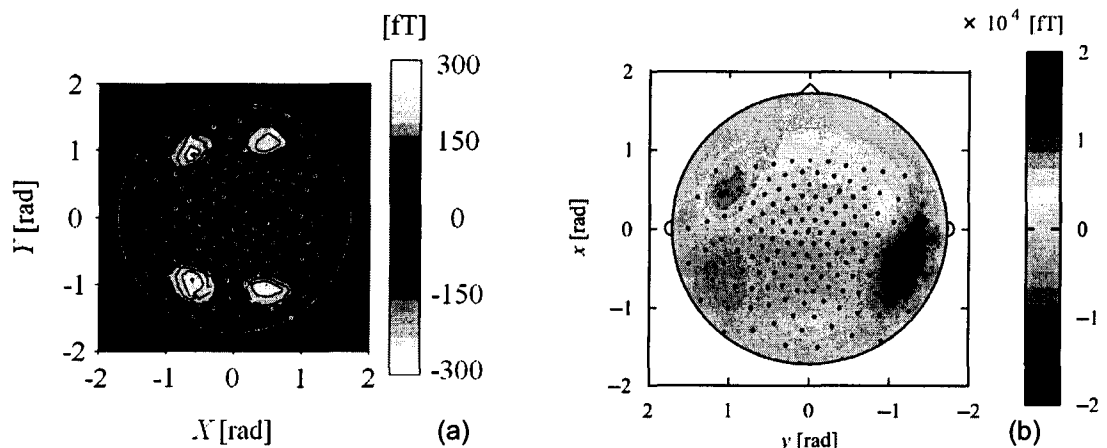


**Figure 3.6: Spatial magnetic flux density distribution when (a) 2 helical coils (b) 4 helical coils were energized simultaneously.**

Meanwhile, the planar view of the spatial distribution of the resulting magnetic flux density at a particular time instance is shown in Figure 3.6. The inverse analysis method described above was applied to the magnetic flux density data measured by the MEG gradiometers. The resulting magnetic field distribution after TSVD was applied is shown in Figure 3.7. Figure 3.7 also displays the localization results of dipoles after data clustering analysis and downhill simplex method were applied, respectively.

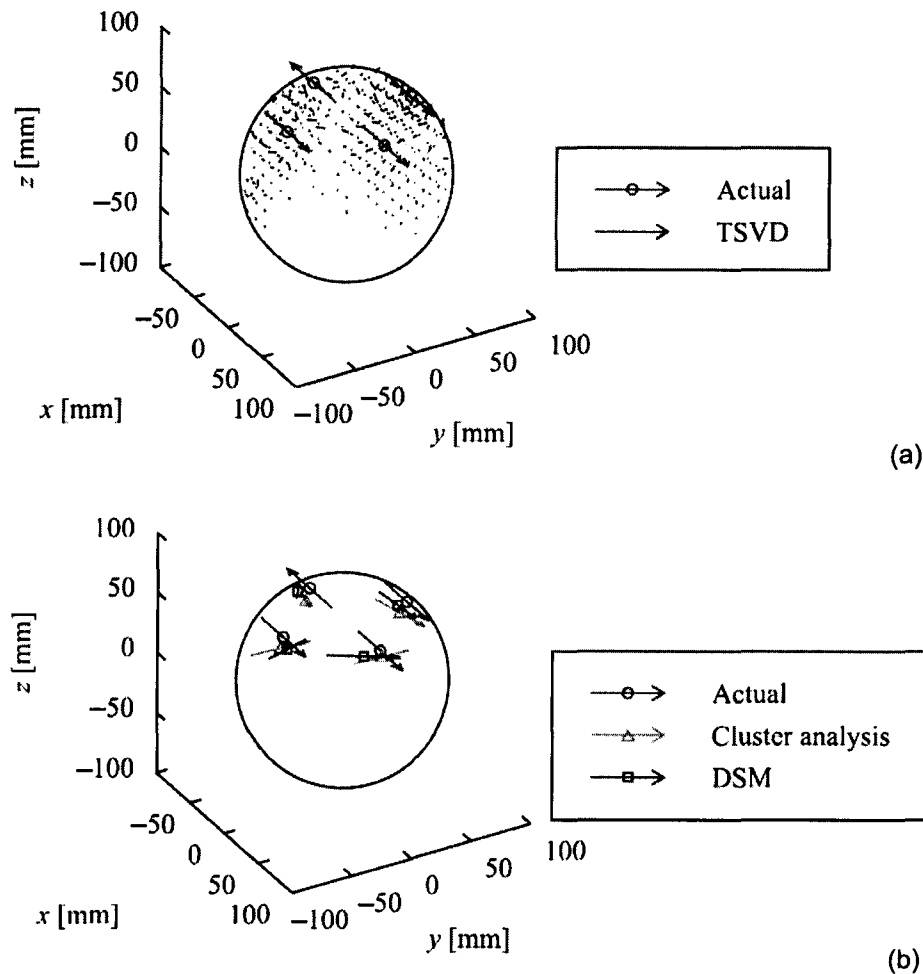


**Figure 3.7:** (a) Magnetic flux density distribution after truncated singular value decomposition (TSVD) was applied. (b) Localized dipoles after cluster analysis was applied to the TSVD result and after downhill simplex method (DSM) was applied to the cluster analysis result.

### **3.3 Further Improvement in Design**

A more advanced version of brain phantom can be implemented by introducing a graphic user interface that renders the visualization of the waveform shape to be generated. Furthermore, the device needs to allow an arbitrary signal waveform to be defined without having to re-program the control algorithm of the microcontroller. The rest of the thesis focuses on the development of an improved mechanism for creating more complex magnetic signals in attempt to more realistically simulate the electromagnetic fields emitted by human brain neurons. Such approach is to be used for further improving the inverse analysis technique developed in association with this study.

## **4: DESIGN OF HARDWARE**

### **4.1 Signal Emitting Mechanism**

A magnetic field can be generated by applying electric signals to a coil attached to the output of a signal generating circuit via a twisted pair of wires, which ensures a detectable magnetic field is created only in the vicinity of the coil but not along the pair of current conducting wires. Conventionally, magnetic fields are produced by using a solenoid, a tightly wound helical coil of wire, which can be modelled as a magnetic dipole. However, the ion exchange associated with neuronal activities is more realistically modelled as the emergence of current dipoles. The study of the novel dipole localization method in the present research attempted both approaches by using both helical coils and triangular coils.

As previously mentioned, the use of a symmetrical twisted pair of wires immersed in saline water provides an eligible model of a current dipole. The use of isosceles-triangle coils in constructing the brain phantom was proposed to provide several advantages [28]. Using a triangular coil eliminates the need of liquid medium for ion exchange while still providing a similar electrical current path. Not using electrolyte to form a circuit loop eliminates the non-linearity between the generated magnetic field and the applied voltage and achieves higher mechanical accuracy. Moreover, it provides more simplicity for the experimental setup and eliminates the problem of electrode degradation.

## 4.2 Control Electronics

The requirement of a graphic user interface that facilitates the real-time control of the waveform generation can be met by integrating a computer to the design. The concept of the design involves a computer connected to a central control unit (CCU) that distributes waveform parameters and control commands to an intended waveform-generating unit. Figure 4.1 demonstrates the block diagram of the design. Notably, as shown in Figure 4.1, the communication established between the host PC and the CCU developed using the protocol supplied by Atmel® allows bidirectional packet transfer. This feature can be exploited to ensure that the CCU correctly receives the data issued by the host PC during the implementation. On the other hand, the unidirectional data transfer between the CCU and each channel is limited by the different logic voltage levels between them. More specifically, logic level '1' has a voltage level of 3.3 V on the CCU, while logic level '1' on each waveform-generating circuit has a voltage of 5 V. This difference in voltage level presents a limitation on the speed of the circuit, which, however, is not of top priority at the present stage.

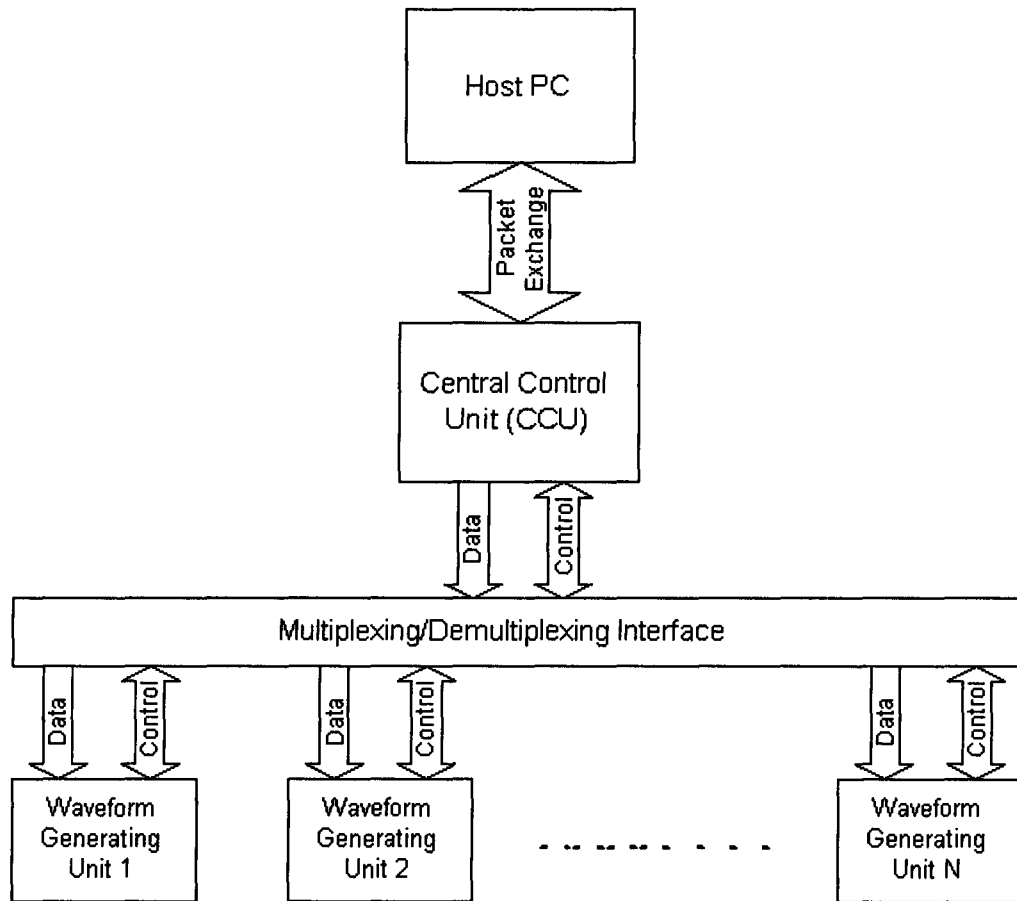


**Figure 4.1: Modified design of the overall simulated-brainwave-generating electronics.**

The CCU that facilitates the communication between the host computer and the peripheral, and the management of the data and instructions sent by the computer is implemented using an AT90USBKEY board supplied with AT90USB1287 microcontroller by Atmel®. The board was specifically designed to allow fast data transfer between the host PC and the on-board microcontroller. The communication between the host computer and the AT90USBKEY is established through USB ports on both the host and the receiving AT90USBKEY. Upon receiving the data, the CCU distributes them to the microcontroller of a specific waveform-generating unit (WGU) through a demultiplexing circuit (Refer

to Appendix A3 for detailed layout of the circuit) consisted of stacks of quad 2-channel multiplexer/demultiplexer microchips (MC14551). The use of a demultiplexing circuit introduces expandability to the design at the expense of response time. The limitation of such implementation is that the more layers the network contains, the longer it takes the signal to propagate from the CCU to each individual unit. The block diagram of the dataflow in each individual signal generating unit (SGU), including the WGU and the output coil, is shown in Figure 4.2. The detailed schematic is included in Appendix A2.

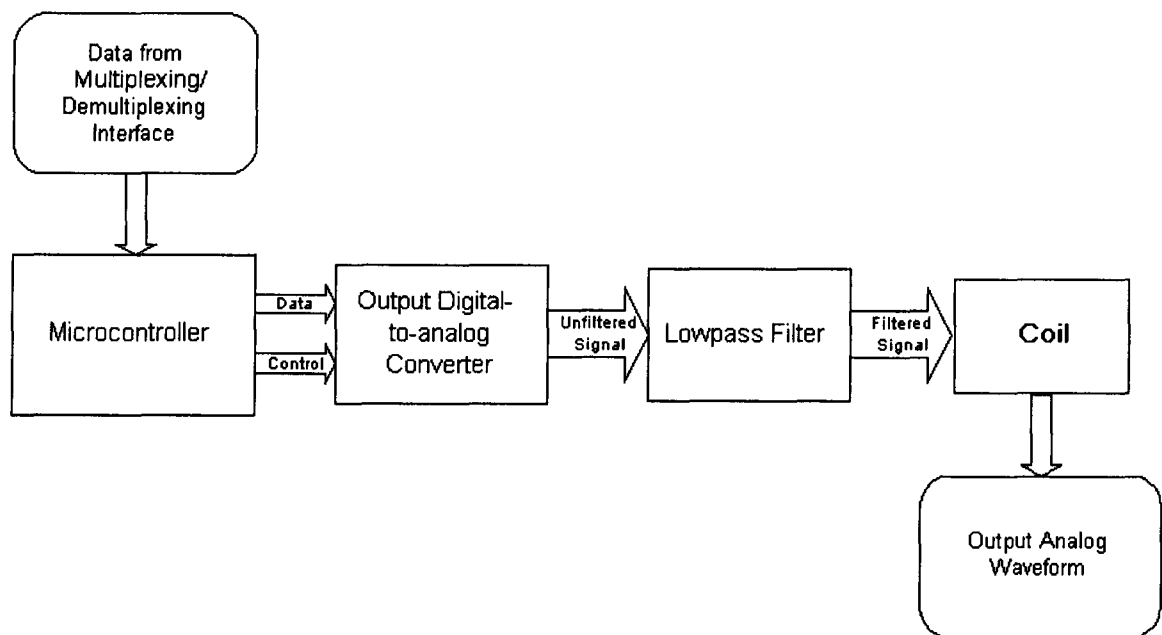


**Figure 4.2: Dataflow among components in a signal generating unit.**

### 4.3 Signal Filtering

The signals generated at the output of each digital-to-analog converter (DAC) were observed to contain multiple frequency components, even when the



intended signal was a sinusoidal function of single frequency component. This was attributed to the method by which the signal was produced. Figure 4.3 shows an example of an unfiltered output signal of the DAC. Instead of a desired smooth sinusoidal signal, the signal exhibited step-like slope. Such a signal could be inferred as a mixture of a low-frequency pure sinusoidal signal and a high-frequency step function, while the step function signal was composed of a wide range of frequencies. Since this unfiltered signal contained the unwanted high-frequency portion added to the signal to be generated, an output lowpass filter was used to remove the unwanted frequency components.

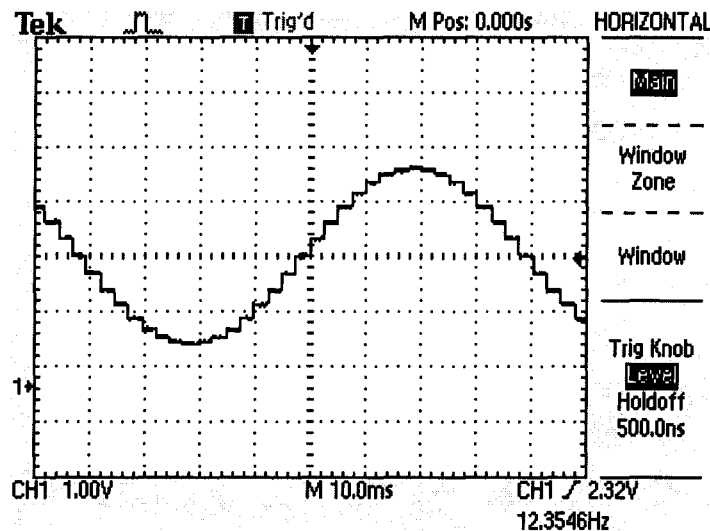


Figure 4.3: Unfiltered sinusoidal signal at the output ( $V_{pk-pk} = 3.2$  V, period = 81 ms).

A fourth-order Butterworth low-pass filter was implemented by cascading two second-order switched-capacitor filter blocks. Using an LTC1060 switched-capacitor filter chip by Linear Technology, the cut-off frequency of this low-pass filter is adjustable based on the frequency of the input clock signal. In the present implementation, the clock signal for the low-pass filter is generated using a pin on

the same microcontroller used for controlling the DAC. The particular pin selected was dedicated to the output of a built-in counter on ATmega32. Figure 4.4 demonstrates the relationship between the input and resulting cut-off frequencies of the low-pass filter implemented after calibration. The observed nonlinearity at high-frequency region of the curve resulted from the particular mechanism for generating the clock signal. Using the Clear Timer on Compare Match Mode for the built-in counter (Refer to the ATmega32 microcontroller datasheet released by Atmel®), the counter output toggled when the counter value was decremented to zero and reset. Therefore, the initial counter value was proportional to the period of the clock signal it generated. Meanwhile, the cut-off frequency of the output filter was governed by the frequency of the clock signal. Hence, given a desired output cut-off frequency, the initial counter value that was proportional to the reciprocal of the desired cut-off frequency was computed by dividing a pre-determined constant value with the desired cut-off frequency. As this frequency increased, the resolution of the division result significantly decreased, since the counter value was an unsigned 8-bit integer limited by the microcontroller. For the current implementation, cut-off frequencies beyond approximately 600 Hz are not required, as most of the brainwaves emitted by normal human brains have frequencies below 200 Hz. The magnitude and phase diagrams of the frequency response of the 4<sup>th</sup>-order output low-pass filter are shown in Figure 4.5, with the cut-off frequency set at approximately 100 Hz. A very sharp increase in signal attenuation can be observed as frequency increased above 100 Hz. Also observable is the phase shift of the output signal

was approximately  $-180^\circ$  at the frequency of 100 Hz, which indicated the frequency response of the filter had 4 poles located near the cut-off frequency.

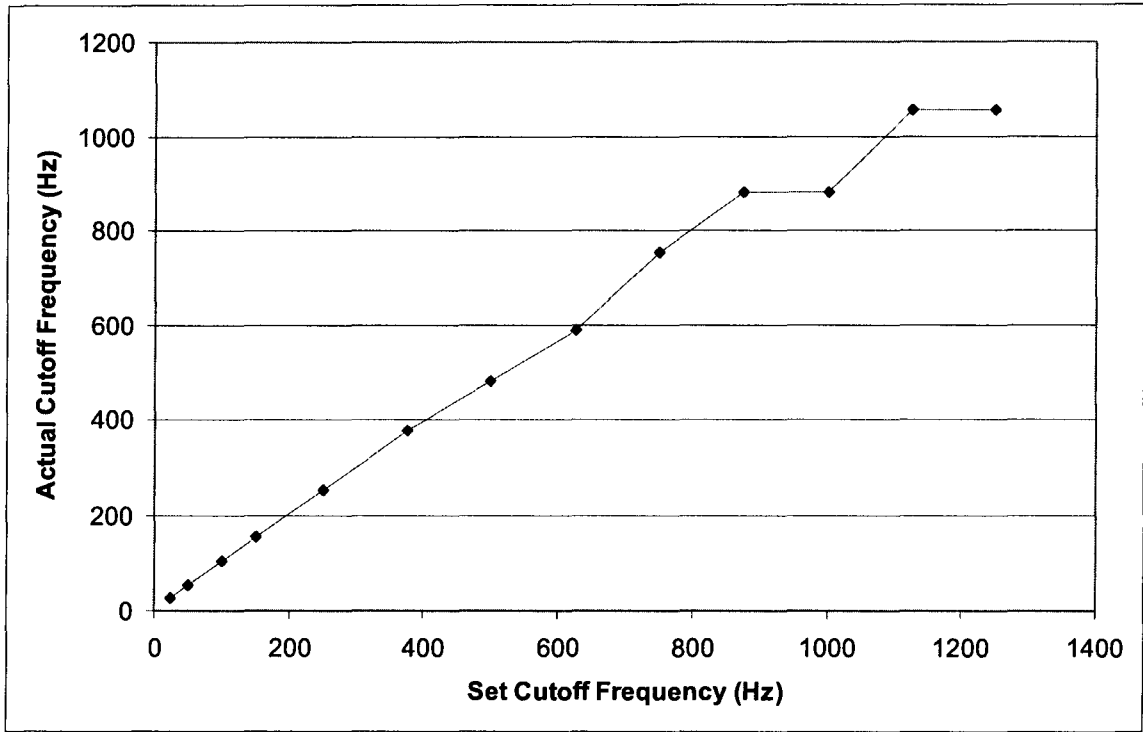


Figure 4.4: Resulting cutoff frequency in comparison with the input cutoff frequency of the implementation.

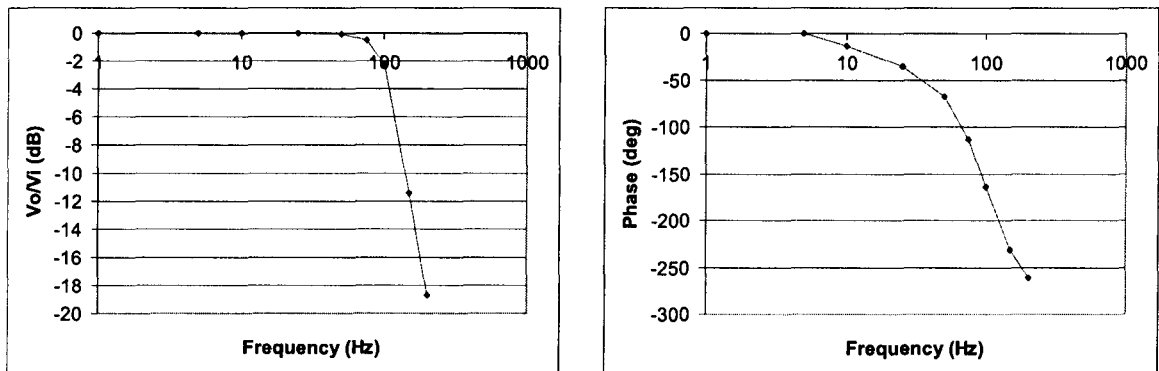


Figure 4.5: (a) Magnitude response and (b) phase shift of the output filter.

The attenuation of unwanted high-frequency components present in the output signal is evident by comparing the unfiltered and filtered output signals both in time and frequency domains, as shown in Figures 4.6 and 4.7.

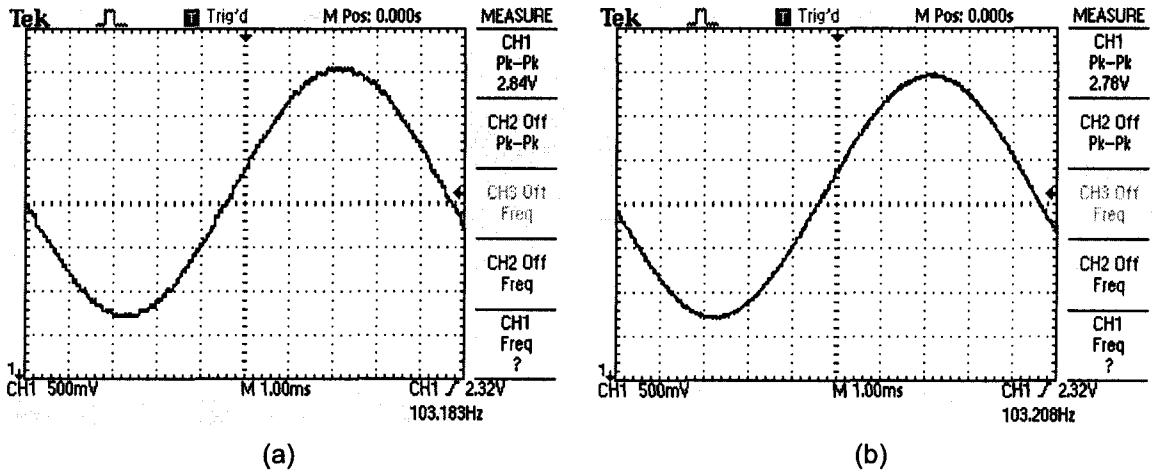


Figure 4.6: (a) Unfiltered and (b) filtered signals at the output ( $V_{pk-pk} = 2.78$  V, period = 9.7 ms).

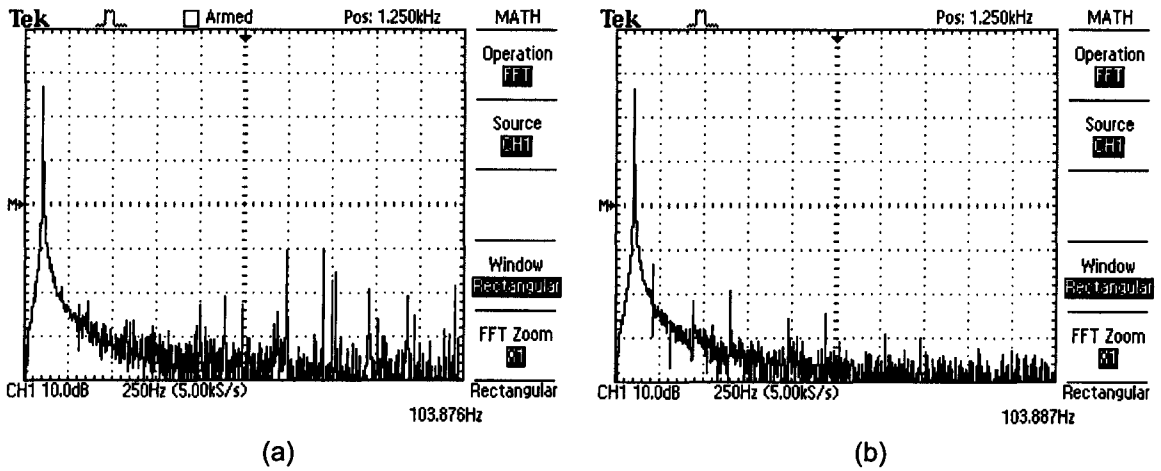
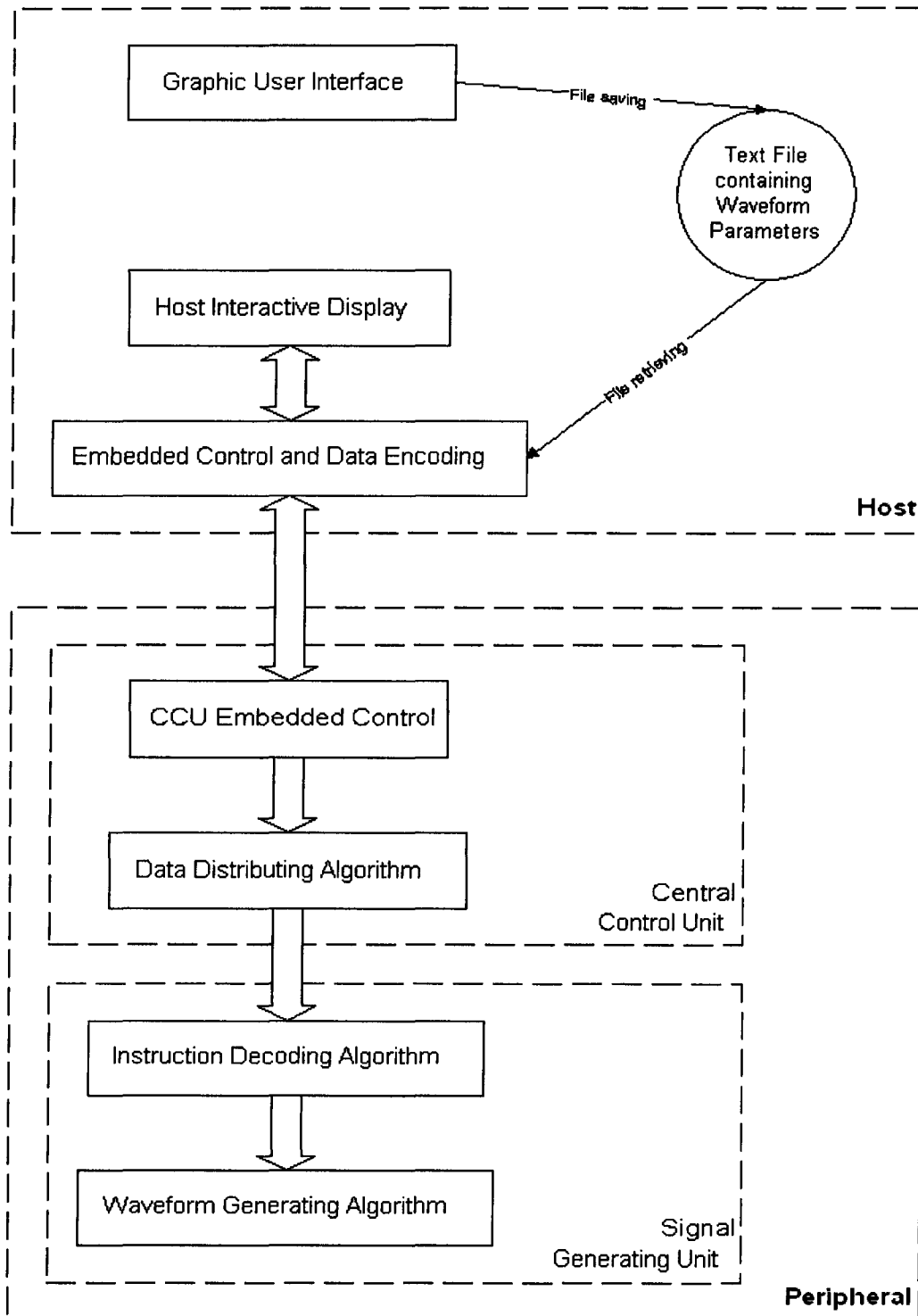


Figure 4.7: Frequency spectra of (a) unfiltered and (b) filtered signals.

## **5: DESIGN OF ALGORITHM**

### **5.1 Overall Design Structure**

The algorithm developed for the design includes the display of a graphic user interface (GUI), the embedded control algorithm, and the communication between microcontrollers, as the block diagram of the overall design algorithm shown in Figure 5.1. On the host PC, a signal-manipulating GUI was designed to handle the input of signal parameters and the corresponding mathematical processing. Due to the low priority for the need of continuous and synchronous data transfer between the GUI and the embedded control, the input signal parameters are stored in specific sequence in a text file, which can be subsequently retrieved by the embedded control algorithm. The control algorithm then encodes the data from the text file to a specific packet format developed to be transferred to the peripheral over a USB connection. A host interactive display, which was based on the real-time exchange of data packets between the host PC and the central control unit, was also programmed to allow real-time control of the peripheral, including data sending, signal starting and stopping, and other possible control instructions in further expansion. Upon receiving the data packets, each of which contains both instruction and coefficient data, the CCU decodes the instruction and determines what subsequent operation is to be performed and which signal generating unit (SGU) the instruction is intended for.



**Figure 5.1: Overall representation of data exchange between interconnected control algorithm blocks**

## 5.2 Graphic User Interface

The construction of a simple signal waveform, such as a sinusoidal function composed of one single frequency component, requires parameters such as amplitude, frequency, and phase to be defined. A graphic user interface was developed to handle the input of values and manipulate the desired waveform using Matlab. Matlab was chosen in this application, owing to its mathematical processing capability and the GUI programming tool it provided. In the present application, parameters and coefficients were organized in groups, each representing the data to be transferred to one single signal-generating unit, referred to as a channel in this article. These data were stored as comma-separated values in a text file with a specific file name. Once started, the program loaded the data from the file and stored them in the form of a matrix in the program memory. Upon the selection of a particular channel, the plotting area on the GUI displayed the waveform defined by the currently stored values of the parameters and coefficients associated with the channel. To provide a mechanism for composing more complex waveforms, the GUI was designed to handle waveforms of a maximum of five frequency components, each also with a different amplitude and phase delay. Based on Fourier Theorem, a periodic signal waveform can be constructed from a series of basic sinusoidal waves of different frequencies [29]. Since human brainwaves normally consist of only several frequency components, a mechanism for composing a complex signal containing a large number of frequency components is not needed in this application. Furthermore, the cut-off frequency at the output can be arbitrarily

defined over a certain range from the GUI. The Matlab GUI developed in this study is shown in Figure 5.2 below. Refer to Appendix B for the Matlab source code. Figure 5.3 demonstrates the customized interactive GUI implemented using Atmel® AtUsbHid Library built from Microsoft Foundation Class Library. The C++ source code for the interactive GUI is included in Appendix C.

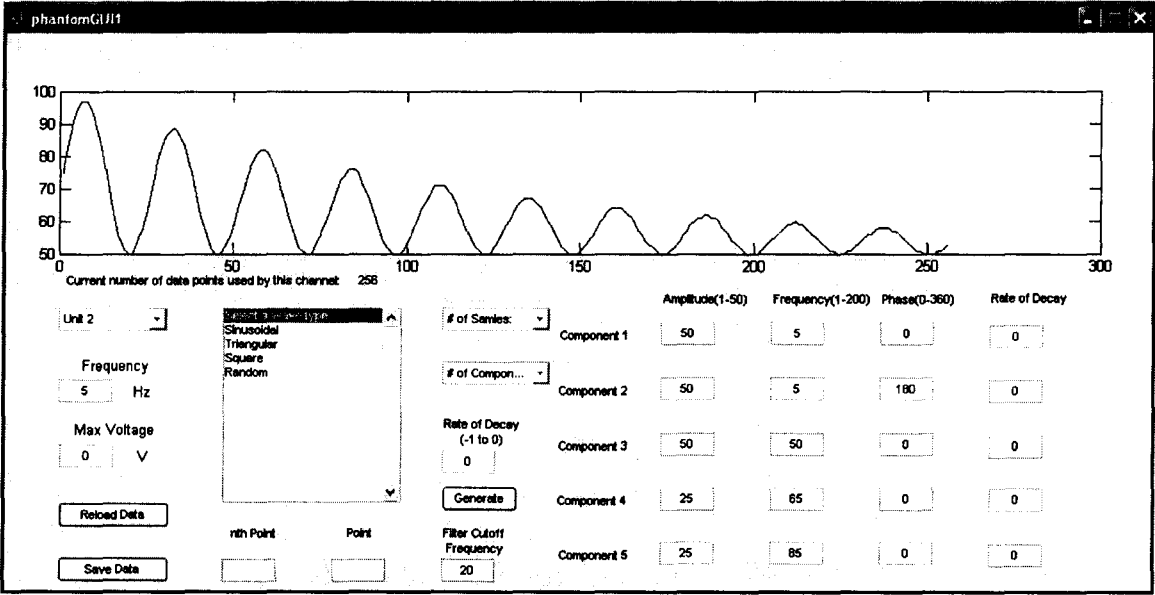


Figure 5.2: Graphic user interface for composing the output signal waveform (programmed in Matlab).

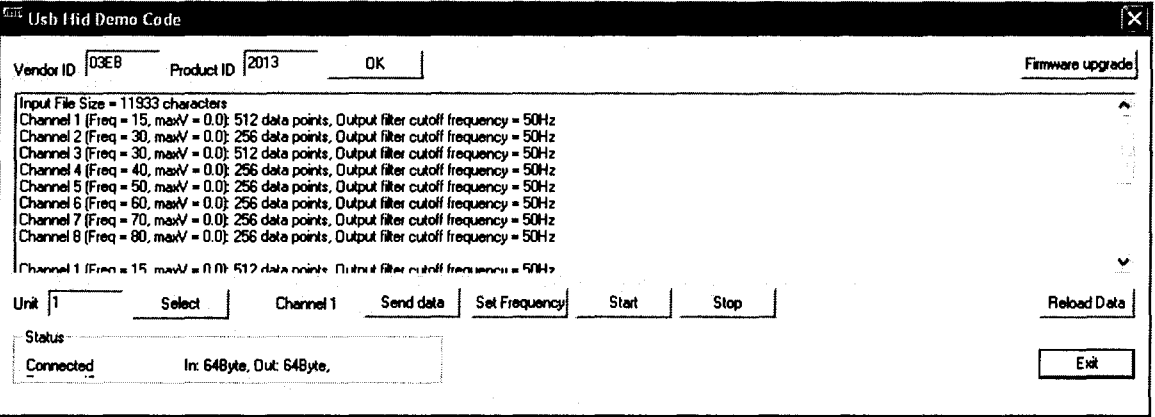


Figure 5.3: Real-time interactive graphic user interface dialog on host PC.



The flowchart in Figure 5.4 illustrates the algorithm for implementing the waveform composing Matlab GUI.

### **5.3 Signal Generating Algorithm**

The generation of signal waveform was accomplished by the use of a DAC, of which the output voltage level depended on the input binary code of the DAC at a particular time instance. A microcontroller was required to store a series of binary codes and transmit them one-by-one sequentially to the DAC with a fixed time interval, in order to form a specific waveform. The time interval between every two consecutive coefficients would be inversely proportional to the pre-defined frequency components of the signal. An 1Hz sinusoidal signal, for example, would have a time interval of 62.5  $\mu$ S, while an 100Hz sinusoidal signal would have a time interval of 0.625  $\mu$ S, if 16 sample points are used to compose one period of the signal. More specifically, the program computes the corresponding value to be loaded in the interval counter based on the frequency of the signal. The flowchart of the signal-generating algorithm is shown in Figure 5.5.

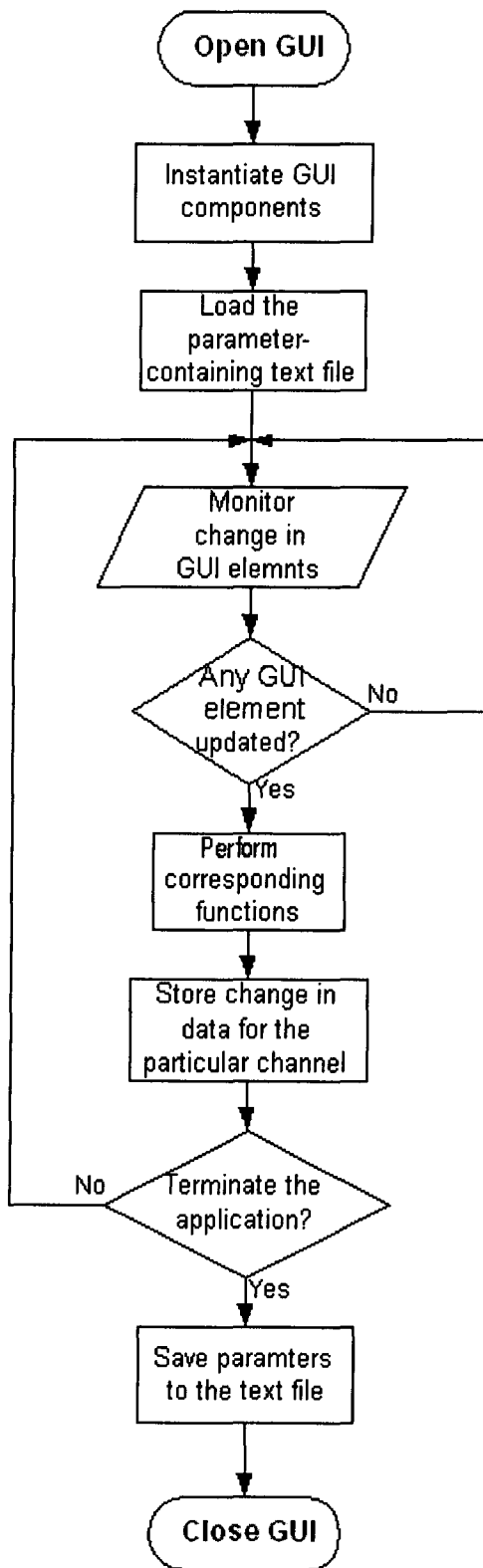


Figure 5.4: Control algorithm of the Matlab GUI on host PC.

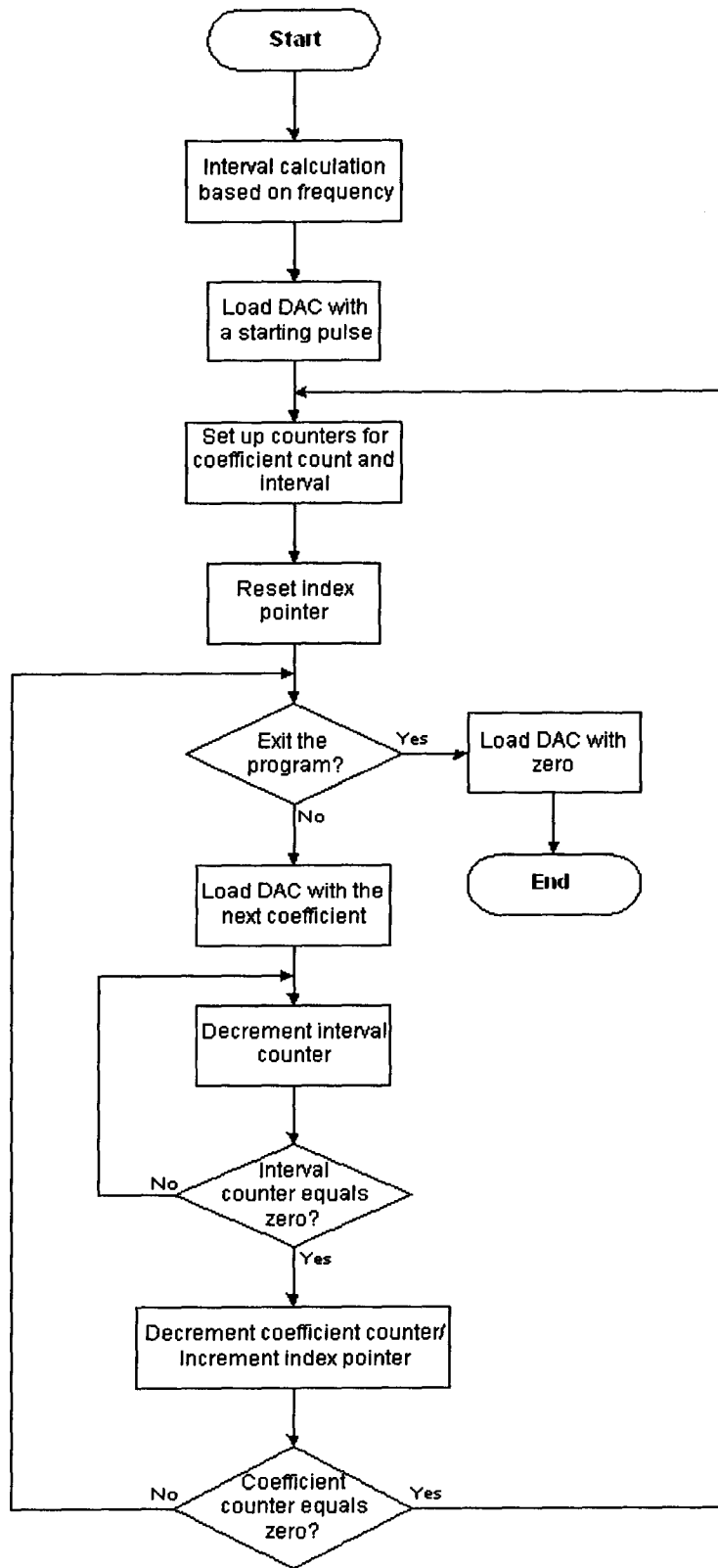
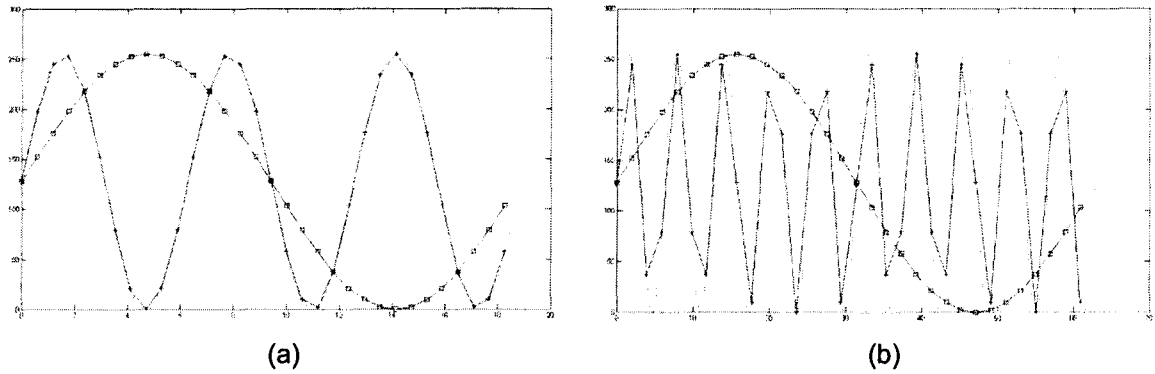


Figure 5.5: Implementation of the signal generating algorithm of SGU.

To generate a sinusoidal signal with one single frequency component, the total number of data points does not have significant effect on the shape of the waveform, as the frequency is varied, since it is the time interval between any two consecutive points that determines the frequency, and this time interval is dependent on the embedded waveform-generating algorithm. However, in the case when two or more frequencies exist in a signal, the higher frequency components might be significantly distorted, when the number of data points is not enough to portray the shape of the fast-varying components. The effect is demonstrated below in Figure 5.6. For a signal of two frequency components, as the frequency of one component is 10 times that of the other component, the higher frequency component is more distorted compared with the case when the frequency of one component is 3 times that of the other. Such distortion shows that in the present implementation, the larger the difference between the frequencies of the fast-varying and the slow-varying components, the fixed number of data points is less able to present the details contained in the fast-varying component. The resolution is limited by the number of data points used to construct one period of the fast varying signal. Figure 5.7 shows the same sinusoidal waveform represented by different numbers of data points. However, the trade-off of using more data points is the demand of more memory space on the microcontroller to store these data and a longer delay in data transfer between the CCU and the peripheral. Moreover, the control of the signal frequency will deviate from linearity, as will be shown in the next section. The on-

chip EEPROM of the ATmega32 microcontroller used for storing the data points in the implementation allows a maximum of 1024 data points.



**Figure 5.6: Representation of a sinusoidal signal (a) 3 times and (b) 10 times of the coexisting fundamental frequency, both with 32 quantization coefficients.**

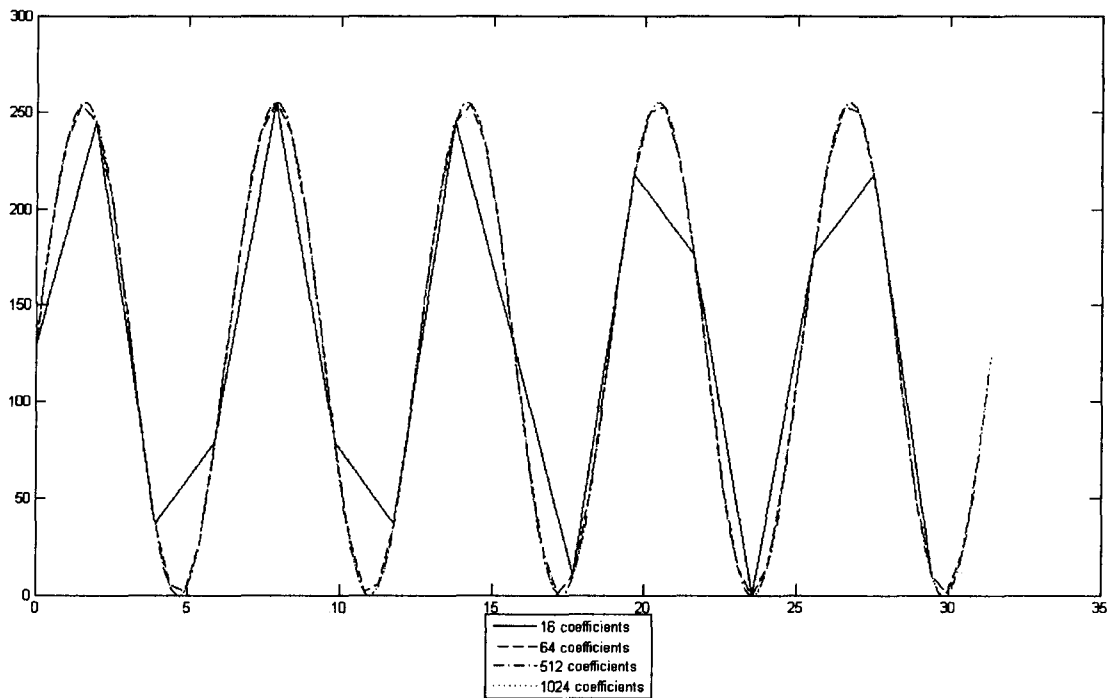


**Figure 5.7: A sinusoidal signal composed of different numbers of quantization coefficients.**

Another advantage of representing a signal with a larger number of data points is the reduction of high-frequency components of the signal generated,

which usually consist of unwanted noise. Such effect can also be illustrated in the frequency domain. Figure 5.8 below shows the frequency responses of an 100-Hz sinusoidal signal, constructed using different numbers of data points. It can be observed that as the number of data points representing a single period increases, the number and magnitude of higher-frequency spikes are reduced. However, representing a signal waveform with a larger number of quantization coefficients using the present signal generating method is not without its trade-off, as will be explained in the next section.

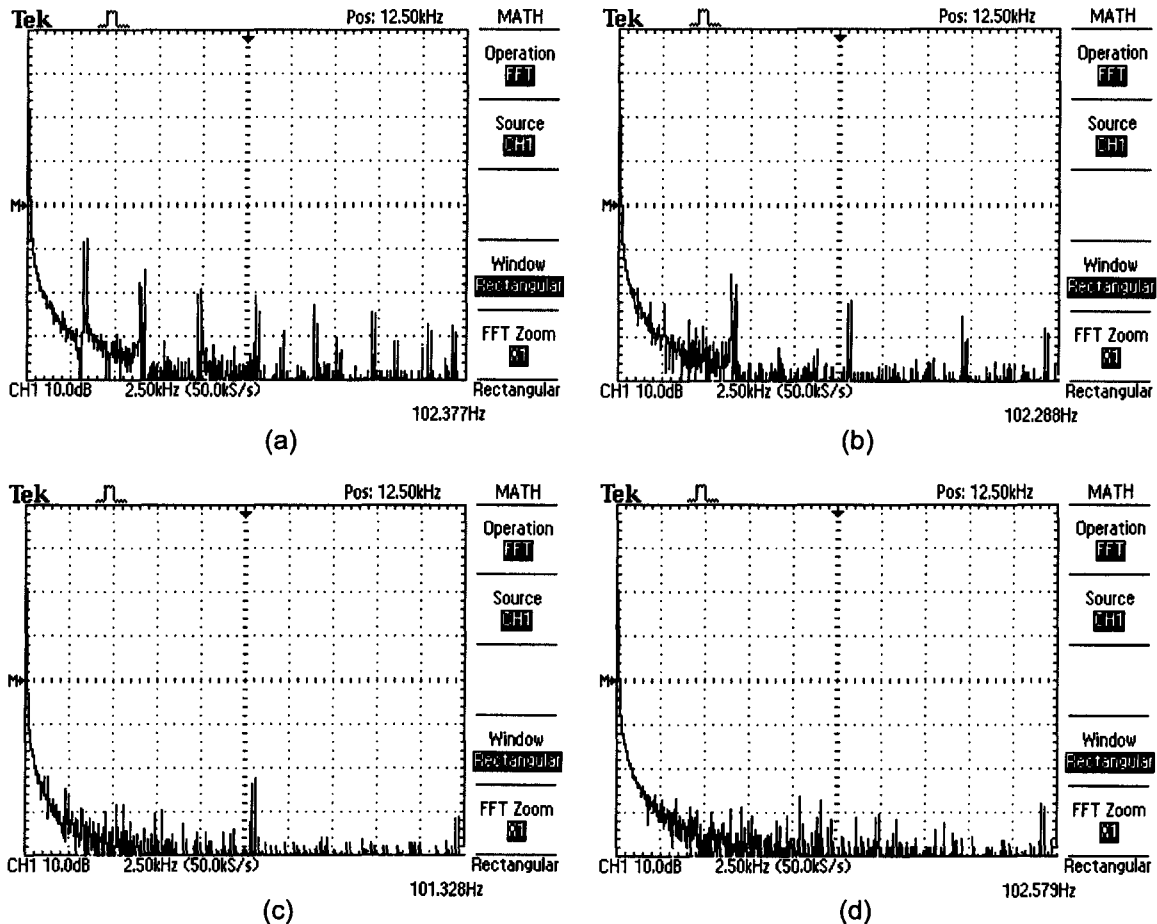


**Figure 5.8: Frequency spectra of an unfiltered sinusoidal signal of 100Hz fundamental frequency formed with (a) 32, (b) 64, (c) 128, and (d) 256 quantization coefficients**

## 5.4 Frequency Calibration

As mentioned previously, the frequency of a generated waveform is controlled by adjusting the length of interval between consecutive voltage points. The frequencies of produced waveforms, therefore, need to be calibrated against the desired frequency of the signal. To accomplish this, a sinusoidal signal with a single desired frequency is defined and compared with the actual signal waveform generated. Figure 5.9 shows that the relationship between the resulting frequency and the value set from the GUI when different numbers of data points are used to compose a single period of the waveform. It can be observed that with the current waveform-generating algorithm, the output frequency levels off at high frequency region. Furthermore, as more data points are used to compose a period, the actual output frequency levels off at a lower value.

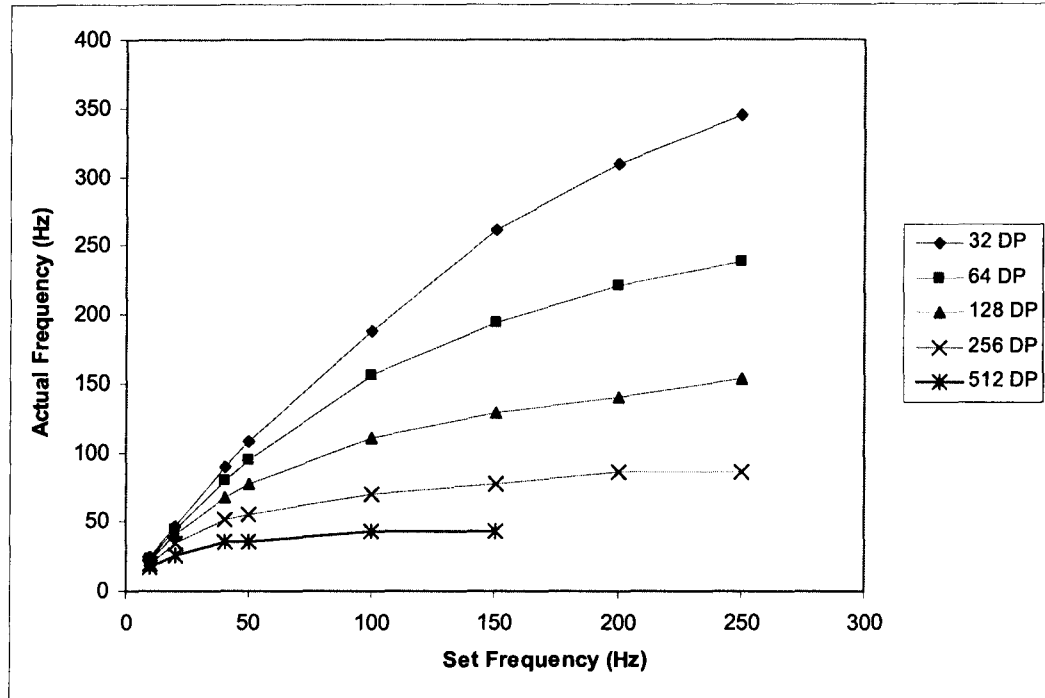


**Figure 5.9: Relationship between resulting frequency of the output sinusoidal signal and the input value of frequency for different number of quantization coefficients before frequency calibration.**

The lower-frequency regions of the curves exhibit more linearity between the output frequency and the set value and thus can provide more linear control of the desired signal frequency. Therefore, it is of great interest to adapt the waveform-generating algorithm to the more linear low-frequency regions. By increasing the length of interval between consecutive output data points, the lower-frequency regions of the curves can be extracted to span the input value range. This was accomplished by doubling the initial count of the counter for controlling the interval between consecutive points. However, the output frequency range is only limited to the lower half of the curves shown. By setting the system clock of the microcontroller to a higher speed, the resulting output frequency can be increased. Figure 5.10 below shows the resulting relationship



as the length between the data points was doubled, while the system clock was increased from the original 1 MHz to 4 MHz. It can be observed that with the same operating conditions, the resulting output frequency exhibited a larger degree of linearity over the desired range.

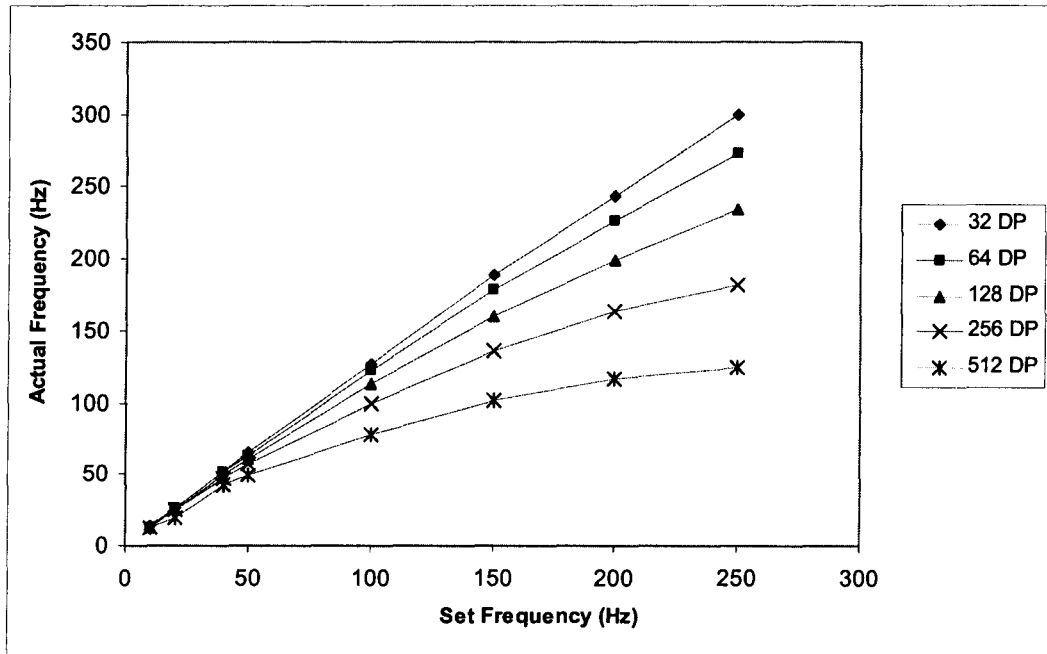


**Figure 5.10: Relationship between resulting frequency of the output sinusoidal signal and the input value of frequency after frequency calibration.**

## 5.5 Embedded Control and Communication

The communication between the host computer and the CCU and between the CCU and any of the SGU is accomplished by the exchange of data packets having data bytes in a specific sequence. These data packets are constructed using a format similar to the format in computer networking protocols, by appending bytes that indicate the command to be executed and relevant parameters to coefficient bytes. Initially, for each single channel, the GUI saves the data in the format shown in Figure 5.11 below, as an array of

parameters followed by the coefficients for constructing a period of signal. The CSV file generated by the GUI contains arrays in such a format, while the number of arrays in the file depends on the total number of SGU attached to the CCU. Once the host interactive display is launched, the embedded control algorithm on the host PC loads the content of the CSV file into its program memory. Every time a function call is made on the host interactive display, one or more packets would be sent to the CCU via the USB connection, including a pilot packet (Packet 1) containing the instruction byte. If the instruction byte in the pilot packet is for coefficient transfer, the number of data packets sent depends on the total number of coefficients (data points) used for constructing a particular waveform. Upon receiving the pilot packet, the microcontroller on the CCU reads byte 6 of the pilot packet that indicates the total number of data points as a multiple of 32 and determines the total number of data packets to be received following the pilot packet. With this implementation, the total number of data points is no longer limited to the maximum number of bytes that can be sent in one single packet, as the USB communication protocol provided by Atmel® limits the maximum number of bytes in a packet to 64 bytes. Figure 5.12 shows the structure of packets sent to the CCU by the host PC for each data transfer. In the pilot packet, depending on the command to be executed, the corresponding instruction byte following the channel ID of the intended unit is attached to the front of an array containing various signal parameters, such as the base frequency, max voltage, and etc.. Upon receiving these data packets, the CCU initiates an external interrupt on the intended SGU, and the data are re-directed

to the intended channel via the demultiplexing circuit. The source code of the CCU embedded algorithm is included in Appendix D. While the microcontroller on each SGU is pre-programmed with an unique channel ID, the addition of channel ID byte to the packet to be sent can prevent any unintended SGU to execute the command. For example, if a propagation delay caused by the demultiplexing network results in the data packets being routed to an unintended channel, the SGU at the receiving end would discard the packets because the channel ID in the pilot packet does not match the pre-programmed ID of the receiving SGU. In the present design, the packet can easily accommodate up to 256 channels and 256 different function calls.

Byte 1	Byte 2	Byte 3	Byte 4	Byte 5	Byte 6	...	Byte $n$
Base frequency	Max voltage	Cut-off frequency	Number of coefficients	Coefficient 1	Coefficient 2	...	Coefficient $k$

**Figure 5.11: Data structure of the stored parameters for each individual channel on host PC.**

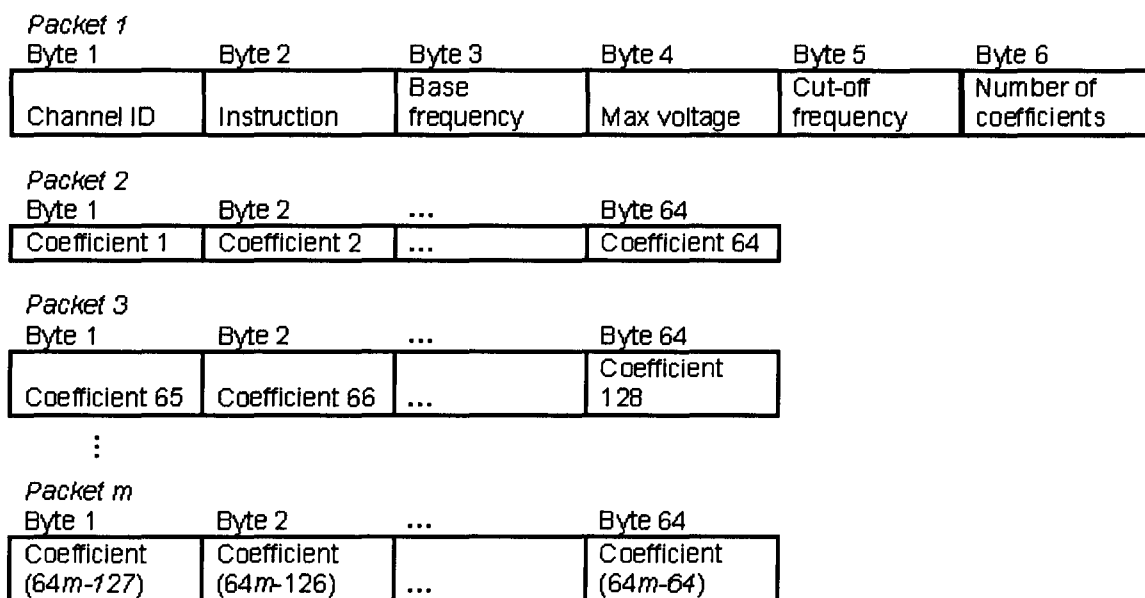


**Figure 5.12: Structure of the packets sent from host PC to CCU during each data transfer.**

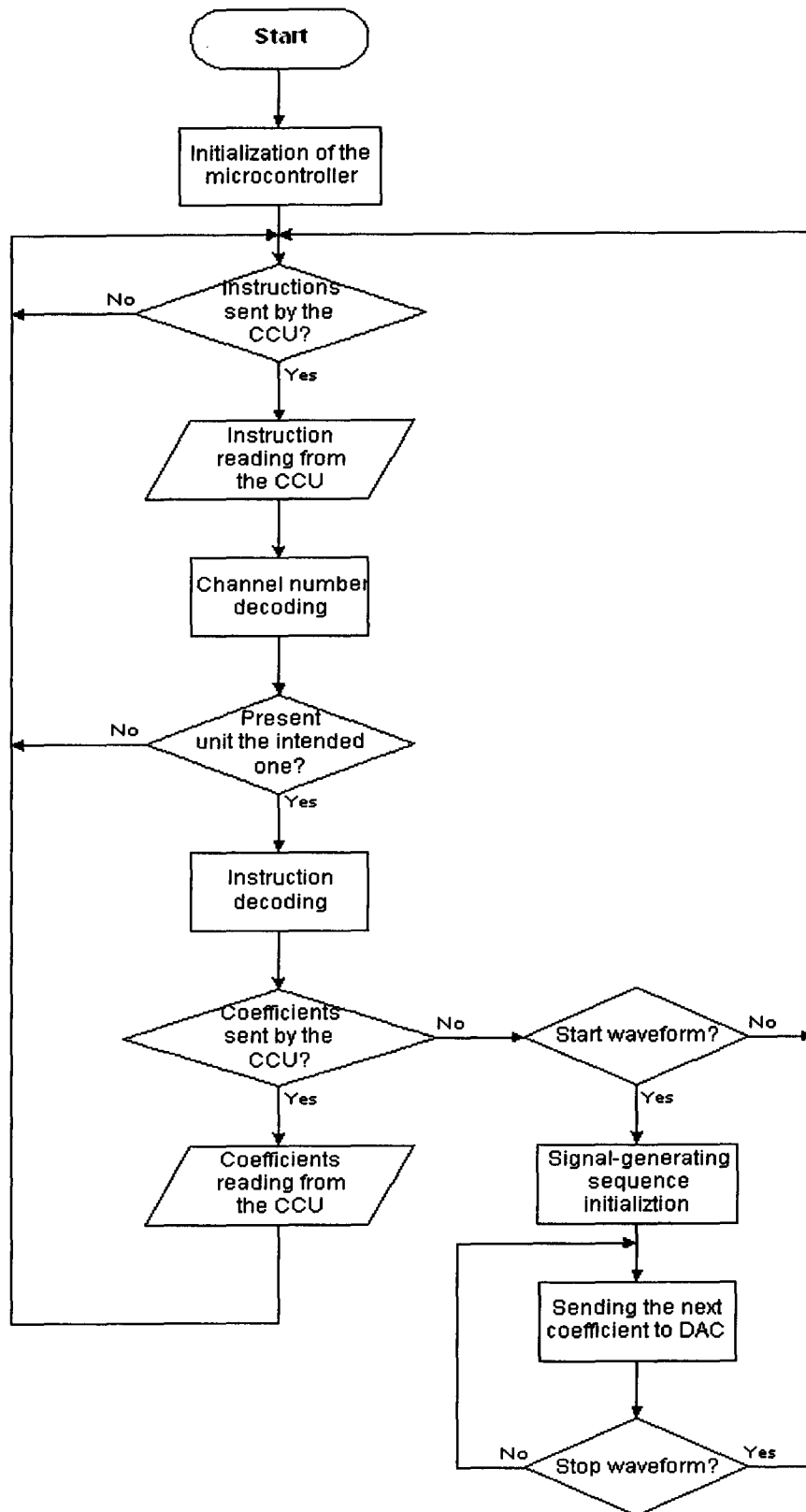
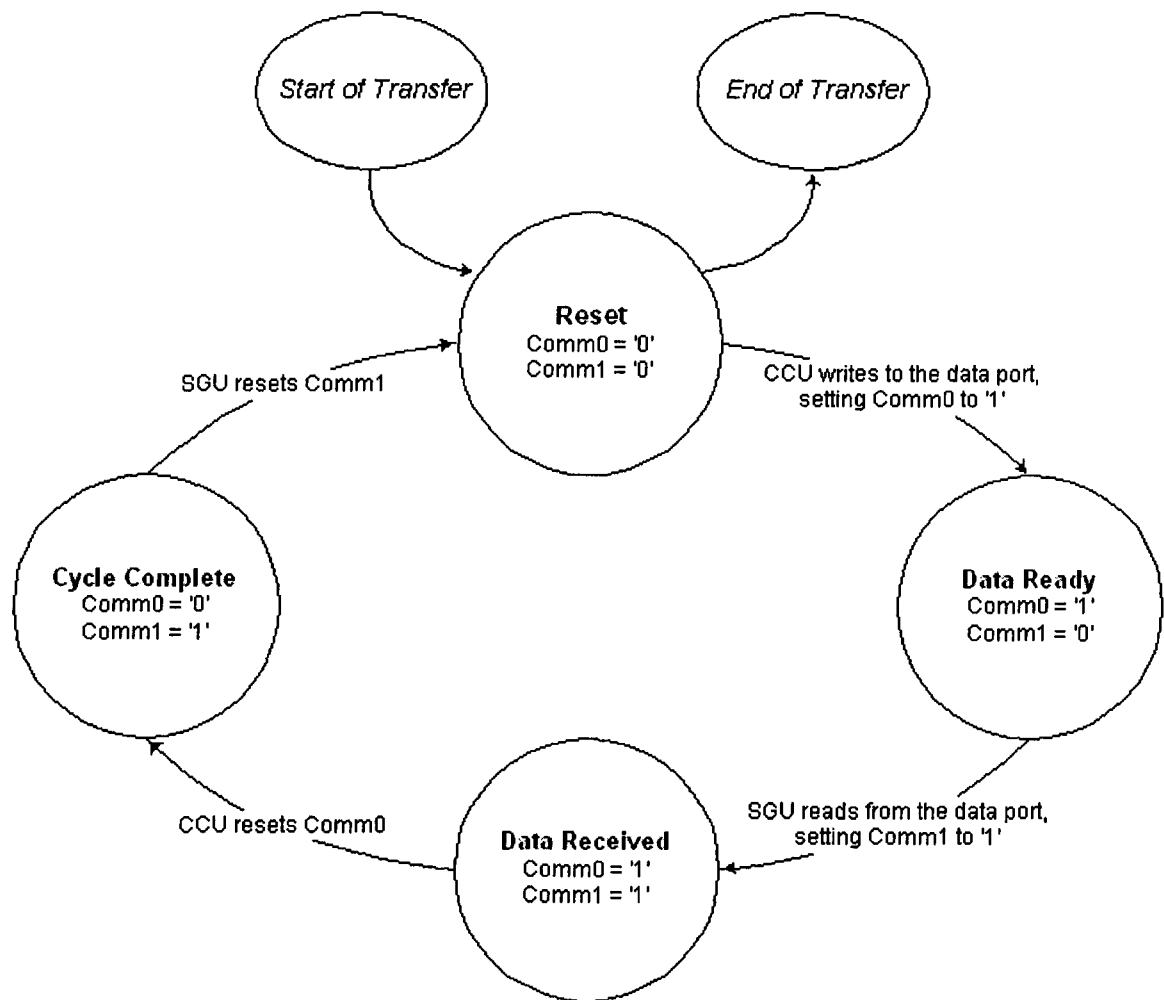


Figure 5.13: Command-decoding algorithm on each SGU.

The command decoding sequence implemented on each SGU microcontroller is illustrated in Figure 5.13. Once the SGU microcontroller receives the pilot packet, and the instruction is decoded to be coefficient transfer, byte-by-byte data transfer is performed between the CCU and the intended SGU. The scheme of coefficient transfer implemented is shown in Figure 5.14. The communication between the CCU and the SGU consists of four states, dictated by Comm0 and Comm1 signal lines. The Comm0 and Comm1 were implemented using a pair of I/O ports between the CCU microcontroller and the SGU microcontroller. Comm0 signal line was configured as an output for the CCU and an input for the SGU. The direction of the Comm1 line was the inverse of that of Comm0. Another connected I/O port between the CCU and the SGU was used for transferring the byte data, with the CCU being the sender and the SGU being the receiver. Upon the start of transfer, both Comm0 and Comm1 lines are reset to '0', and the system is in *Reset* state. After the CCU writes the new byte of coefficient to the data port, it sets Comm0 to '1' to indicate a new byte is ready for the SGU to receive. The system is in *Data Ready* state at this stage. The SGU then reads the new byte of data from the data port and set Comm1 to '1'. The *Data Received* state indicates to the CCU that the current byte has been received and a new byte of coefficient can be written to the data port. Once the CCU detects a '1' on Comm1, it resets Comm0 to '0' to switch to *Cycle Complete* state. Subsequently, the SGU resets Comm0 to '0', and the entire cycle is repeated for each of the coefficients. The end of transfer is done by exiting the loop when all the coefficient bytes are finished transferring. The

communication is achieved by the CCU controlling the status of Comm0 line and the SGU controlling the status of Comm1 line. In any of the states, both the CCU and the SGU should check the status of both the Comm0 and the Comm1 lines and perform the corresponding tasks before altering its own signal line. Refer to Appendix E for the detailed control algorithm for each SGU microcontroller.



**Figure 5.14: Communication states of data point forwarding from CCU to SGU.**

## 6: MEASUREMENT AND ANALYSIS

### 6.1 Experiment and Method

A more delicate method of positioning coils was devised, which allowed more coils to be mounted on a head-shaped object simultaneously. Each coil at the end of a twisted pair was firmly glued on a flat wooden stick with markings indicating every centimetre, as illustrated in Figure 6.1. These markings were later used for determining the relative spatial coordinate of the coils with respect to the reference points in the Polhemus measurement system.

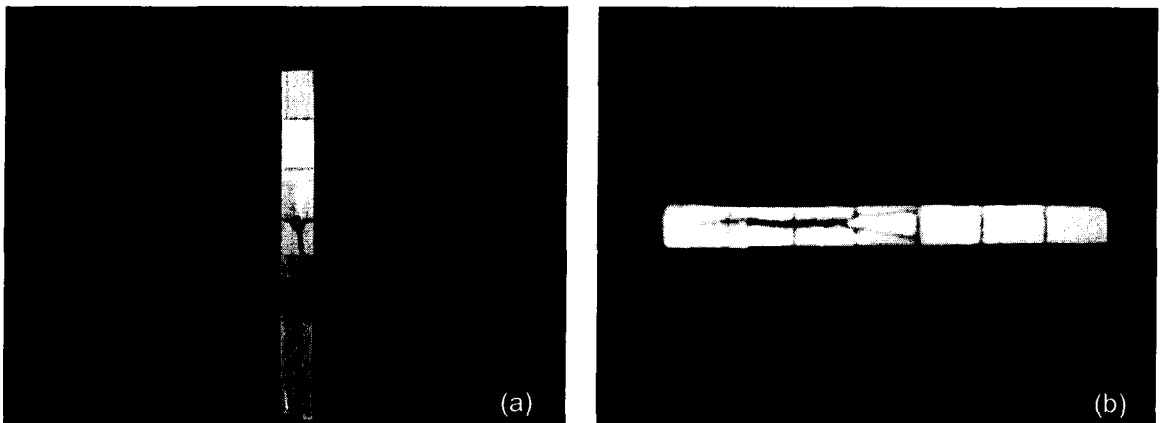


**Figure 6.1:** (a) A helical coil (3 loops) and (b) an isosceles triangular coil fixed on a wooden stick. The distance between two adjacent marked lines on the stick is 1 cm.

These sticks were then mounted on a plastic skull fixed on the base, as shown in Figure 6.2 below. Holes were drilled at spots evenly distributed on the plastic skull. Then a sheet of rubber layer was glued on the surface of the skull. Holes were opened on the rubber sheet at the corresponding locations. Then these sticks with the coils attached were inserted into the holes on the skull and

held in place by the rubber sheet. Three reference coils (not shown in Figure 6.2) which define the nasion, left ear, and right ear positions were fixed on the base instead of the corresponding positions on the plastic skull. The reference coils also emitted signals recorded by the MEG system; these signals were used for determining the relative location and orientation of the test subject in the measurement cavity. The overall control and signal generating electronics used in the experiment is shown in Figure 6.3.

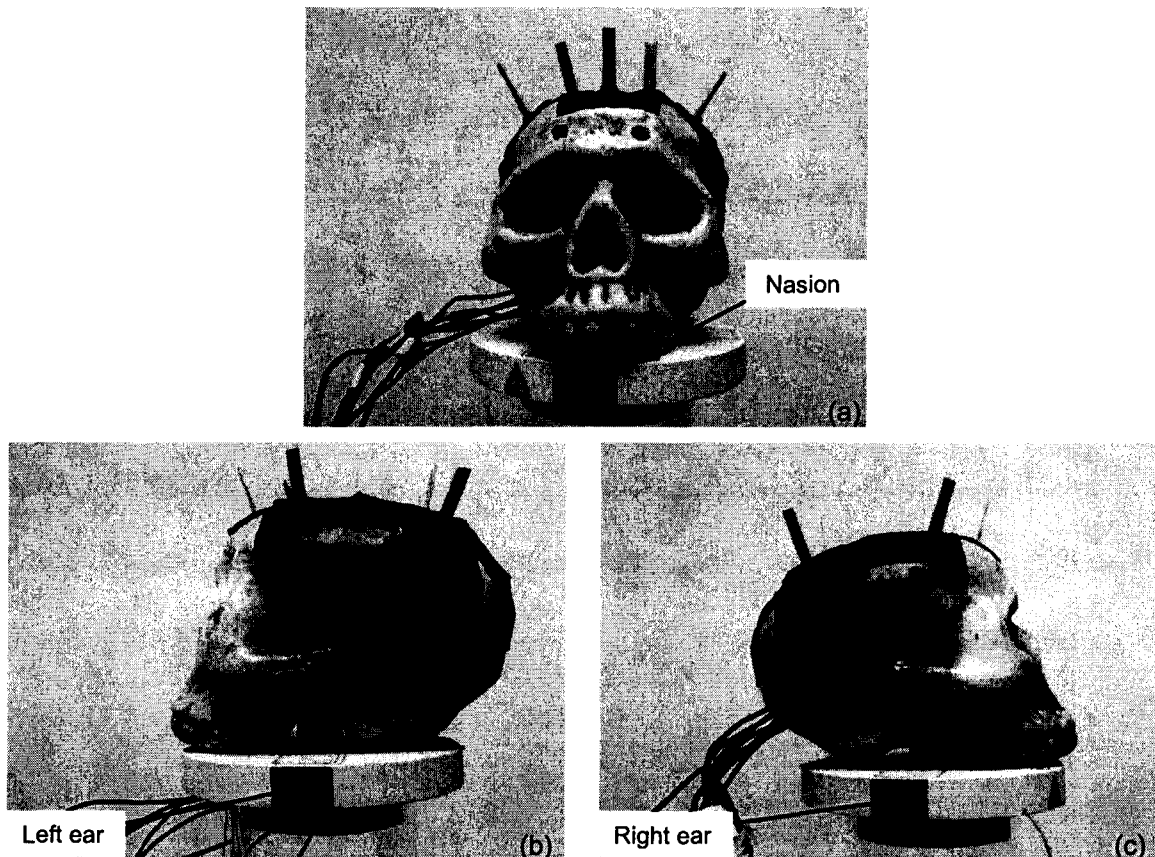


**Figure 6.2: (a) Front view, (b) left-side view, and (c) right-side view of coil placements on a plastic skull covered with a layer of rubber sheet mounted on a plastic base.**



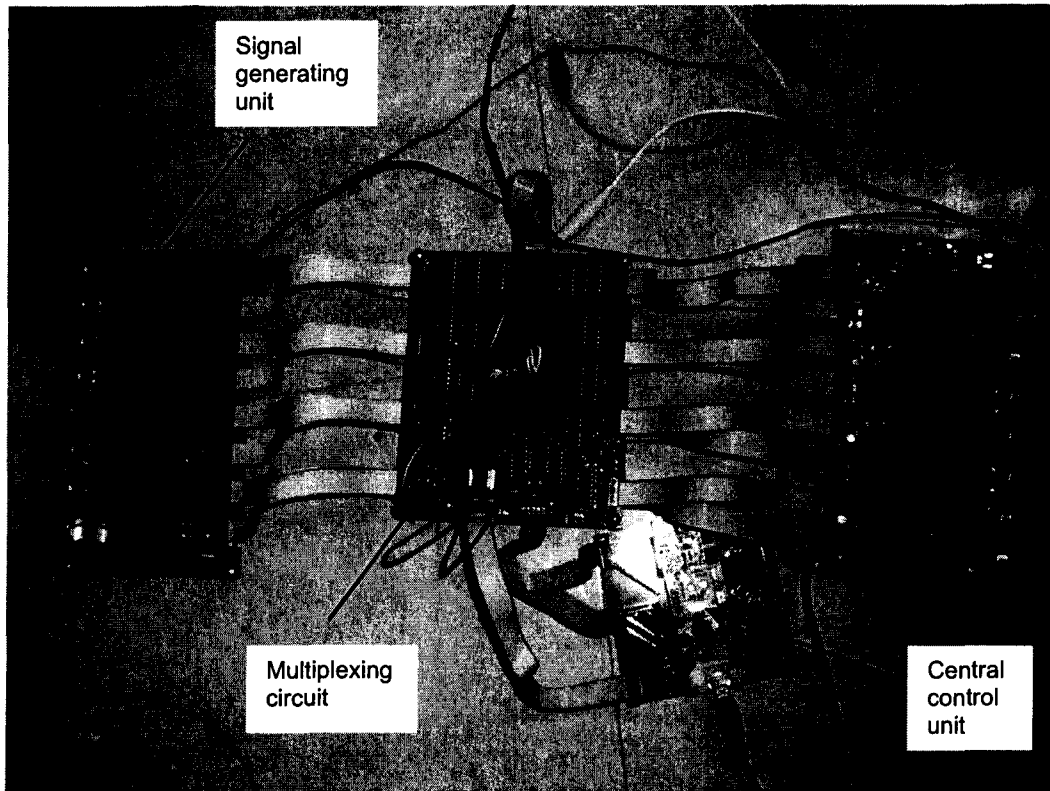


**Figure 6.3: Final assembled magnetic-field-emitting circuit**

The information about the actual spatial locations of the coils was required for the inverse analysis results to be compared with, so the performance of the inverse analysis method developed could be evaluated. To obtain such information, a spatial coordinate locating system developed by Polhemus was used. It was necessary to minimize the shifting of the coil locations with respect to the three reference coils between the MEG and Polhemus recordings. The Polhemus system used in the present is shown in Figure 6.4. The spatial coordinates recorded by the Polhemus FASTRAK® system were used for determining the relative positions of the test coils and reference coils on the phantom and was later used for verifying the spatial localization capability of the inverse analysis method developed in association with this study.

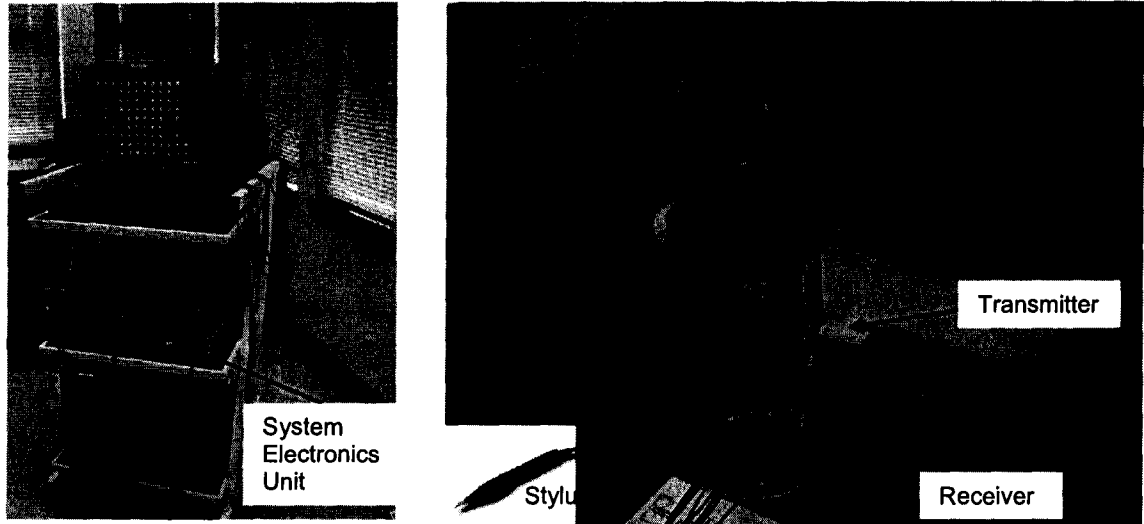


**Figure 6.4:** Polhemus FASTRAK® 3D Digitizer used for localizing points in 3D space, including a transmitter and a receiver fixed around the test skull during the experiment and a stylus used for physically locating the coils on the skull.

## 6.2 MEG Measurement using Helical Coils

Measurement was taken using helical coils mounted on the surface of the plastic skull with relative locations of which the planar view is illustrated in Figure 6.5. All coils were wound with the best attempt to keep the geometry the same.

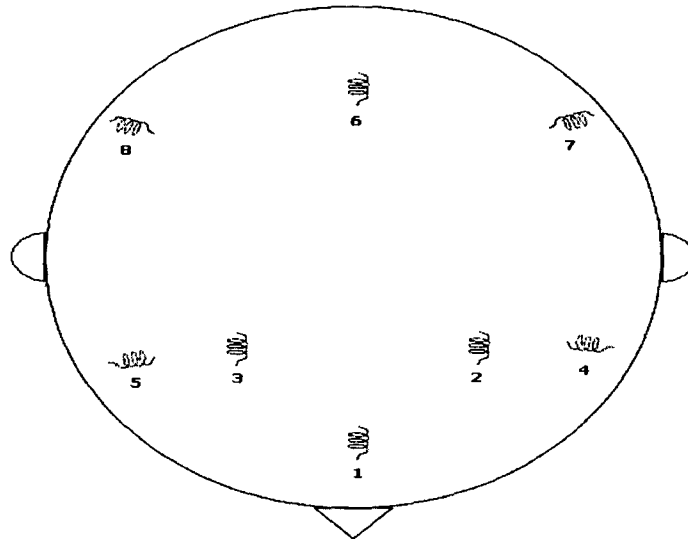


**Figure 6.5:** Relative locations of the helical coils on the head surface.

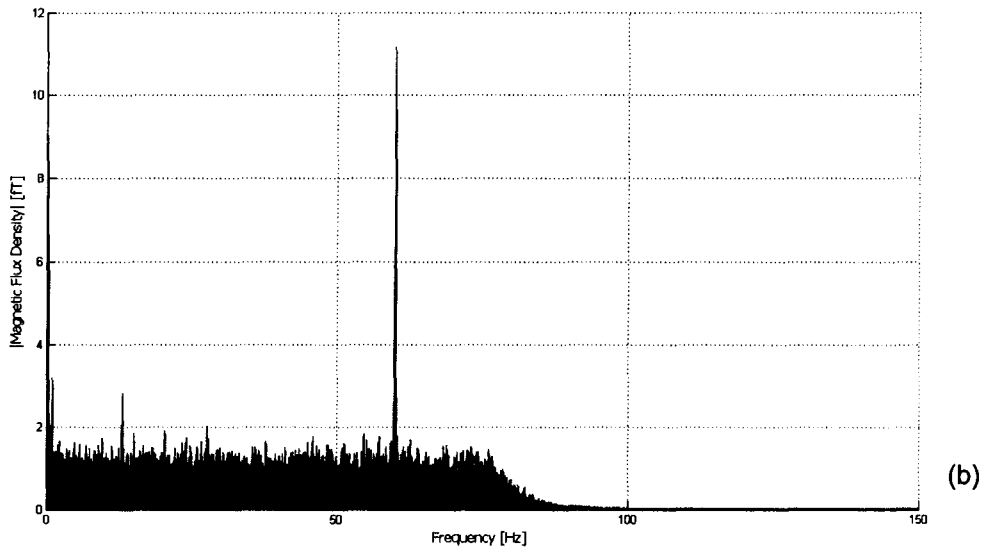
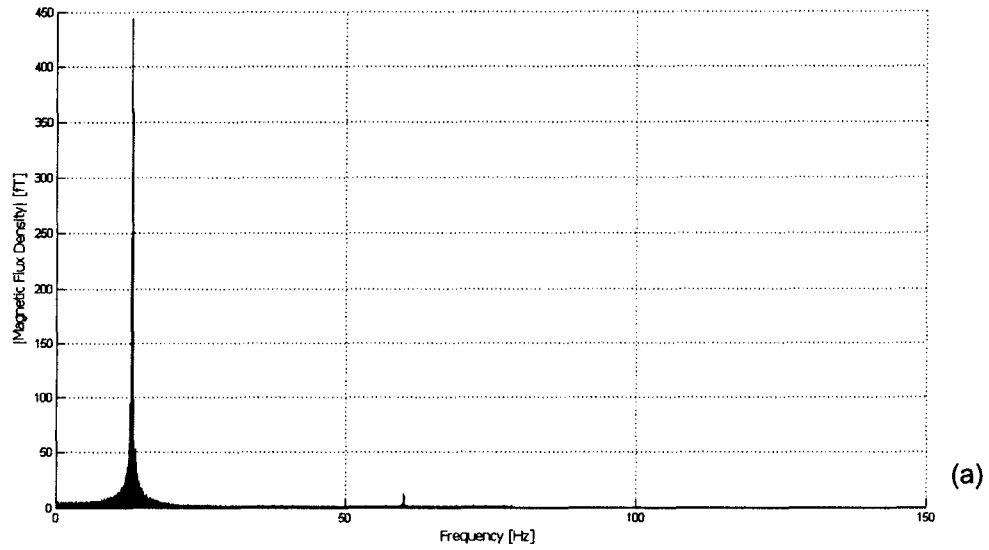


**Figure 6.6: Frequency spectra of (a) all coils at 13 Hz, maximum current and (b) all coils at 13 Hz, minimum current.**

The frequency spectra of measured magnetic flux density under various test conditions are shown in Figures 6.6 and 6.7. It can be observed all the intended frequency components were visible in the recorded magnetic fields. Notably the signal at 60 Hz was likely due to the noise present in the power supply.

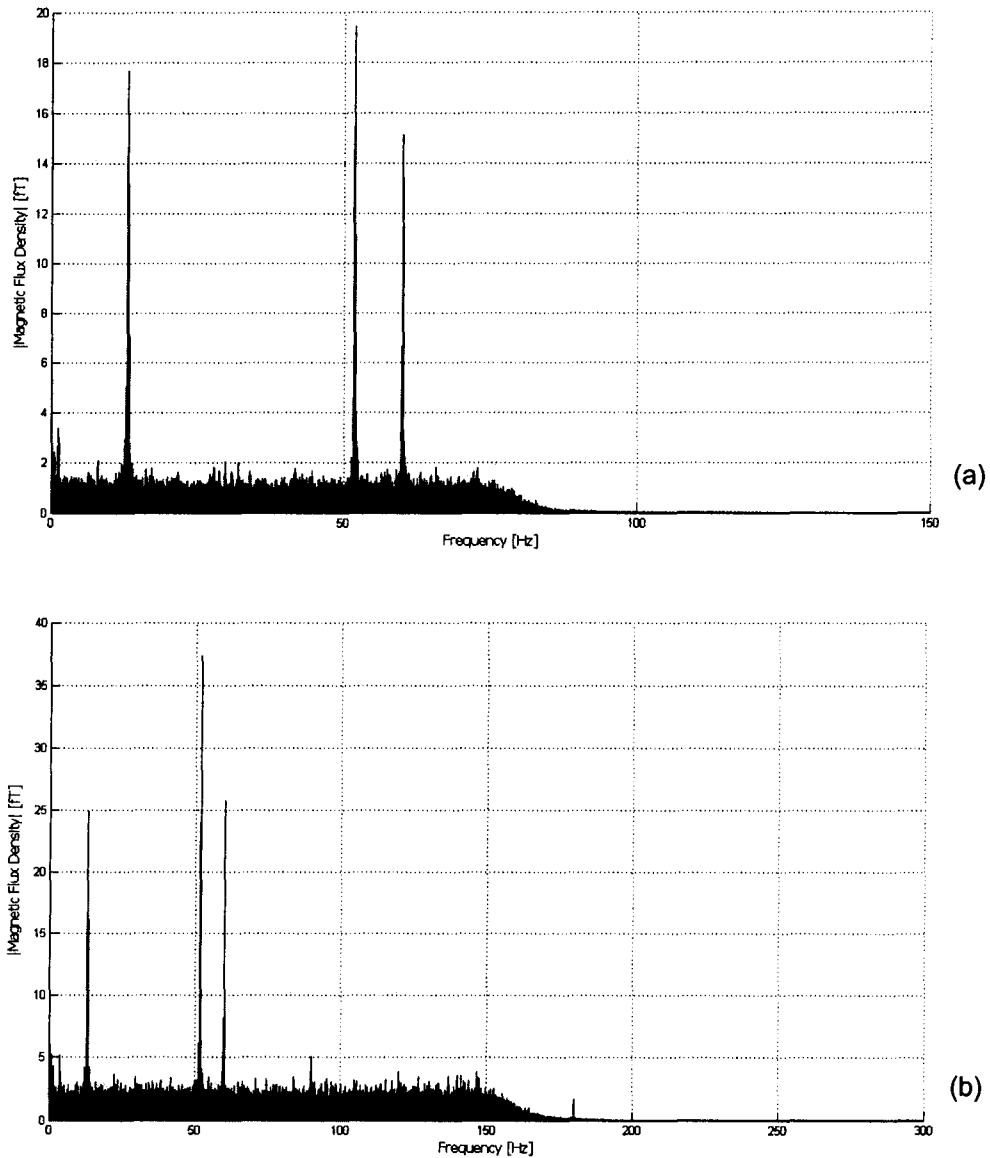


**Figure 6.7: Frequency spectra of (a) coil 4 at 50 Hz, the rest at 13 Hz, half current and (b) coil 4 at 50 Hz, coil 7 at 90 Hz, the rest at 13 Hz, half current.**

### 6.3 Simulated Magnetic Field Pattern of a Triangular Coil

An experimental approach of the study was to use triangular shaped coils to generate current dipoles. To study the behaviour of current dipoles generated by triangular coils, simulations were performed using COMSOL Multiphysics software [30]. Models of isosceles triangles were constructed using copper as the

material, as illustrated in Figure 6.8. Each side of the triangle consisted of a long cylindrical shape with a diameter of 0.15 mm. Since the wire had a constant resistance, the current in the coil was proportional to the applied voltage. The current density through any cross sections along the long axis of all three cylinders would be constant. Notably the corner effect of the triangular shape was neglected in the simulation models constructed. Nonetheless, the relatively small thickness of the wire compared to the dimensions of the triangular shapes simulated, the corner effect would not result in significant difference between the simulated and actual magnetic fields.

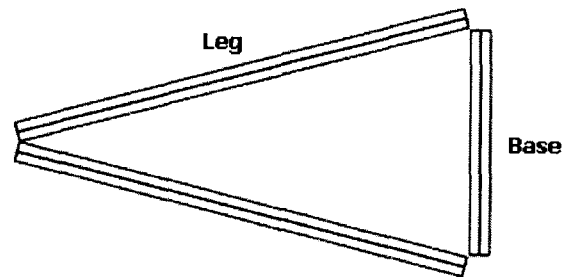


**Figure 6.8: Example triangular coil model constructed in COMSOL.**

The orientation of the coil in the simulated space is shown in Figure 6.9 below. The coils were oriented with the base side of the triangle parallel to the x-axis at  $z = 0$  of the simulated space.

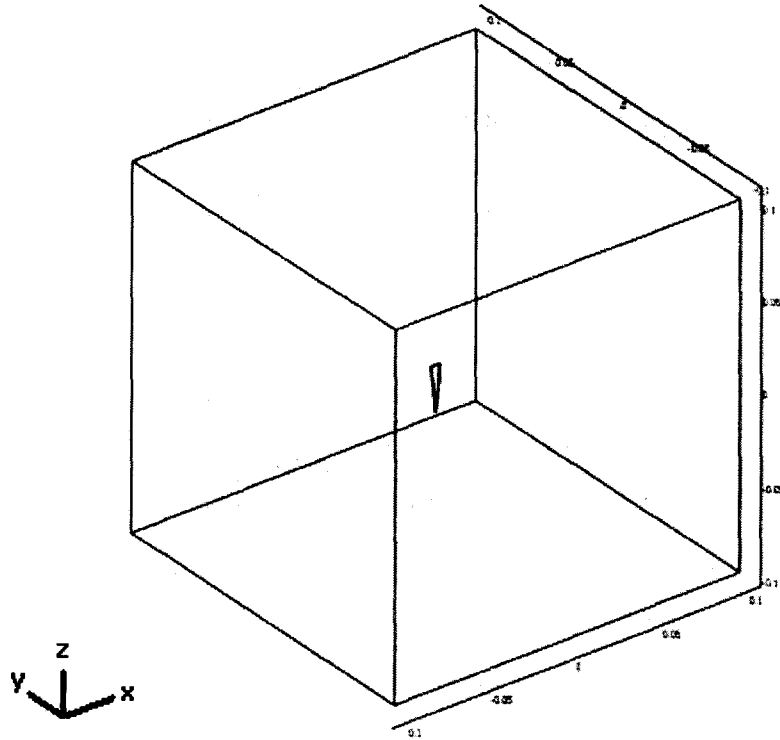


**Figure 6.9: Simulated space in COMSOL, consisting of a cube of 10-cm side length.**

It was of interest to investigate on the magnetic flux density generated by the coil in each dimension of the simulated space. The patterns of the axial components of magnetic flux density in the  $xy$ ,  $yz$ ,  $zx$  planes 5 cm from the origin are shown in Figure 6.10, respectively. By varying the leg length of the triangular coil while keeping the base length constant at 5 mm, the magnetic flux density normal to any plane in the simulated space can be compared. Since magnetoencephalography detects only the tangential component of the source current, it is of interest to monitor  $z$ -component of the magnetic flux density in the  $xy$ -plane, which is parallel to the base side of the triangular coil.

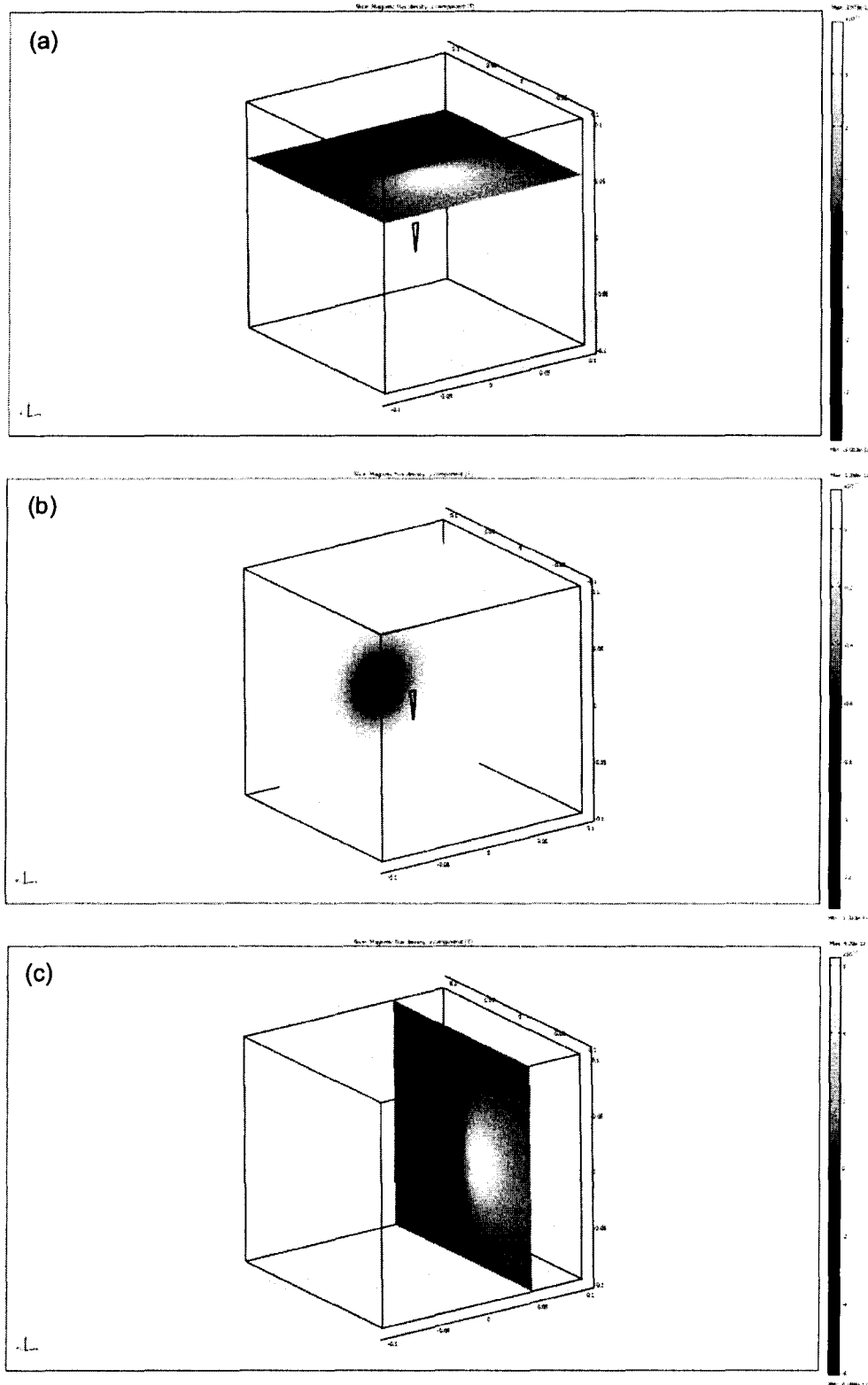


**Figure 6.10: (a) Z-component on xy-plane ( $z = 5 \text{ cm}$ ), (b) y-component on zx-plane ( $y = 5 \text{ cm}$ ), and (c) x-component on yz-plane ( $x = 5 \text{ cm}$ ) of the magnetic field generated by the simulated triangular coils.**

Simulation results indicated the locations of maximum z-component of the magnetic flux density on a given xy-plane remained unchanged irrespective to the change of base and leg lengths, as long as the origin was fixed at the center of the base (See Appendix F). Nonetheless, the maximum y-component on any given zx-plane varied as the geometry of the triangle was changed. It appeared to be located at the same x and z coordinates as the triangle's centroid.

The maximum z-component magnetic flux density normal to the xy-plane at  $z = 5$  cm, and the y-component along the y-axis on the zx-plane at  $y = 5$  cm for various leg-to-base ratios of the coil are shown in Figures 6.11 and 6.12, respectively, while the base was kept constant at 5 mm.

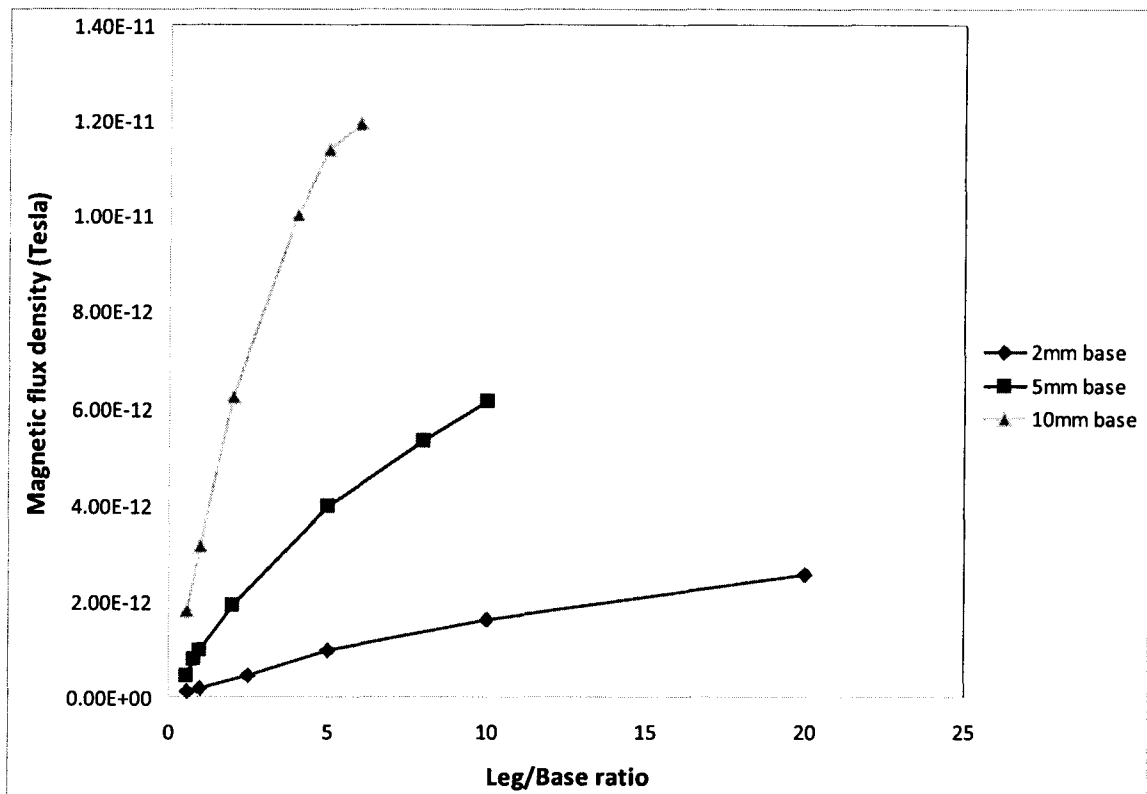


Figure 6.11: Max z-component magnetic flux density in the xy-plane at  $z = 5$  cm from origin of isosceles triangular coils.



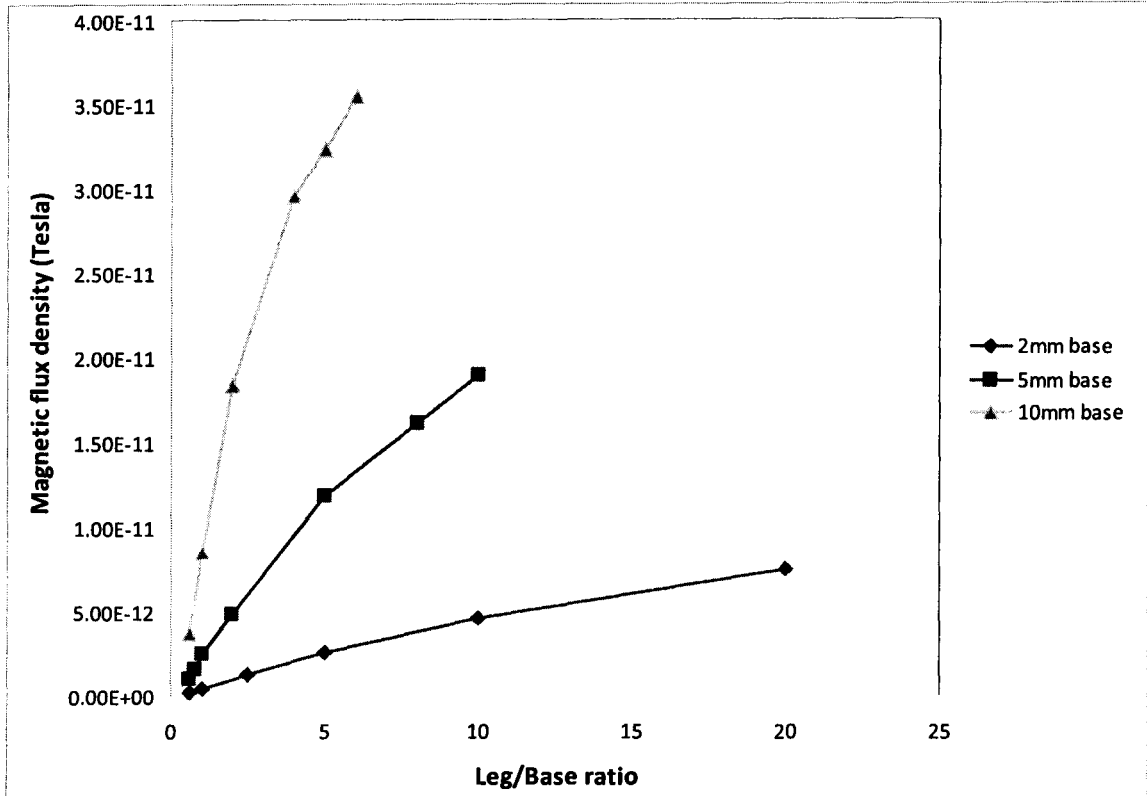
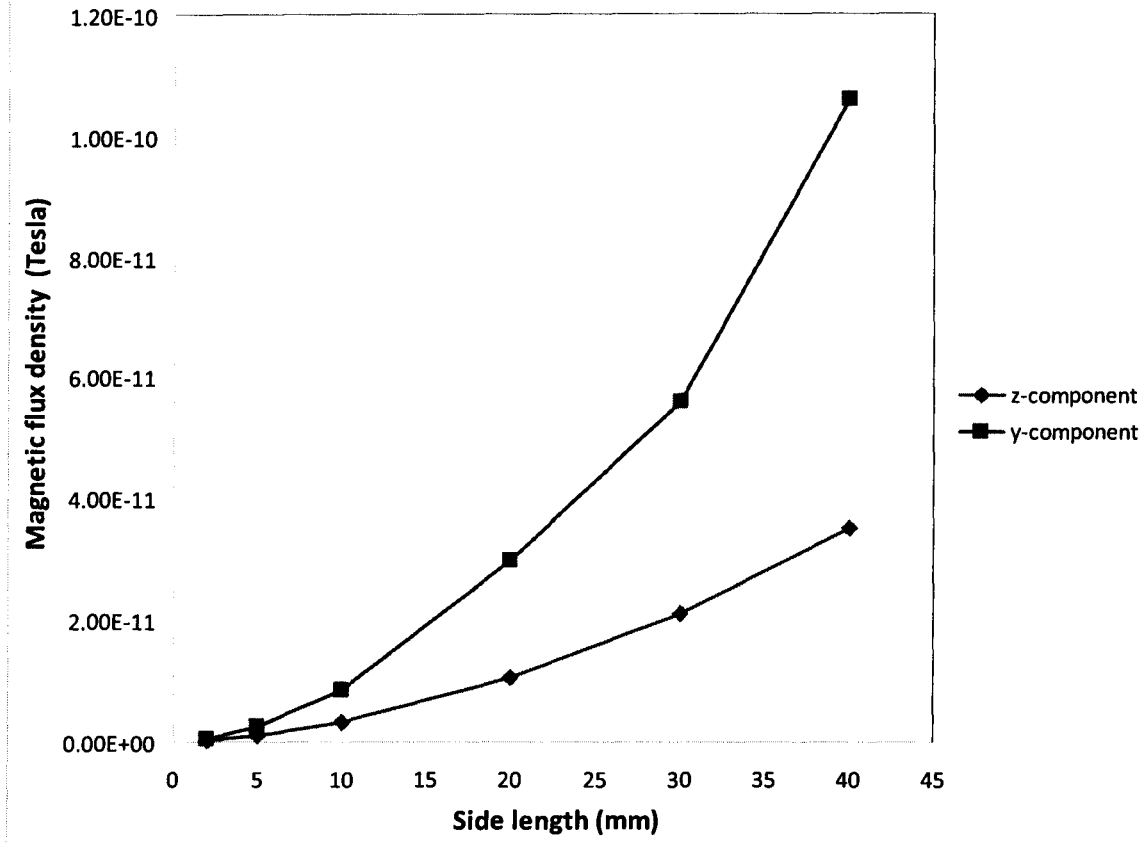


Figure 6.12: Y-component magnetic flux density in the zx-plane at  $y = 5 \text{ cm}$  ( $x = 0, z = 0$ ) from origin of isosceles triangular coils

The simulated magnetic flux densities appeared to level off at different values of leg-to-base ratio, when the base length was varied, for both z- and y-components. Next, the effect of increasing the length of the base side of the coil was to be modeled. By constructing an equilateral triangular coil with various side lengths, the magnetic flux density normal to the planes at the same above mentioned positions in the simulated space was modeled, as shown in Figure 6.13 below.



**Figure 6.13: Max magnetic flux density in the plane perpendicular to the axial component at 5 cm from origin of equilateral triangular coils.**

The simulation result indicated that as the leg-to-base ratio increased, the y-component of the resulting magnetic field at the vicinity of the origin behaved more similarly to a current dipole.

### 6.4 MEG Measurement using Triangular Coils

MEG data were recorded using triangular coils mounted on the plastic skull, as mentioned in the method above. The relative locations of the coils on the test skull are illustrated in Figure 6.14 below. Table 6.1 shows the measured dimensions of different triangular coils tested.

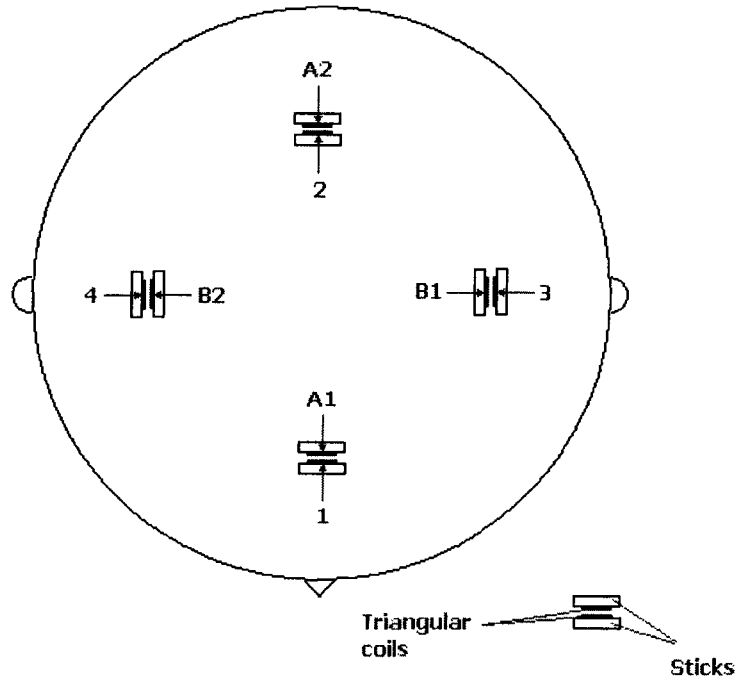


**Figure 6.14: Relative locations of the triangular coils on the head surface.**

**Table 6.1: Measured base and side lengths of different types of triangular coils used in the experiment.**

Coil	Base length (mm)	Side length (mm)
1, 2, 3, 4	7.0	7.0
A1, A2	4.9	13.5
B1, B2	3.8	13.5

The experimental conditions of a sequence of test cases using these triangular coils connected to the waveform generating circuit developed are recorded in Table 6.2. The same waveform and output resistance were used across these test cases.

**Table 6.2: Coils energized in different test cases in the experiment.**

Test case	Coils energized
1	1
2	A1
3	2
4	A2
5	1, 2
6	A1, A2
7	3, 4
8	B1, B2
9	1, 2, 3, 4
10	A1, B1, B2
11	1, 2, 3, 4, A1, A2, B1, B2

The actual locations of the MEG sensors are evenly distributed around the measured space, illustrated in Figure 6.15. Each channel consists of an inner sensor and an outer sensor.

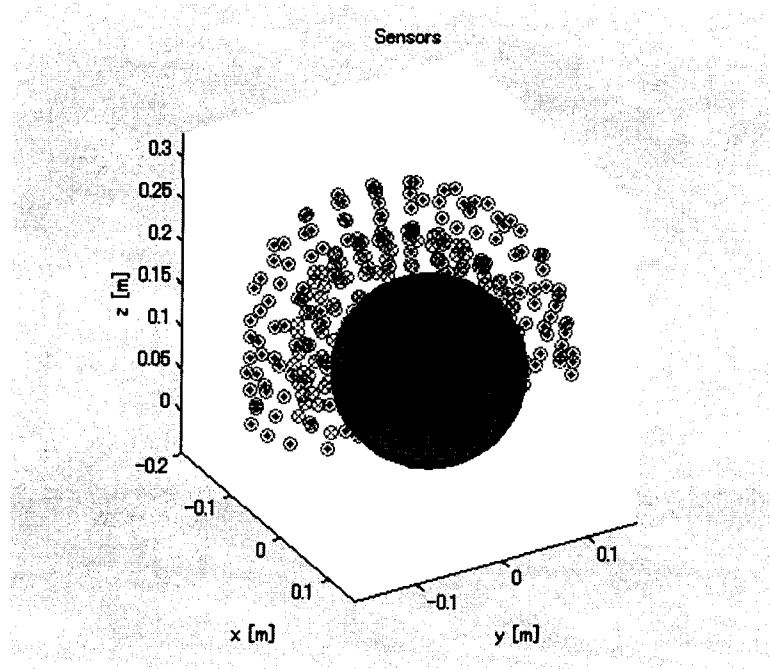


**Figure 6.15: Spatial distribution of sensors around the measured space, for a total of 151 channels, each having an inner and an outer sensors.**

The spatial distribution maps of measured magnetic fields at a particular time instance for different test cases are shown in Figure 6.16 below. In this case, time was equal to 1.1 seconds since the beginning of recording. The artifact of using a triangular coil to simulate a current dipole can be observed towards the back of the measuring space, as sensors were located more towards the posterior of the measuring cavity to cover the surface of occipital cortex. As indicated by COMSOL simulation in the previous section, a triangular coil produces a magnetic field, the pattern of which contains the characteristics of both a magnetic dipole and a current dipole.

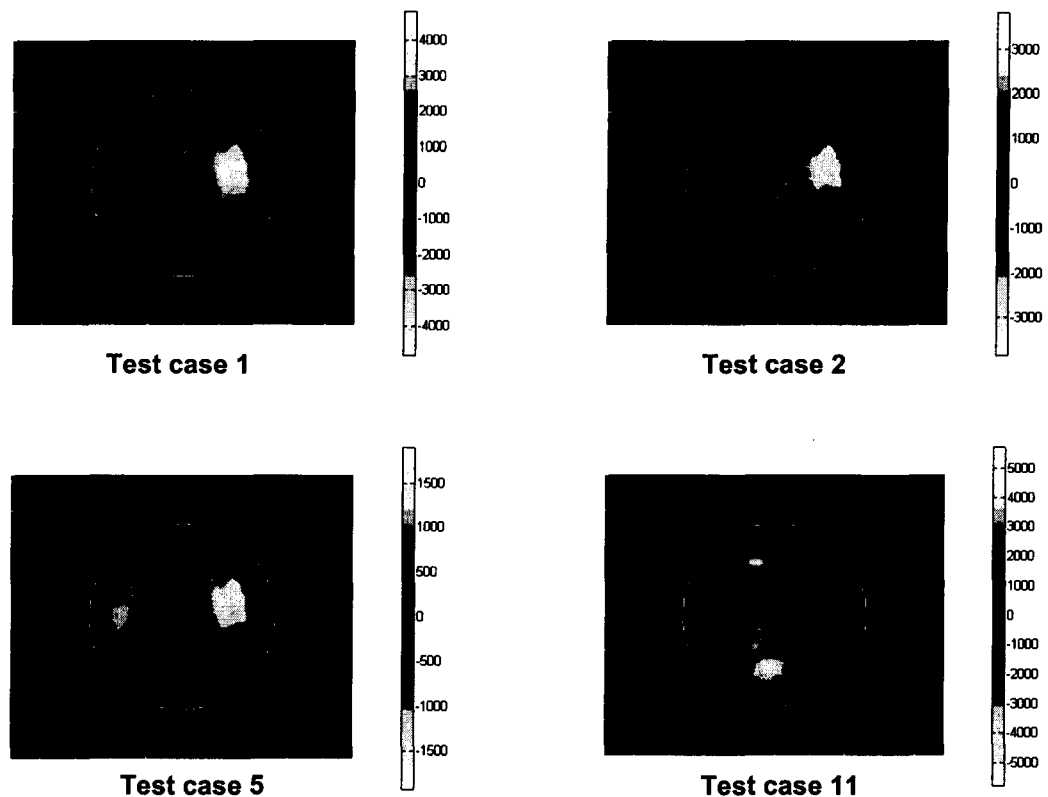
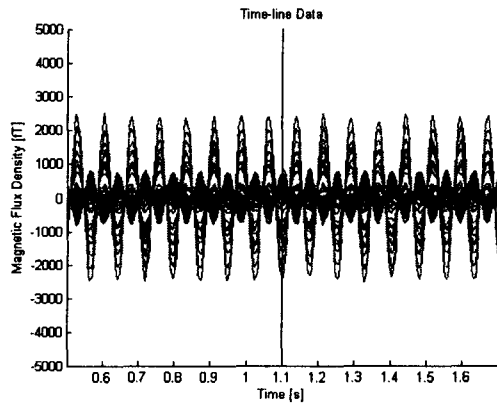
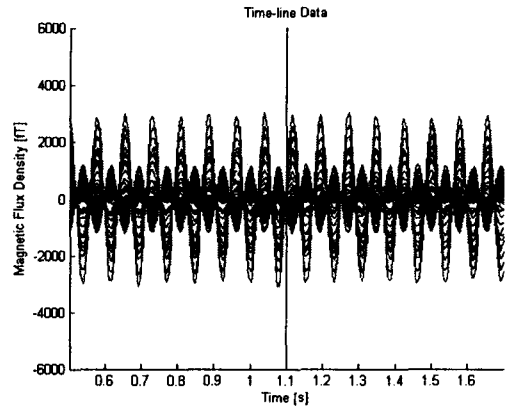


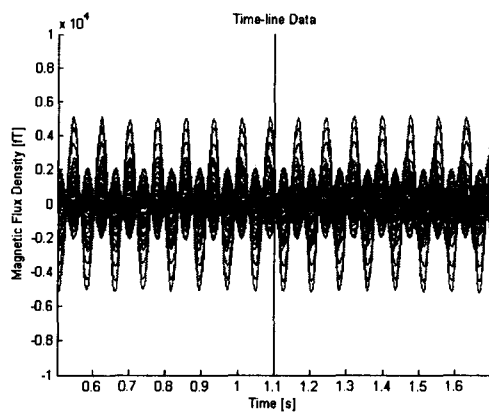
**Figure 6.16: Spatial magnetic flux density distribution of test cases 1, 2, 5, 11 at time equal to 1.1 seconds after the start of recording (Unit: fT).**



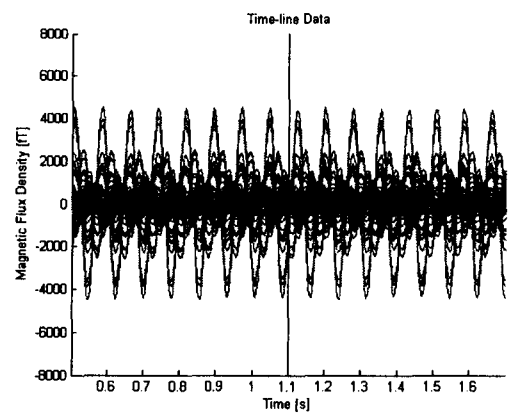
**Test case 1**



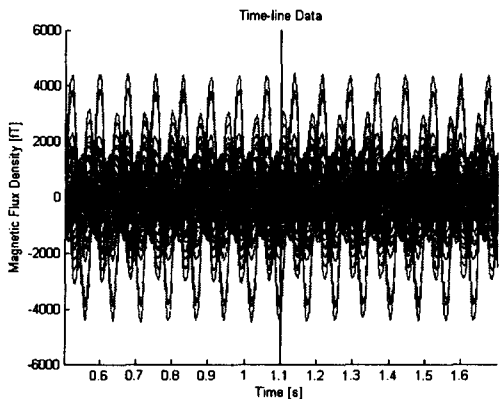
**Test case 2**



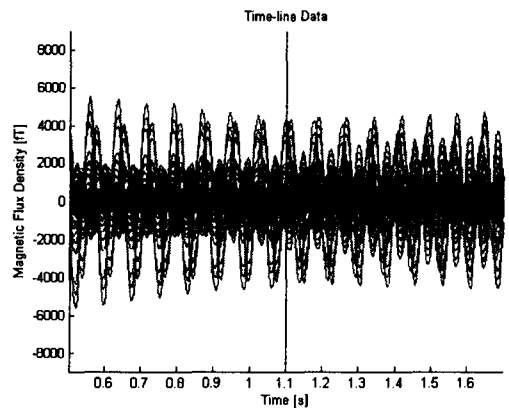
**Test case 7**



**Test case 8**



**Test case 10**



**Test case 11**

**Figure 6.17: AC component of the recorded magnetic flux densities on all channels for test cases 1, 2, 7, 8, 10, and 11.**

The AC components of the measured magnetic flux density with respect to time at different channels are shown in Figure 6.17 above. Excluding the DC

component allows the signals emitted by different sources to be more distinguishable.

Comparing the AC component of experimental magnetic flux density across test cases 1 and 2, 3 and 4, 7 and 8 reveals consistency between the simulated and experimental data of change in magnetic flux density with respect to the geometry change of the triangular coil. The increase in the recorded magnetic field complexity is observable, as the number of magnetic field sources increases. Also noticeable in the figure is the opposite magnetic field associated with the induced current on the other coil when only one single coil was energized, due to the arranged proximity in locations for each pair of coils. The resulting magnetic flux density and locations of dipoles obtained from each of the TSVD, data clustering, and downhill simplex computation inverse analysis steps for several experimental trials are illustrated sequentially in Figure 6.18 (See Appendix G for the inverse analysis results of the other test cases). The actual locations of the dipoles derived from the Polhemus measurement are also shown in the figure. It can be observed that the inversely mapped dipole locations converged more toward the actual locations after each subsequent step.

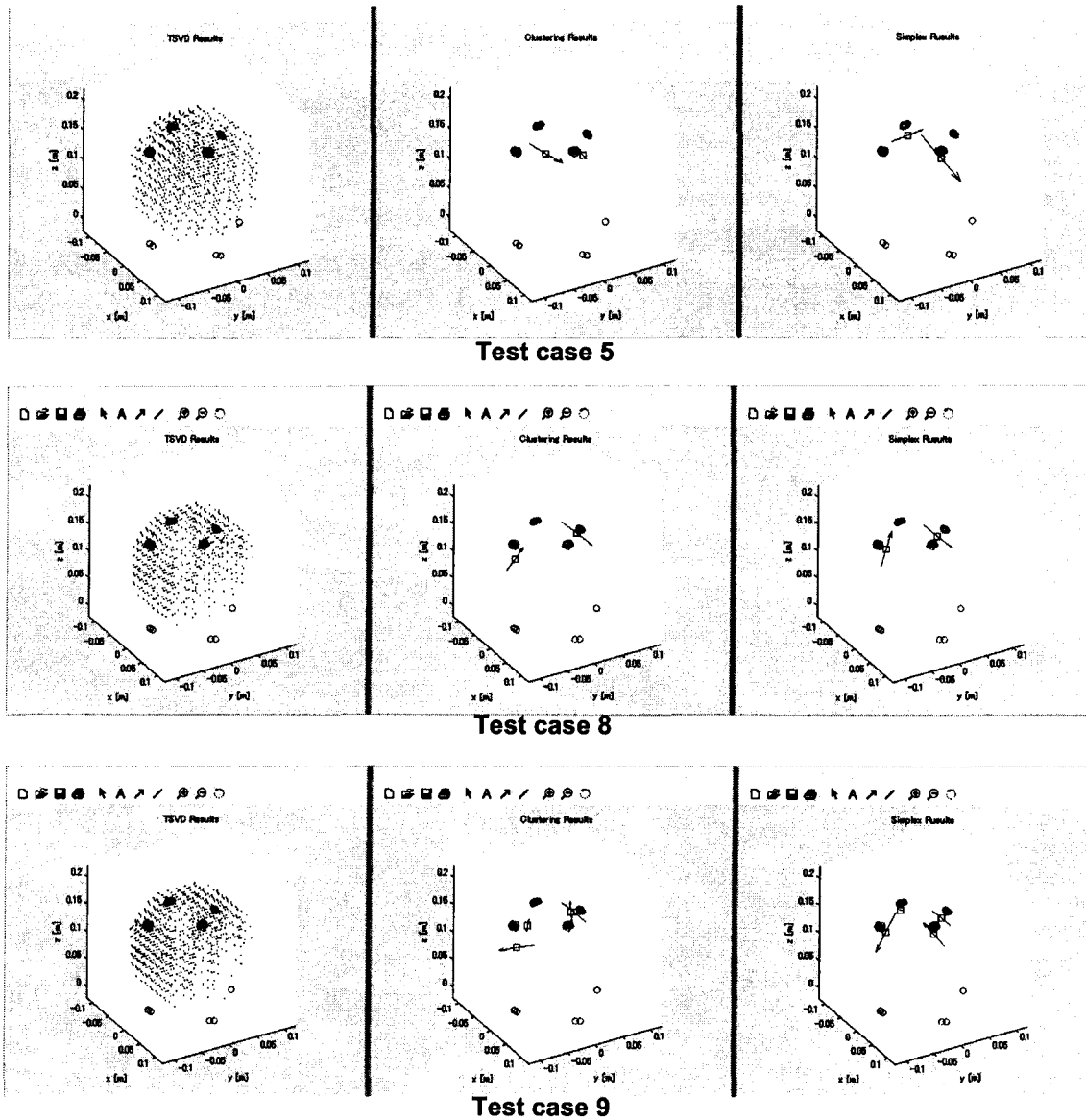


**Figure 6.18: Left – Resulting magnetic flux density distribution after TSVD; middle – Resulting dipole locations after data clustering; right – Adjusted dipole locations after downhill simplex computation of test cases 5, 8, and 9.**

The resulting dipole moments from inverse analysis for different test cases are listed in Table 6.3. The results were grouped into dipole numbers according to their associated coils. The orthogonality for each dipole across different test cases was also calculated. As shown by the table, the directionality of each individual inversely mapped dipole moment was fairly consistent across different



test cases. However, the analysis result exhibited a large variation in terms of the magnitude for the same dipole across different cases.

**Table 6.3: Resulting dipole moments for the dipole associated with each coil across different test cases from the inverse analysis and their correlation.**

Dipole	Test case	Dipole moment (nA·m <sup>2</sup> )				Orthogonality	
		x-comp	y-comp	z-comp	Magnitude	With test case	[a·b]/[ a  b ]
1	1	-11.4126	-2.64473	4.2279	12.4546045	5	-0.99712
	5	4.44082	0.694774	-1.79769	4.84100016	8	-0.99722
	8	-9.07006	-2.16781	3.86496	10.0947167	1	0.998896
2	3	9.08655	0.745644	4.78266	10.2953976	5	0.989986
	5	4.00989	0.247444	2.89069	4.94939744	8	0.968141
	8	2.25881	-0.25313	1.01386	2.48881679	3	0.982892
A1	2	9.99079	1.81074	-3.97841	10.9051552	6	0.997893
	6	13.8897	2.01862	-6.43405	15.4400645	9	0.996194
	9	12.0714	2.11669	-4.43003	13.031663	2	0.999632
A2	4	-15.3359	2.13292	-7.68465	17.2856305	6	-0.98913
	6	11.8206	-2.03927	8.30499	14.5896561	—	—
B1	7	-3.46474	4.62228	5.79692	8.18377524	9	-0.9823
	9	3.66125	-6.27462	-5.18878	8.92743219	—	—
B2	7	-0.54642	7.23373	-7.91303	10.7350581	9	0.998203
	9	-0.25029	2.21183	-2.17895	3.11490925	—	—
3	8	4.06249	-8.84695	-8.80414	13.1257469	—	—
4	8	0.485255	-5.99561	6.46891	8.83343695	—	—

## **7: CONCLUSION AND FUTURE WORK**

### **7.1 Conclusion**

Cognitive science and brain clinical research can benefit from MEG, provided that a reliable inverse analysis technique for localizing the active regions in the brain can be developed. A consistent electronic method was devised to provide the ground truth for the verification of a novel inverse analysis technique developed by attempting to physically simulate the magnetic fields emitted by active brain neurons. Moreover, the feasibility of using triangular coils to simulate current dipoles, which more faithfully represent neuronal activities, was also studied. Both simulation and experiment revealed that triangular coils with finite base lengths still produce magnetic field patterns of magnetic dipoles. Another drawback of using coils for emitting magnetic signal observed is the undesirable induction across coils of close spatial proximity. The inverse analysis method developed in association with the present study provided accurate estimate of the actual dipole location and directionality, while the consistency for estimating the dipole magnitude requires improvement.

### **7.2 Future Work**

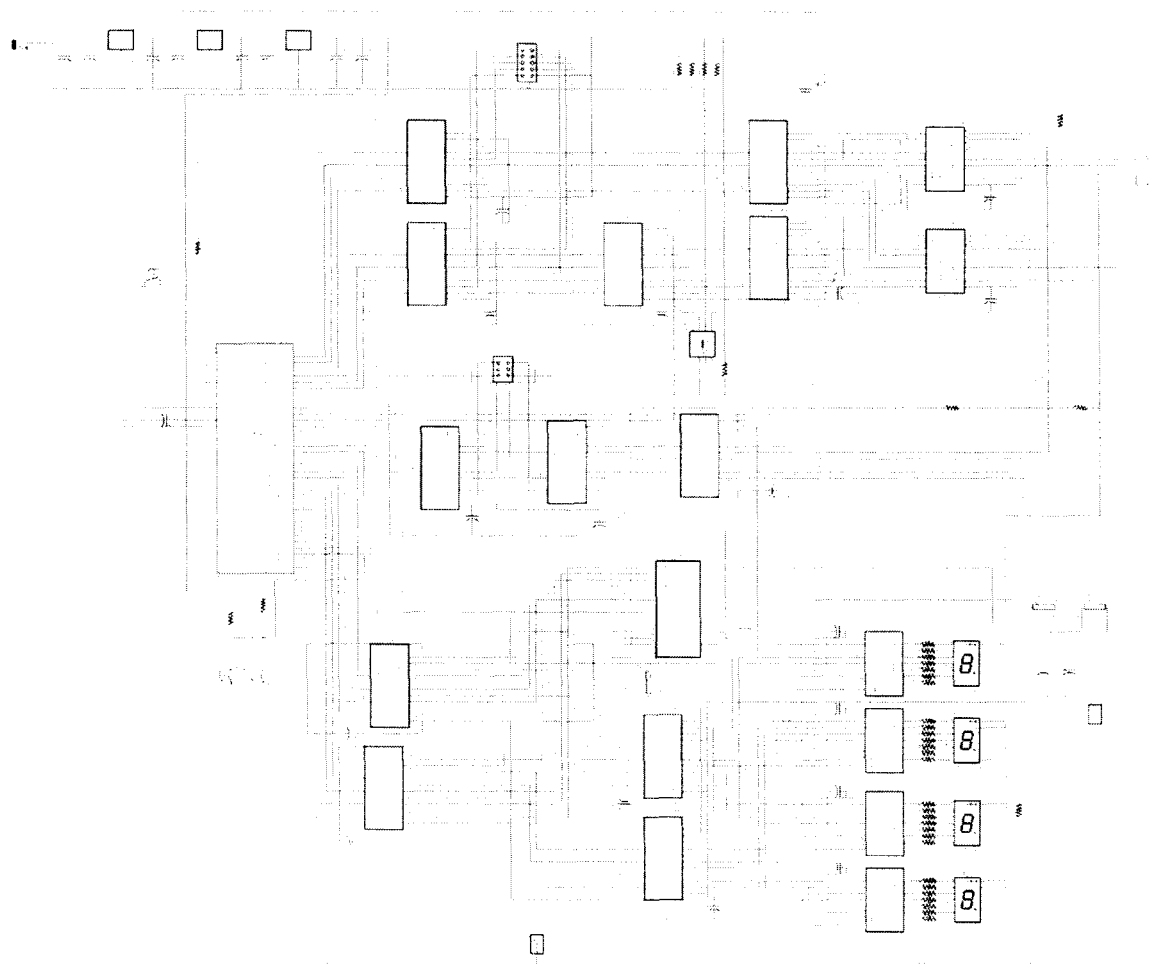
Using the signal generating mechanism developed in the present study, a more complex combination of signals across different sources can be devised in the next phase of inverse analysis method development. Moreover, the use of triangular coils with finite base lengths still does not truly simulate a current

dipole, which can more realistically model the ion exchange process in a cluster of active brain neuron than a magnetic dipole. A more sophisticated approach might involve the use of capacitive elements in the circuit to store charges until a controlled triggering event. How to avoid the interference of the generated signal due to the triggering mechanism is also subject to further study. In the electronics aspect, the method for emitting magnetic signal in the present study does not allow controllable synchronization of signals across different signal generating units. Having more synchronized signal across different sources might pose more challenge to the inverse analysis. The future aim is to allow the signal pattern resulting from the MEG recording of human subjects to be replicated on the signal-generating device before the spatial mapping of sources can be proceeded. A more finely calibrated spatial fixation of the coils is also subject to more development for any clinical purposes.

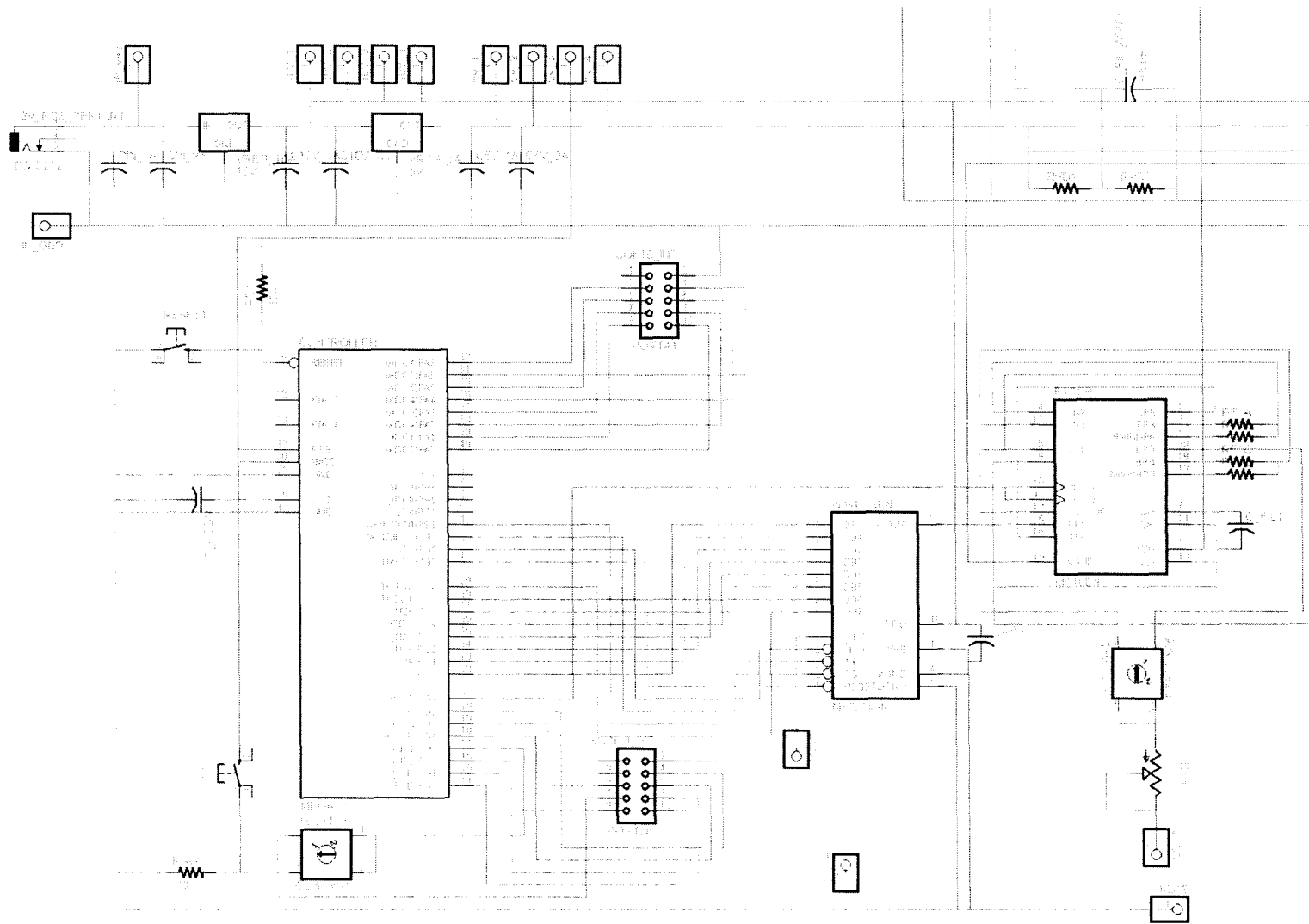
## **APPENDICES**

## Appendix A: Schematic Drawings

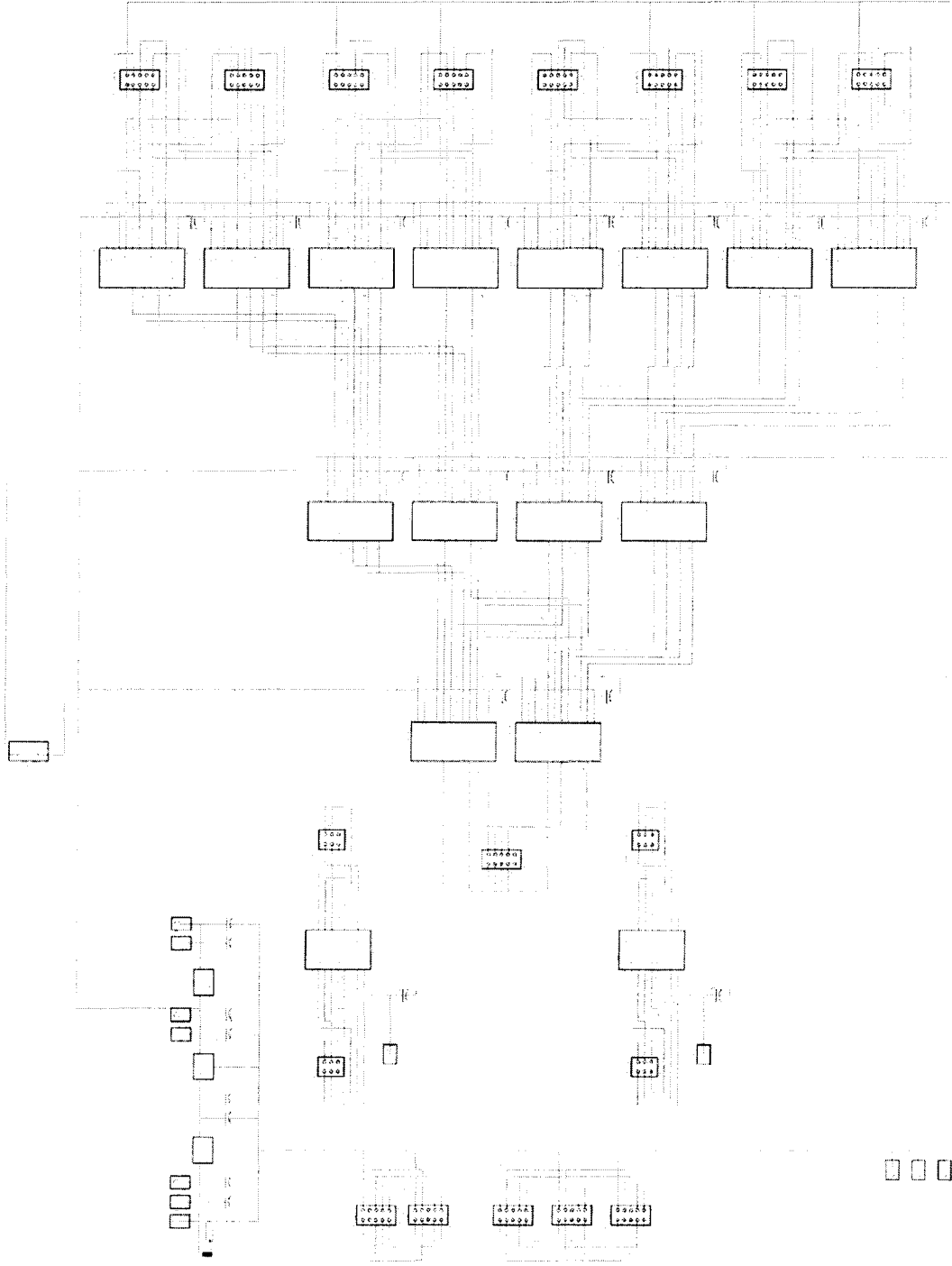
### Appendix A1: Schematic of standalone waveform-generating unit in previous implementation



**Appendix A2: Schematic drawing of waveform-generating unit developed for this thesis work**



**Appendix A3: Schematic drawing of the MUX/DeMUX circuit**



## Appendix B: Matlab Code for Waveform-composing GUI

Note: The following code should be saved as phantomGUI1.m in the same directory as the phantomGUI1.fig file and executed in Matlab program.

```
function varargout = phantomGUI1(varargin)
%PHANTOMGUI1 M-file for phantomGUI1.fig
%   PHANTOMGUI1, by itself, creates a new PHANTOMGUI1 or raises the existing
%   singleton*.
%
%   H = PHANTOMGUI1 returns the handle to a new PHANTOMGUI1 or the handle to
%   the existing singleton*.
%
%   PHANTOMGUI1('Property','Value',...) creates a new PHANTOMGUI1 using the
%   given property value pairs. Unrecognized properties are passed via
%   varargin to phantomGUI1_OpeningFcn. This calling syntax produces a
%   warning when there is an existing singleton*.
%
%   PHANTOMGUI1('CALLBACK') and PHANTOMGUI1('CALLBACK',hObject,...) call the
%   local function named CALLBACK in PHANTOMGUI1.M with the given input
%   arguments.
%
%   *See GUI Options on GUIDE's Tools menu. Choose "GUI allows only one
%   instance to run (singleton)".
%
% See also: GUIDE, GUIDATA, GUIHANDLES
% Created by Jeff Liu
% Last Modified by GUIDE v2.5 30-Nov-2010 14:39:56

% Begin initialization code - DO NOT EDIT
gui_Singleton = 1;
gui_State = struct('gui_Name',       mfilename, ...
                  'gui_Singleton',  gui_Singleton, ...
                  'gui_OpeningFcn', @phantomGUI1_OpeningFcn, ...
                  'gui_OutputFcn',  @phantomGUI1_OutputFcn, ...
                  'gui_LayoutFcn',  [], ...
                  'gui_Callback',    []);
if nargin && ischar(varargin{1})
    gui_State.gui_Callback = str2func(varargin{1});
end
if nargout
    [varargout{1:nargout}] = gui_mainfcn(gui_State, varargin{:});
else
    gui_mainfcn(gui_State, varargin{:});
end
% End initialization code - DO NOT EDIT
%=====
% --- Executes just before phantomGUI1 is made visible.
function phantomGUI1_OpeningFcn(hObject, eventdata, handles, varargin)
handles.output = hObject;
handles.Coeff = [];
handles.Comp = [];
% Data Structure:
% handles.Coeff = Channel 1: baseFreq, maxV, 3dB_Freq, numCoeff/32, Coeff(1), Coeff(2), Coeff(3), ...,
%                 Coeff(numCoeff)
%                 Channel 2: baseFreq, maxV, 3dB_Freq, numCoeff/32, Coeff(1), Coeff(2), Coeff(3), ...,
%                 Coeff(numCoeff)
%                 Channel 3: ...
%                 .
```



```

%
% Channel n:
% handles.Comp = Channel 1: Comp1_Amp, Comp1_Freq, Comp1_Phase, Comp1_ROD, Comp2_Amp,
Comp2_Freq, ..., Comp5_Phase, Comp5_ROD
% Channel 2: ...
%
%
%
guidata(hObject, handles); % Update handles structure
%=====
function varargout = phantomGUI1_OutputFcn(hObject, eventdata, handles)
varargout{1} = handles.output;
%=====
% This function responds to an input to the frequency edit box by checking
% the validity of the input value and displaying it.
function edit_freq_Callback(hObject, eventdata, handles)
handles_Val = handles.unitSelect;
val = get(handles_Val, 'Value');
handles_Val = handles.edit_freq;
input = str2num(get(hObject, 'String'));
%Input value limited from 0 to 255.
if (isempty(input) | (input<0) | (input>255))
    edit_Val = get(handles_Val, 'Value');
    set(hObject, 'String', edit_Val);
else
    handles.Coeff(val-1, 1) = input;
    set(handles_Val, 'Value', handles.Coeff(val-1, 1));
end
guidata(hObject, handles);
%=====
function edit_freq_CreateFcn(hObject, eventdata, handles)
if ispc
    set(hObject, 'BackgroundColor', 'white');
else
    set(hObject, 'BackgroundColor', get(0, 'defaultUicontrolBackgroundColor'));
end
%=====
% This function responds to an input to the max voltage edit box by checking
% the validity of the input value and displaying it.
function edit_maxV_Callback(hObject, eventdata, handles)
handles_Val = handles.unitSelect;
val = get(handles_Val, 'Value');
handles_Val = handles.edit_maxV;
input = str2num(get(hObject, 'String'));
%Input value limited from 0 to 10.0.
if (isempty(input) | (input<0.0) | (input>10.0))
    edit_Val = get(handles_Val, 'Value');
    set(hObject, 'String', edit_Val);
else
    handles.Coeff(val-1, 2) = input;
    set(handles_Val, 'Value', handles.Coeff(val-1, 2));
end
guidata(hObject, handles);
%=====
function edit_maxV_CreateFcn(hObject, eventdata, handles)
if ispc
    set(hObject, 'BackgroundColor', 'white');
else
    set(hObject, 'BackgroundColor', get(0, 'defaultUicontrolBackgroundColor'));
end
%=====
% This function responds to a selection of channel by displaying all
% coefficients and parameters of the newly selected channel.

```

```

function unitSelect_Callback(hObject, eventdata, handles)
val = get(hObject,'Value');
string_list = get(hObject,'String');
selected_string = string_list{val}; % convert from cell array
if (val ~= 1)
    numCoeff = 32*handles.Coeff(val-1,4);
    hObject = handles.CurNumSam;
    set(hObject,'String',num2str(numCoeff));
    x = 1:1:numCoeff;
    y = handles.Coeff(val-1,5:numCoeff+4);
    axes(handles.plot1)
    plot(x,y);
    handles_Val(1) = handles.Amp1;
    handles_Val(2) = handles.Freq1;
    handles_Val(3) = handles.Pha1;
    handles_Val(4) = handles.numPer1;
    handles_Val(5) = handles.Amp2;
    handles_Val(6) = handles.Freq2;
    handles_Val(7) = handles.Pha2;
    handles_Val(8) = handles.numPer2;
    handles_Val(9) = handles.Amp3;
    handles_Val(10) = handles.Freq3;
    handles_Val(11) = handles.Pha3;
    handles_Val(12) = handles.numPer3;
    handles_Val(13) = handles.Amp4;
    handles_Val(14) = handles.Freq4;
    handles_Val(15) = handles.Pha4;
    handles_Val(16) = handles.numPer4;
    handles_Val(17) = handles.Amp5;
    handles_Val(18) = handles.Freq5;
    handles_Val(19) = handles.Pha5;
    handles_Val(20) = handles.numPer5;
    handles_3dBFreq = handles.cutoffFreq;
    for i = 1:20
        set(handles_Val(i),'Value',handles.Comp(val-1,i));
        cellVal = get(handles_Val(i),'Value');
        hObject = handles_Val(i);
        set(hObject,'String',cellVal);
    end
    set(handles_3dBFreq,'Value',handles.Coeff(val-1,3));
    cellVal = get(handles_3dBFreq,'Value');
    hObject = handles_3dBFreq;
    set(hObject,'String',cellVal);
    handles_Val(1) = handles.edit_freq;
    handles_Val(2) = handles.edit_maxV;
    for i = 1:2
        set(handles_Val(i),'Value',handles.Coeff(val-1,i));
        cellVal = get(handles_Val(i),'Value');
        hObject = handles_Val(i);
        set(hObject,'String',cellVal);
    end
end
guidata(hObject, handles); %updates the handles
%=====
function unitSelect_CreateFcn(hObject, eventdata, handles)
if ispc
    set(hObject,'BackgroundColor','white');
else
    set(hObject,'BackgroundColor',get(0,'defaultUicontrolBackgroundColor'));
end
%=====
function typeSelect_Callback(hObject, eventdata, handles)

```

```

%=====
function typeSelect_CreateFcn(hObject, eventdata, handles)
if ispc
    set(hObject,'BackgroundColor','white');
else
    set(hObject,'BackgroundColor',get(0,'defaultUicontrolBackgroundColor'));
end
%=====
function numSelect_Callback(hObject, eventdata, handles)
%=====
function numSelect_CreateFcn(hObject, eventdata, handles)
if ispc
    set(hObject,'BackgroundColor','white');
else
    set(hObject,'BackgroundColor',get(0,'defaultUicontrolBackgroundColor'));
end
%=====
% This function responds to when the Reload button is pushed by retrieving
% the data with the corresponding file name stored in a specific sequence.
function Reload_Callback(hObject, eventdata, handles)
handles.Coeff = csvread('testData2_Coeff.dat');
handles.Comp = csvread('testData2_Comp.dat');
menuHandle = handles.unitSelect;
set(menuHandle,'Value',1);
menuHandle = handles.typeSelect;
set(menuHandle,'Value',1);
menuHandle = handles.samSelect;
set(menuHandle,'Value',1);
guidata(hObject,handles);
%=====
% This function responds to when the Save button is pushed by storing
% the data with the corresponding file name stored in a specific sequence.
function Save_Callback(hObject, eventdata, handles)
csvwrite('testData2_Coeff.dat',handles.Coeff);
csvwrite('testData2_Comp.dat',handles.Comp);
%=====
% This function responds to when the Generate button is pushed by
% generating a series of coefficients with specified parameters for a given
% channel and displaying the resulting waveform.
function Generate_Callback(hObject, eventdata, handles)
contHandles = handles.unitSelect;
unitItem = get(contHandles,'Value');
contHandles = handles.typeSelect;
typeItem = get(contHandles,'Value');
contHandles = handles.samSelect;
samItem = get(contHandles,'Value');
contHandles = handles.numSelect;
numItem = get(contHandles,'Value');
if (samItem == 2)
    numCoeff = 64;
elseif (samItem == 3)
    numCoeff = 128;
elseif (samItem == 4)
    numCoeff = 192;
elseif (samItem == 5)
    numCoeff = 256;
elseif (samItem == 6)
    numCoeff = 384;
elseif (samItem == 7)
    numCoeff = 512;
end
if (unitItem ~= 1 & samItem ~= 1 & numItem ~= 1)

```

```

handles.Coeff(unitItem-1,4) = numCoeff/32;
x = (pi/numCoeff):(pi/(numCoeff/2)):(2*pi-(pi/numCoeff));
for i = 1:(numItem-1)
    A(i,:) = handles.Comp(unitItem-1,4*i-3:4*i);
end
if (typeItem == 1)
    y = handles.Coeff(unitItem-1,5:numCoeff+4);
elseif (typeItem == 2)
    [baseFreq,ind] = min(A(1:numItem-1,2));
    if (A(ind,4) ~= 1)
        A(ind,4) == 1;
    end
    for i = 1:(numItem-1)
        if ((A(i,4)>(A(i,2)/baseFreq)) | (A(i,4)==0))
            A(i,4) = (A(i,2)/baseFreq);
        end
        yComp(i,1:A(i,4)*numCoeff*baseFreq/A(i,2)) =
uint8(((sin(x(1:numCoeff*A(i,4)*baseFreq/A(i,2))*A(i,2)/baseFreq+2*pi*A(i,3)/360)+1)/2).*A(i,1));
        yComp(i,A(i,4)*numCoeff*baseFreq/A(i,2)+1:numCoeff) = A(i,1)/2;
        %yComp(i,:) = uint8(((sin(x*A(i,2)/baseFreq+2*pi*A(i,3)/360)+1)/2).*A(i,1));
        %yComp(i,:) = uint8(((sin(x*A(i,2)/baseFreq)+1)/2)*A(i,1));
    end
    y = sum(yComp,1);
    [topFreq,ind] = max(A(1:numItem-1,2));
    contHandles = handles.decay1;
    decayVal = get(contHandles,'Value');
    range = max(y);
    for i = 1:numCoeff
        y(1,i) = uint8((y(1,i)-range/2)*exp((decayVal*i*topFreq)/(numCoeff*baseFreq))+range/2);
    end
elseif (typeItem == 3)
    [baseFreq,ind] = min(A(1:numItem-1,2));
    for i = 1:(numItem-1)
        for j = 1:2:(2*A(i,2)/baseFreq)-1
            for k = 1:numCoeff*baseFreq/(2*A(i,2))
                yTemp(((numCoeff*baseFreq*(j-1))/(2*A(i,2)))+k) = (A(i,1)*A(i,2)/(numCoeff*baseFreq/2))^k - 1;
                yTemp(((numCoeff*baseFreq*j)/(2*A(i,2)))+k) = A(i,1) -
(A(i,1)*A(i,2)/(numCoeff*baseFreq/2))^(k-1) - 1;;
                %yComp(i,((numCoeff*baseFreq*(j-1))/(2*A(i,2)))+1:((numCoeff*baseFreq*j)/(2*A(i,2)))) =
(256*A(i,2)/(numCoeff*baseFreq/2))^i - 1;
                %yComp(i,((numCoeff*baseFreq*j)/(2*A(i,2)))+1:((numCoeff*baseFreq*(j+1))/(2*A(i,2)))) = 256 -
(256/(numCoeff/2))^(i-((numCoeff/2)+1)) - 1;;
            end
        end
        yComp(i,1:numCoeff-(numCoeff*baseFreq*A(i,3)/(360*A(i,2)))) =
yTemp((numCoeff*baseFreq*A(i,3)/(360*A(i,2)))+1:numCoeff);
        yComp(i,numCoeff-(numCoeff*baseFreq*A(i,3)/(360*A(i,2)))+1:numCoeff) =
yTemp(1:(numCoeff*baseFreq*A(i,3)/(360*A(i,2))));
    end
    y = uint8(sum(yComp,1));
elseif (typeItem == 4)
    [baseFreq,ind] = min(A(1:numItem-1,2));
    for i = 1:(numItem-1)
        for j = 1:2:(2*A(i,2)/baseFreq)-1
            %yComp(i,((numCoeff*baseFreq*(j-1))/(2*A(i,2)))+1:((numCoeff*baseFreq*j)/(2*A(i,2)))) = A(i,1);
            %yComp(i,((numCoeff*baseFreq*j)/(2*A(i,2)))+1:((numCoeff*baseFreq*(j+1))/(2*A(i,2)))) = 0;
            yTemp(((numCoeff*baseFreq*(j-1))/(2*A(i,2)))+1:((numCoeff*baseFreq*j)/(2*A(i,2)))) = A(i,1);
            yTemp(((numCoeff*baseFreq*j)/(2*A(i,2)))+1:((numCoeff*baseFreq*(j+1))/(2*A(i,2)))) = 0;
        end
        yComp(i,1:numCoeff-(numCoeff*baseFreq*A(i,3)/(360*A(i,2)))) =
yTemp((numCoeff*baseFreq*A(i,3)/(360*A(i,2)))+1:numCoeff);

```

```

        yComp(i,numCoeff-(numCoeff*baseFreq*A(i,3)/(360*A(i,2)))+1:numCoeff) =
yTemp(1:(numCoeff*baseFreq*A(i,3)/(360*A(i,2))));
    end
    y = uint8(sum(yComp, 1));
elseif (typeltem == 5)
    y = uint8(rand(1,numCoeff).*255);
else
end
x = 1:1:numCoeff;
handles.Coeff(unitItem-1,5:numCoeff+4) = y;
axes(handles.plot1)
if ((typeltem == 1) | (typeltem == 5))
    plot(x,y);
else
    if numItem == 2
        plot(x,yComp(1,:),'g',x,y,'b');
    elseif numItem == 3
        plot(x,yComp(1,:),'g',x,yComp(2,:),'y',x,y,'b');
    elseif numItem == 4
        plot(x,yComp(1,:),'g',x,yComp(2,:),'y',x,yComp(3,:),'m',x,y,'b');
    elseif numItem == 5
        plot(x,yComp(1,:),'g',x,yComp(2,:),'y',x,yComp(3,:),'m',x,yComp(4,:),'c',x,y,'b');
    elseif numItem == 6
        plot(x,yComp(1,:),'g',x,yComp(2,:),'y',x,yComp(3,:),'m',x,yComp(4,:),'c',x,yComp(5,:),'r',x,y,'b');
    end
end
hObject = handles.CurNumSam;
set(hObject,'String',num2str(numCoeff));
elseif (unitItem ~= 1 & samItem ~= 1 & numItem == 1)
handles.Coeff(unitItem-1,4) = numCoeff/32;
x = (pi/numCoeff):(pi/(numCoeff/2)):(2*pi-(pi/numCoeff));
if (typeltem == 1)
    y = handles.Coeff(unitItem-1,5:numCoeff+4);
elseif (typeltem == 2)
    y = uint8(((sin(x)+1)/2).*255);
elseif (typeltem == 3)
    for i = 1:numCoeff/2
        y(i) = (256/(numCoeff/2))^i - 1;
    end
    for i = (numCoeff/2)+1:numCoeff
        y(i) = 256 - (256/(numCoeff/2))^(i-((numCoeff/2)+1)) - 1;
    end
elseif (typeltem == 4)
    y(1:(numCoeff/2)) = 255;
    y((numCoeff/2)+1:numCoeff) = 0;
elseif (typeltem == 5)
    y = uint8(rand(1,numCoeff).*255);
else
end
x = 1:1:numCoeff;
handles.Coeff(unitItem-1,5:numCoeff+4) = y;
axes(handles.plot1)
plot(x,y);
hObject = handles.CurNumSam;
set(hObject,'String',num2str(numCoeff));
end
guidata(hObject,handles);
%=====
function samSelect_Callback(hObject, eventdata, handles)
%=====
function samSelect_CreateFcn(hObject, eventdata, handles)
if ispc

```

```

        set(hObject,'BackgroundColor','white');
    else
        set(hObject,'BackgroundColor',get(0,'defaultUicontrolBackgroundColor'));
    end
    %=====
    % This function responds to when a specific coefficient number is selected
    % by highlighting the coefficient selected on the waveform displayed in
    % red. The selected coefficient number should be between 1 and the total
    % number of samples used.
    function samNum_Callback(hObject, eventdata, handles)
    handles_Val = handles.unitSelect;
    unitItem = get(handles_Val,'Value');
    handles_Val = handles.samNum;
    input = uint16(str2num(get(hObject,'String')));
    %Input value limited from 1 to the total number of sample points.
    if (unitItem ~= 1)
        numSam = 32*handles.Coeff(unitItem-1,4);
        if (isempty(input) | (input<1) | (input>numSam))
            edit_Val = get(handles_Val,'Value');
            set(hObject,'String',edit_Val);
        else
            set(handles_Val,'Value',input);
            handles_Val = handles.samVal;
            set(handles_Val,'Value',handles.Coeff(unitItem-1,input+4));
            hObject = handles_Val;
            set(hObject,'String',handles.Coeff(unitItem-1,input+4));
            %plots the waveform with the specified point highlighted
            %x = 0:(pi/(numSam/2)):((numSam-1)*pi/(numSam/2));
            x = 1:1:numSam;
            y = handles.Coeff(unitItem-1,5:numSam+4);
            axes(handles.plot1)
            %plots the x and y data of selected sample point in red
            plot(x,y,x(input),y(input),'r');
        end
    end
    guidata(hObject, handles);
    %=====
    function samNum_CreateFcn(hObject, eventdata, handles)
    if ispc
        set(hObject,'BackgroundColor','white');
    else
        set(hObject,'BackgroundColor',get(0,'defaultUicontrolBackgroundColor'));
    end
    %=====
    % This function responds to when the value of a selected coefficient number
    % is modified by checking the validity of input value, storing and
    % displaying the new value on the waveform in red.
    function samVal_Callback(hObject, eventdata, handles)
    handles_Val = handles.unitSelect;
    unitItem = get(handles_Val,'Value');
    handles_Val = handles.samVal;
    input = uint8(str2num(get(hObject,'String')));
    %Input value ranges from 0 to 255 (byte).
    if (unitItem ~= 1)
        numSam = 32*handles.Coeff(unitItem-1,4);
        if (isempty(input) | (input<0) | (input>255))
            edit_Val = get(handles_Val,'Value');
            set(hObject,'String',edit_Val);
        else
            handles_Val = handles.samNum;
            edit_Val = get(handles_Val,'Value');
            handles.Coeff(unitItem-1,edit_Val+4) = input;
        end
    end
end

```

```

handles_Val = handles.samVal;
set(handles_Val,'Value',input);
set(hObject,'String',input);
%plots the waveform with the specified point highlighted
%x = 0:(pi/(numSam/2)):((numSam-1)*pi/(numSam/2));
x = 1:1:numSam;
y = handles.Coeff(unitItem-1,5:numSam+4);
axes(handles.plot1)
%plots the x and y data of selected sample point in red
plot(x,y,x(edit_Val),y(edit_Val),'*r');
end
end
guidata(hObject, handles);
%=====
function samVal_CreateFcn(hObject, eventdata, handles)
if ispc
    set(hObject,'BackgroundColor','white');
else
    set(hObject,'BackgroundColor',get(0,'defaultUicontrolBackgroundColor'));
end
%=====
% This function responds to when the value of the filter cutoff frequency
% is modified by checking the validity of input value and storing the new
% value. The resulting value would be the stored value multiplied by 5.
function cutoffFreq_Callback(hObject, eventdata, handles)
handles_Val = handles.unitSelect;
unitItem = get(handles_Val,'Value');
handles_Val = handles.cutoffFreq;
input = uint8(str2num(get(hObject,'String')));
%Input value ranges from 0 to 100.
if (unitItem ~= 1)
    if (isempty(input) | (input<0) | (input>100))
        edit_Val = get(handles_Val,'Value');
        set(hObject,'String',edit_Val);
    else
        handles.Coeff(unitItem-1,3) = input;
        set(handles_Val,'Value',handles.Comp(unitItem-1,3));
    end
end
end
guidata(hObject, handles);
%=====
function cutoffFreq_CreateFcn(hObject, eventdata, handles)
if ispc
    set(hObject,'BackgroundColor','white');
else
    set(hObject,'BackgroundColor',get(0,'defaultUicontrolBackgroundColor'));
end
%=====
% This function responds to when the value of waveform decay is modified by
% checking the validity of input value and storing the new value. The value
% is used for calculating the exponent of a exponential decay function. -1
% represents the max decay rate and 0 represents no decay.
function decay1_Callback(hObject, eventdata, handles)
handles_Val = handles.unitSelect;
unitItem = get(handles_Val,'Value');
handles_Val = handles.decay1;
input = str2num(get(hObject,'String'));
%Input value should be between -1 and 0 (double).
if (unitItem ~= 1)
    if (isempty(input) | (input<-1) | (input>0))
        edit_Val = get(handles_Val,'Value');
        set(hObject,'String',edit_Val);
    end
end
end

```

```

        else
            set(handles_Val,'Value',input);
        end
    end
end
guidata(hObject, handles);
%=====
function decay1_CreateFcn(hObject, eventdata, handles)
if ispc
    set(hObject,'BackgroundColor','white');
else
    set(hObject,'BackgroundColor',get(0,'defaultUicontrolBackgroundColor'));
end
set(hObject,'Value',0);
set(hObject,'String',0);
guidata(hObject, handles);
%=====
% This parameter governs the amplitude of component 1.
function Amp1_Callback(hObject, eventdata, handles)
handles_Val = handles.unitSelect;
unitItem = get(handles_Val,'Value');
handles_Val = handles.Amp1;
input = uint8(str2num(get(hObject,'String')));
%Input value should be between 0 and 50 for each component.
if (unitItem ~= 1)
    if (isempty(input) | (input<0) | (input>50))
        %set(hObject,'String','0')
        edit_Val = get(handles_Val,'Value');
        set(hObject,'String',edit_Val);
    else
        handles.Comp(unitItem-1,1) = input;
        set(handles_Val,'Value',handles.Comp(unitItem-1,1));
    end
end
guidata(hObject, handles);
%=====
function Amp1_CreateFcn(hObject, eventdata, handles)
if ispc
    set(hObject,'BackgroundColor','white');
else
    set(hObject,'BackgroundColor',get(0,'defaultUicontrolBackgroundColor'));
end
%=====
% This parameter governs the frequency of component 1.
function Freq1_Callback(hObject, eventdata, handles)
handles_Val = handles.unitSelect;
unitItem = get(handles_Val,'Value');
handles_Val = handles.Freq1;
input = uint8(str2num(get(hObject,'String')));
%Input value should be between 1 and 200 for each component.
if (unitItem ~= 1)
    if (isempty(input) | (input<1) | (input>200))
        %set(hObject,'String','0')
        edit_Val = get(handles_Val,'Value');
        set(hObject,'String',edit_Val);
    else
        handles.Comp(unitItem-1,2) = input;
        set(handles_Val,'Value',handles.Comp(unitItem-1,2));
    end
end
end
guidata(hObject, handles);
%=====
function Freq1_CreateFcn(hObject, eventdata, handles)

```



```

if ispc
    set(hObject,'BackgroundColor','white');
else
    set(hObject,'BackgroundColor',get(0,'defaultUicontrolBackgroundColor'));
end
end
%=====
% This parameter governs the phase delay of component 1.
function Pha1_Callback(hObject, eventdata, handles)
handles_Val = handles.unitSelect;
unitItem = get(handles_Val,'Value');
handles_Val = handles.Pha1;
input = uint8(str2num(get(hObject,'String')));
%Input value should be between 0 and 360 for each component.
if (unitItem ~= 1)
    if (isempty(input) | (input<0) | (input>360))
        %set(hObject,'String','0')
        edit_Val = get(handles_Val,'Value');
        set(hObject,'String',edit_Val);
    else
        handles.Comp(unitItem-1,3) = input;
        set(handles_Val,'Value',handles.Comp(unitItem-1,3));
    end
end
end
guidata(hObject, handles);
%=====
function Pha1_CreateFcn(hObject, eventdata, handles)
if ispc
    set(hObject,'BackgroundColor','white');
else
    set(hObject,'BackgroundColor',get(0,'defaultUicontrolBackgroundColor'));
end
end
%=====
% This parameter governs the rate of decay of component 1.
function RofDecay1_Callback(hObject, eventdata, handles)
handles_Val = handles.unitSelect;
unitItem = get(handles_Val,'Value');
handles_Val = handles.RofDecay1;
input = str2num(get(hObject,'String'));
%Input value should be between -1 and 0 (double) for each component.
if (unitItem ~= 1)
    if (isempty(input) | (input<-1) | (input>0))
        edit_Val = get(handles_Val,'Value');
        set(hObject,'String',edit_Val);
    else
        handles.Comp(unitItem-1,4) = input;
        set(handles_Val,'Value',handles.Comp(unitItem-1,4));
    end
end
end
guidata(hObject, handles);
%=====
function RofDecay1_CreateFcn(hObject, eventdata, handles)
if ispc
    set(hObject,'BackgroundColor','white');
else
    set(hObject,'BackgroundColor',get(0,'defaultUicontrolBackgroundColor'));
end
end
%=====
% Note: The same sets of function calls for controlling the parameters of
% components 2 to 5 are not shown.

```

## Appendix C: C++ Code for Interactive Host GUI

Note: The following code should be saved as `UsbHidDemoCodeDlg.cpp` to replace the file with the same name and compiled together with modified `UsbHidDemoCode.rc`, `UsbHidDemoCodeDlg.h`, and `resource.h` files in the `UsbHidDemoCode` project provided by Atmel®

```
// UsbHidDemoCodeDlg.cpp : implementation file
//
// This program has been modified by Jeff to accommodate functions required for
// implementing the interactive GUI for Phantom host PC using the functions of
// the AtUsbHid library. The library functions prototypes can be found in the
// last part of the AtUsbHid.h file.
#include "stdafx.h"
#include "UsbHidDemoCode.h"
#include "UsbHidDemoCodeDlg.h"
#include <winuser.h>
#include <windows.h>
#include <dbt.h>
#ifdef _DEBUG
#define new DEBUG_NEW
#undef THIS_FILE
static char THIS_FILE[] = __FILE__;
#endif
// Include Atmel Hid Usb
#include "AtUsbHid.h"
#define DEFAULT_VID 0x03EB
#define DEFAULT_PID 0x2013
#define DEFAULT_UNIT 1
// Global variables for storing the data structure
int coeffArray[8][516];
short totPckt,pcktNum,curUnit;
bool morePckt;
const short totNumPoints = 2000;
/*-----*/
FUNCTION: handleError
PURPOSE: Call when an error is return by a function call
PARAMETERS: DWORD errorCode - error code that represent the error
COMMENTS: Modified for Phantom project
/*-----*/
void handleError(DWORD errorCode)
{
    switch(errorCode)
    {
        case ERROR_MOD_NOT_FOUND:
            AfxMessageBox( "Could not find Atmel USB HID DLL: AtUsbHid.dll\nPlease update the
            PATH variable.\n", MB_ICONSTOP,0);
            exit(-1);
            break;
        case ERROR_USB_DEVICE_NOT_FOUND:
            OutputDebugString("Error: Could not open the device.\n");
            break;
        case ERROR_USB_DEVICE_NO_CAPABILITIES:
            OutputDebugString("Error: Could not get USB device capabilities.\n");
            break;
        case ERROR_WRITE_FAULT:
    }
}
```

```

        OutputDebugString("Error: Could not write.\n");
        break;
    case ERROR_READ_FAULT:
        OutputDebugString("Error: Could not read.\n");
        break;
    default:
        OutputDebugString("Error: Unknown error code.\n");
    }
}
///////////////////////////////////////////////////////////////////
// CAboutDlg dialog used for App About
class CAboutDlg : public CDialog
{
public:
    CAboutDlg();
// Dialog Data
    ///{AFX_DATA(CAboutDlg)
    enum { IDD = IDD_ABOUTBOX };
    ///}AFX_DATA
    // ClassWizard generated virtual function overrides
    ///{AFX_VIRTUAL(CAboutDlg)
    protected:
    virtual void DoDataExchange(CDataExchange* pDX); // DDX/DDV support
    ///}AFX_VIRTUAL
// Implementation
protected:
    ///{AFX_MSG(CAboutDlg)
    ///}AFX_MSG
    DECLARE_MESSAGE_MAP()
};
CAboutDlg::CAboutDlg() : CDialog(CAboutDlg::IDD)
{
    ///{AFX_DATA_INIT(CAboutDlg)
    ///}AFX_DATA_INIT
}
void CAboutDlg::DoDataExchange(CDataExchange* pDX)
{
    CDialog::DoDataExchange(pDX);
    ///{AFX_DATA_MAP(CAboutDlg)
    ///}AFX_DATA_MAP
}
BEGIN_MESSAGE_MAP(CAboutDlg, CDialog)
    ///{AFX_MSG_MAP(CAboutDlg)
    // No message handlers
    ///}AFX_MSG_MAP
END_MESSAGE_MAP()
/////////////////////////////////////////////////////////////////
// CUsbHidDemoCodeDlg dialog
CUsbHidDemoCodeDlg::CUsbHidDemoCodeDlg(CWnd* pParent /*=NULL*/)
: CDialog(CUsbHidDemoCodeDlg::IDD, pParent)
{
    ///{AFX_DATA_INIT(CUsbHidDemoCodeDlg)
    m_PID = _T("2013");
    m_VID = _T("03EB");
    m_UNIT = 1;
    ///}AFX_DATA_INIT
    // Note that LoadIcon does not require a subsequent DestroyIcon in Win32
    m_hIcon = AfxGetApp()->LoadIcon(IDR_MAINFRAME);
}
void CUsbHidDemoCodeDlg::DoDataExchange(CDataExchange* pDX)
{
    CDialog::DoDataExchange(pDX);
}

```

```

//{{AFX_DATA_MAP(CUsbHidDemoCodeDlg)
DDX_Control(pDX, IDC_SetFreq, m_SetFreq);
DDX_Control(pDX, IDC_RELOAD, m_Reload);
DDX_Control(pDX, IDC_STOP, m_Stop);
DDX_Control(pDX, IDC_START, m_Start);
DDX_Control(pDX, IDC_CHECK, m_Check);
DDX_Control(pDX, IDC_FW_UPGRADE, m_FwUpgrade);
DDX_Control(pDX, IDC_LIST, m_RecievedData);
DDX_Control(pDX, IDC_STATUS_TEXT, m_Status);
DDX_Control(pDX, IDC_SEND, m_Send);
DDX_Text(pDX, IDC_PID, m_PID);
DDV_MaxChars(pDX, m_PID, 4);
DDX_Text(pDX, IDC_VID, m_VID);
DDV_MaxChars(pDX, m_VID, 4);
DDX_Text(pDX, IDC_UNIT, m_UNIT);
//
DDX_Control(pDX, IDC_STATIC_CH, m_Channel);
//}}AFX_DATA_MAP
}
BEGIN_MESSAGE_MAP(CUsbHidDemoCodeDlg, CDialog)
//{{AFX_MSG_MAP(CUsbHidDemoCodeDlg)
ON_WM_SYSCOMMAND()
ON_WM_PAINT()
ON_WM_QUERYDRAGICON()
ON_BN_CLICKED(IDC_SEND, SendData)
ON_WM_TIMER()
ON_BN_CLICKED(IDC_PW_UPGRADE, OnFwUpgrade)
ON_BN_CLICKED(IDC_BUTTON_VID_PID, OnButtonVidPid)
ON_BN_CLICKED(IDC_CHECK, OnCheck)
ON_BN_CLICKED(IDC_START, OnStart)
ON_BN_CLICKED(IDC_STOP, OnStop)
ON_BN_CLICKED(IDC_RELOAD, OnReload)
ON_BN_CLICKED(IDC_SetFreq, OnSetFreq)
//}}AFX_MSG_MAP
ON_WM_DEVICECHANGE()
END_MESSAGE_MAP()
////////////////////////////////////
// CUsbHidDemoCodeDlg message handlers
BOOL CUsbHidDemoCodeDlg::OnInitDialog()
{
    CDialog::OnInitDialog();
    char Display[220] = "";
    char temp[5];
    // Add "About..." menu item to system menu.
    // IDM_ABOUTBOX must be in the system command range.
    ASSERT((IDM_ABOUTBOX & 0xFFF0) == IDM_ABOUTBOX);
    ASSERT(IDM_ABOUTBOX < 0xF000);
    CMenu* pSysMenu = GetSystemMenu(FALSE);
    if (pSysMenu != NULL)
    {
        CString strAboutMenu;
        strAboutMenu.LoadString(IDS_ABOUTBOX);
        if (!strAboutMenu.IsEmpty())
        {
            pSysMenu->AppendMenu(MF_SEPARATOR);
            pSysMenu->AppendMenu(MF_STRING, IDM_ABOUTBOX, strAboutMenu);
        }
    }
    // Set the icon for this dialog. The framework does this automatically
    // when the application's main window is not a dialog
    SetIcon(m_hIcon, TRUE);           // Set big icon
    SetIcon(m_hIcon, FALSE);        // Set small icon
}

```

```

// Set default Vid and Pid
Vid = DEFAULT_VID;
Pid = DEFAULT_PID;
Unit = DEFAULT_UNIT;
pcktNum = 0;
morePckt = false;
// Disable All Push Button until connection
DisableButton();
//Display all the coefficients of the channel
strcat(Display,"Channel ");
_itoa(Unit, temp, 10); //Convert the integer to the corresponding string, ex. 13 -> "13"
strcat(Display, temp);
m_Channel.SetWindowText(Display);
Display[0] = '\0';
// Explicitely load the AtUsbHid library.
hLib = LoadLibrary(AT_USB_HID_DLL);
if (hLib == NULL)
{
    handleError(GetLastError());
    return 0;
}
// Get USB HID library functions addresses.
if (loadFuncPointers(hLib)==NULL) {
    AfxMessageBox( "Could not get USB HID library functions
addresses",MB_ICONSTOP,0);
    return 0;
}
// Modification starts here - for reading in the text file containing the data in specific order
CFile inputFile;
inputFile.Open( "C:\\MATLAB7\\work\\testData2_Coeff.dat", CFile::modeRead); //specifies the
path of the text file
char totInput[totNumPoints];
CString Element = "";
short i,j,k;
short a = 0;
short b = 0;
short c = 0;
bool flag = 0; //flag for implementing maxV cell (maxV cell is implemented as b7..b4 as the
higher decimal place and b3..b0 as lower decimal place)
long filePointer = 0;
long fileSize = inputFile.GetLength();
UINT IBytesRead;
while(filePointer < (fileSize/totNumPoints)+1)
{
    IBytesRead = inputFile.Read (totInput,totNumPoints);
    for(i=0; i<totNumPoints; i++)
    {
        if (a<8)
        {
            if(!(totInput[i] == ',' ) && !(totInput[i] == '.' ) && !(totInput[i] == '\n')){
                Element = Element + totInput[i];
            }
            else{
                if(totInput[i] == ','){
                    if (flag == 1)
                    {
                        flag = 0;
                        coeffArray[a][b] = coeffArray[a][b] +
_ttoi(Element);
                    }
                    else{
                        coeffArray[a][b] = _ttoi(Element);
                    }
                }
            }
        }
        //Convert the string to the corresponding integer, ex. "45" -> 45
    }
}

```

```

    }
    Element = "";
    b++;
} else if (totInput[j] == '.')
{
    coeffArray[a][b] = _ttoi(Element)*10;
    Element = "";
    flag = 1;
} else{
    coeffArray[a][b] = _ttoi(Element);
    Element = "";
    a++;
    b = 0;
}
}
}
}
filePointer = filePointer++;
}
inputFile.Close();
//The following segment of code is for displaying the content of the text file on the interactive GUI
totInput[0] = '\0';
strcat(Display, "Input File Size = ");
_itoa(fileSize, temp, 10);
strcat(Display, temp);
strcat(Display, " characters");
AddRecievedData(Display);
Display[0] = '\0';
for(j=0; j<8; j++)
{
    strcat(Display, "Channel ");
    itoa(j+1, temp, 10); //Convert the integer to the corresponding string, ex. 13 -> "13"
    strcat(Display, temp);
    strcat(Display, " (Freq = ");
    _itoa(coeffArray[j][0], temp, 10); //char *_itoa(int value, char * string, int radix)
    strcat(Display, temp);
    strcat(Display, ", maxV = ");
    _itoa((coeffArray[j][1]/10), temp, 10);
    strcat(Display, temp);
    strcat(Display, ".");
    _itoa((coeffArray[j][1] % 10), temp, 10);
    strcat(Display, temp);
    strcat(Display, "): ");
    _itoa(32*coeffArray[j][3], temp, 10);
    strcat(Display, temp);
    strcat(Display, " data points, ");
    _itoa(5*coeffArray[j][2], temp, 10);
    strcat(Display, "Output filter cutoff frequency = ");
    strcat(Display, temp);
    strcat(Display, "Hz");
    AddRecievedData(Display);
    Display[0] = '\0';
}
//Displays the default Channel 1 on GUI initiation
AddRecievedData("");
strcat(Display, "Channel ");
itoa(1, temp, 10); //Convert the integer to the corresponding string, ex. 13 -> "13"
strcat(Display, temp);
strcat(Display, " (Freq = ");
_itoa(coeffArray[0][0], temp, 10); //char *_itoa(int value, char * string, int radix)
strcat(Display, temp);
strcat(Display, ", maxV = ");

```

```

        _itoa((coeffArray[0][1]/10), temp, 10);
        strcat(Display, temp);
        strcat(Display, ".");
        _itoa((coeffArray[0][1] % 10), temp, 10);
        strcat(Display, temp);
        strcat(Display, "):");
        _itoa(32*coeffArray[0][3], temp, 10);
        strcat(Display, temp);
        strcat(Display, " data points, ");
        _itoa(5*coeffArray[0][2], temp, 10);
        strcat(Display, "Output filter cutoff frequency = ");
        strcat(Display, temp);
        strcat(Display, "Hz");
        AddRecievedData(Display);
        Display[0] = '\0';
        for (k=0; k<8; k++)
        {
            for(i=k*32+4; i<k*32+36; i++)
            {
                _itoa(coeffArray[0][i], temp, 10);
                strcat(Display,temp);
                strcat(Display,",");
            }
            AddRecievedData(Display);
            Display[0] = '\0';
        }
        AddRecievedData("");
        // try to connect Device
        ConnectDevice();
        DYNCALL(hidRegisterDeviceNotification)((m_hWnd));
        return TRUE; // return TRUE unless you set the focus to a control
    }
void CUsbHidDemoCodeDlg::OnSysCommand(UINT nID, LPARAM lParam)
{
    if ((nID & 0xFFF0) == IDM_ABOUTBOX)
    {
        CAboutDlg dlgAbout;
        dlgAbout.DoModal();
    }
    else
    {
        CDialog::OnSysCommand(nID, lParam);
    }
}
// Original code
void CUsbHidDemoCodeDlg::OnPaint()
{
    if (IsIconic())
    {
        CPaintDC dc(this); // device context for painting

        SendMessage(WM_ICONERASEBKGND, (LPARAM) dc.GetSafeHdc(), 0);

        // Center icon in client rectangle
        int cxIcon = GetSystemMetrics(SM_CXICON);
        int cyIcon = GetSystemMetrics(SM_CYICON);
        CRect rect;
        GetClientRect(&rect);
        int x = (rect.Width() - cxIcon + 1) / 2;
        int y = (rect.Height() - cyIcon + 1) / 2;

        // Draw the icon
    }
}

```

```

        dc.DrawIcon(x, y, m_hIcon);
    }
    else
    {
        CDialog::OnPaint();
    }
}
// Original code
HCURSOR CUsbHidDemoCodeDlg::OnQueryDragIcon()
{
    return (HCURSOR) m_hIcon;
}
/*-----
FUNCTION: SendData
PURPOSE: Send the data over the the USB key as packets
          Executed when Send Data button is pushed
COMMENTS: Created for Phantom project
-----*/
void CUsbHidDemoCodeDlg::SendData()
{
    m_Send.SetWindowText(_T("Send Data"));
    DeactivateButton();
    short i;
    char *outArray = 0;
    CString packet = "";
    char Display[50] = "";
    char cell[3];
    if((m_UNIT < 9)&&(m_UNIT > 0)){
        Unit = m_UNIT;
        strcat(Display,"Sending data to Channel ");
        itoa(Unit, cell, 10); //Convert the integer to the corresponding string, ex. 13 -> "13"
        strcat(Display, cell);
        AddRecievedData(Display);
        packet = static_cast<char>(Unit);
        packet = packet + static_cast<char>(1);
        for(i=0; i<4; i++)
        {
            packet = packet + static_cast<char>(coeffArray[Unit-1][i]);
        }
        AddRecievedData("Packet sent:");
        outArray = packet.GetBuffer(packet.GetLength());
        DYNCALL(writeData)((UCHAR*)outArray);
        packet.ReleaseBuffer();
        packet.Empty();
        //The following for testing
        _itoa(Unit, cell, 10);
        packet = cell;
        packet = packet + ",";
        _itoa(1, cell, 10);
        packet = packet + cell + ",";
        for(i=0; i<4; i++)
        {
            _itoa(coeffArray[Unit-1][i], cell, 10);
            packet = packet + cell;
            packet = packet + ",";
        }
        _itoa(32*coeffArray[Unit-1][3], cell, 10);
        packet = packet + cell;
        packet = packet + ",";
        AddRecievedData(packet);
        packet.ReleaseBuffer();
        packet.Empty();
    }
}

```



```

        totPckt = coeffArray[Unit-1][3]*32/64;
        morePckt = true;
        curUnit = Unit;
    }
}
/*-----*/
FUNCTION: DisableButton
PURPOSE: Disable All push button
          Change Current Status to Diconnected
          Stop Read Function timer
          Executed when the device is not physically connected
COMMENTS: Modified for Phantom project
/*-----*/
void CUsbHidDemoCodeDlg::DisableButton()
{
    // Disable all push button
    m_Start.EnableWindow(false);
    m_Stop.EnableWindow(false);
    m_Send.EnableWindow(false);
    m_SetFreq.EnableWindow(false);
    // Disable Firmware Upgrade
    m_FwUpgrade.EnableWindow(false);
    // Change push button text display
    m_Start.SetWindowText(_T(""));
    m_Stop.SetWindowText(_T(""));
    m_Send.SetWindowText(_T(""));
    m_SetFreq.SetWindowText(_T(""));
    m_Status.SetWindowText(_T("No Connection"));
    CDialog::KillTimer(1);
    IsConnected = false ;
}
/*-----*/
FUNCTION: DeactivateButton
PURPOSE: Deactivate All button
COMMENTS: Created for Phantom project
/*-----*/
void CUsbHidDemoCodeDlg::DeactivateButton()
{
    // Deactivate All communication button
    m_Start.EnableWindow(false);
    m_Stop.EnableWindow(false);
    m_Send.EnableWindow(false);
    m_SetFreq.EnableWindow(false);
    m_FwUpgrade.EnableWindow(false);
}
/*-----*/
FUNCTION: ConnectDevice
PURPOSE: Connect Device using Current Vid and Pid
          if connection is sucefull, change status to Connected
          if connection fail Status is set to diconnected
COMMENTS: Modified for Phantom project
/*-----*/
void CUsbHidDemoCodeDlg::ConnectDevice()
{
    char Display[50] = "";
    char temp[3];
    // Open our USB device.
    if (DYNCALL(findHidDevice)(Vid, Pid)) {
        EnableButton();
        Unit = DEFAULT_UNIT;
        strcat(Display,"Channel ");
        _itoa(Unit, temp, 10); //Convert the integer to the corresponding string, ex. 13 -> "13"
        strcat(Display, temp);
    }
}

```

```

        m_Channel.SetWindowText(Display);
        Display[0] = '\0';
    }
    else {
        DisableButton();
    }
}
/*-----*/
FUNCTION: EnableButton
PURPOSE: Enable all push button
          Set Read function timer
COMMENTS: Modified for Phantom project
/*-----*/
void CUsbHidDemoCodeDlg::EnableButton()
{
    CString inReport;
    CString outReport;
    CString featureReport;
    // Enable all push button
    m_Start.EnableWindow(true);
    m_Stop.EnableWindow(true);
    m_Send.EnableWindow(true);
    m_SetFreq.EnableWindow(true);
    // Enable Firmware Upgrade
    m_FwUpgrade.EnableWindow(true);
    // Change push button text
    m_Start.SetWindowText(_T("Start"));
    m_Stop.SetWindowText(_T("Stop"));
    m_Send.SetWindowText(_T("Send data"));
    m_SetFreq.SetWindowText(_T("Set Frequency"));
    inReport.Format( "%s: %dByte", " In",DYNCALL(getInputReportLength()));
    outReport.Format( "%s: %dByte", " Out",DYNCALL(getOutputReportLength()));
    featureReport.Format("%s: %dByte", " Feature",DYNCALL(getFeatureReportLength()));
    CString text = "Connected!\t"+inReport+" "+outReport+" "+featureReport;
    m_Status.SetWindowText(text);
    SetTimer(1,50,0);
    IsConnected = true ;
}
/*-----*/
FUNCTION: ActivateButton
PURPOSE: Activate All button
COMMENTS: Modified for Phantom project
/*-----*/
void CUsbHidDemoCodeDlg::ActivateButton()
{
    CString inReport;
    CString outReport;
    CString featureReport;
    //Activate all push button
    m_Start.EnableWindow(true);
    m_Stop.EnableWindow(true);
    m_Send.EnableWindow(true);
    m_SetFreq.EnableWindow(true);
    m_FwUpgrade.EnableWindow(true);
}
/*-----*/
FUNCTION: OnDeviceChange
PURPOSE: This function is call each time a status change for a device using
          ON_WM_DEVICECHANGE()
          The function will check if this our device change it status :
          There is 2 important type of event :
          DBT_DEVICEARRIVAL : in this case, we try to connect a device using

```

```

        current VID and PID
        DBT_DEVICEREMOVECOMPLETE : if our device as been disconnected,
        we close the device properly using closeDevice()
        if OnDeviceChange is called by another device nothing is done
    PARMATERS: UINT nEventType : Event Id
        DWORD dwData : data associated to the Event
    COMMENTS: Original code
    -----*/
    BOOL CUsbHidDemoCodeDlg::OnDeviceChange(UINT nEventType, DWORD dwData)
    {
        int isOurDevice;
        switch(nEventType)
        {
            case DBT_DEVICEARRIVAL :
                isOurDevice=DYNCALL(isMyDeviceNotification(dwData));
                if(isOurDevice&&IsConnected) {
                    OutputDebugString(">>> Our Device Already Connected.\n");
                }
                else {
                    // Connect Only if status is disconnected
                    OutputDebugString(">>> A device has been inserted and is
now available.\n");
                    ConnectDevice();
                }
                break;
            case DBT_DEVICEREMOVECOMPLETE :
                isOurDevice=DYNCALL(isMyDeviceNotification(dwData));
                if(IsConnected&&isOurDevice) {
                    // Close Connection only once
                    DisableButton();
                    DYNCALL(closeDevice());
                    OutputDebugString(">>> A device has been removed.\n");
                }
                break;
            default :
                OutputDebugString(">>> OnDeviceChange : default\n");
                break;
        }
        return TRUE;
    }
}
/*-----

```

FUNCTION: AddRecievedData

PURPOSE: This function add new message to m\_RecievedData CList and remove the 100th oldest message to avoid list to be too big.

PARMATERS:

CString NewData - New string to display in CList

COMMENTS: Original code

```

    -----*/
    void CUsbHidDemoCodeDlg::AddRecievedData(CString NewData)
    {
        m_RecievedData.AddString( NewData );
        // display only last 100 messages recieved
        if(m_RecievedData.GetCount(>100) {
            m_RecievedData.DeleteString(0);
        }
        // Set Focus on Last Element
        int nCount = m_RecievedData.GetCount();
        if (nCount > 0) m_RecievedData.SetCurSel(nCount-1);
    }
}
/*-----

```

FUNCTION: OnTimer

PURPOSE: This function allows us to call the check if a new data has been recieved

If true, the buffer information are display using AddRecievedData  
 The Timer for this function must be killed if Connection  
 is lost using function : CDialog::KillTimer(1);  
 If a device is connected, the timer must be set using :  
 SetTimer(1,50,0);  
 This program has been modified to check if the data for a single channel  
 has been broken down to multiple packets

PARAMETERS: nIDEvent - Timer identifier

COMMENTS: Modified for Phantom project

```

-----*/
void CUsbHidDemoCodeDlg::OnTimer(UINT nIDEvent)
{
    UCHAR sbuffer[512];    //was 255
    char *outArray = 0;
    CString packet = "";
    char cell[3];
    short i;
    if(DYNCALL(readData(sbuffer))!=0) {
        if (pktNum == totPckt)
        {
            morePckt = false;
            pktNum = 0;
        }
        if(!morePckt)
        {
            ActivateButton();
        }
        for(i=0; i<64; i++)
        {
            _itoa(sbuffer[i], cell, 10);
            packet = packet + cell;
            packet = packet + ",";
        }
        AddRecievedData("Received packet:");
        AddRecievedData(packet);
        packet.ReleaseBuffer();
        packet.Empty();
        AddRecievedData("");
        if (morePckt == true)
        {
            AddRecievedData("Packet sent:");
            for(i=0; i<64; i++)
            {
                _itoa(coeffArray[curUnit-1][64*pcktNum+4+i], cell, 10);
                packet = packet + cell;
                packet = packet + ",";
            }
            AddRecievedData(packet);
            packet.ReleaseBuffer();
            packet.Empty();
            for(i=64*pcktNum+4; i<64*pcktNum+68; i++)
            {
                packet = packet + static_cast<char>(coeffArray[curUnit-1][i]);
            }
            outArray = packet.GetBuffer(packet.GetLength());
            DYNCALL(writeData)((UCHAR*)outArray);
            packet.ReleaseBuffer();
            packet.Empty();
            pcktNum++;
        }
    }
}
CDialog::OnTimer(nIDEvent);

```

```

}
/*-----
FUNCTION: OnFwUpgrade
PURPOSE: Call when Firmware Upgrade Button is pressed.
        This function set the device in Firmware upgarde mode using startBootLoader
        Once bootloader mode as been sent, the device is close properly.
        You have the to lauch Flip to load a new firmeare
COMMENTS: Original code for programming purpose
-----*/
void CUsbHidDemoCodeDlg::OnFwUpgrade()
{
    if(IsConnected) { //if our device is attached
        UCHAR* outputReport = new UCHAR[DYNCALL(getFeatureReportLength());
        outputReport[0]=0x55;
        outputReport[1]=0xAA;
        outputReport[2]=0x55;
        outputReport[3]=0xAA;
        if(!DYNCALL(setFeature(outputReport))) {
            // Fail to run bootLoader
            AfxMessageBox( "Can not start Device in Boot Loader mode",
MB_ICONSTOP,0);
        }
        DisableButton();
        DYNCALL(closeDevice()); //close all handles
    }
}
/*-----
FUNCTION: OnCancel
PURPOSE: On one cancel if device is connected, this one is disconnected.
        the application is Unregister from the device notification table using
        hidUnregisterDeviceNotification(m_hWnd)
COMMENTS: Original code
-----*/
void CUsbHidDemoCodeDlg::OnCancel()
{
    if(IsConnected) //if our device is attached
    {
        DYNCALL(closeDevice()); //close all handles
        CDialog::KillTimer(1); //close the timer
    }
    DYNCALL(hidUnregisterDeviceNotification(m_hWnd));
    FreeLibrary(hLib);
    CDialog::OnCancel();
}
/*-----
FUNCTION: OnButtonVidPid
PURPOSE: When clic on button Vid PID
        Vendor ID en Product ID is taken from edit Box and new value
        are change.
COMMENTS: Original code
-----*/
void CUsbHidDemoCodeDlg::OnButtonVidPid()
{
    UpdateData();
    // Try To Convert in Hex
    char VidToConvert[10];
    char PidToConvert[10];
    char * pEnd;
    long newVid;
    long newPid;
    // Get New Vid
    strcpy(VidToConvert,"0x");
}

```

```

    strcat(VidToConvert,m_VID.GetBuffer(m_VID.GetLength()));
    newVid = strtol (VidToConvert,&pEnd,0);
    m_VID.Format("%X",newVid);
    // Get New Pid
    strcpy(PidToConvert,"0x");
    strcat(PidToConvert,m_PID.GetBuffer(m_PID.GetLength()));
    newPid = strtol (PidToConvert,&pEnd,0);
    m_PID.Format("%X",newPid);
    // Upadte
    SetDlgItemText(IDC_VID , m_VID.GetBuffer(m_VID.GetLength()));
    SetDlgItemText(IDC_PID , m_PID.GetBuffer(m_PID.GetLength()));
    if((newVid!=Vid)||newPid!=Pid) {
        Vid=newVid;
        Pid=newPid;
        if(IsConnected) {
            // Close Connection only once
            DisableButton();
            DYNCALL(closeDevice());
        }
        ConnectDevice();
    }
}
//The following code is still under construction. Jeff. 2010Jun17
/*-----*/
FUNCTION: OnCheck
PURPOSE: Executed when a new channel is selected
Also displays the data of the channel and issues the corresponding MUX sel signal
COMMENTS: Created for Phantom project
/*-----*/
void CUsbHidDemoCodeDlg::OnCheck()
{
    UpdateData();
    char *outArray = 0;
    CString packet = "";
    char Display[220] = "";
    char cell[5];
    short i,k;
    // TODO: Add your control notification handler code here
    if((m_UNIT < 9)&&(m_UNIT > 0)&&(Unit != m_UNIT)){
        Unit = m_UNIT;
        //Display the channel selected message
        strcat(Display,"Selected Channel ");
        itoa(Unit, cell, 10); //Convert the integer to the corresponding string, ex. 13 -> "13"
        strcat(Display, cell);
        AddRecievedData(Display);
        Display[0] = '\0';
        //Display all the coefficients of the channel
        strcat(Display,"Channel ");
        itoa(Unit, cell, 10); //Convert the integer to the corresponding string, ex. 13 -> "13"
        strcat(Display, cell);
        m_Channel.SetWindowText(Display);
        strcat(Display, " (Freq = ");
        _itoa(coeffArray[Unit-1][0], cell, 10);
        strcat(Display, cell);
        strcat(Display, ", maxV = ");
        _itoa(coeffArray[Unit-1][1], cell, 10);
        strcat(Display, cell);
        strcat(Display, "): ");
        _itoa(32*coeffArray[Unit-1][3], cell, 10);
        strcat(Display, cell);
        strcat(Display, " data points, ");
        _itoa(5*coeffArray[Unit-1][2], cell, 10);
    }
}

```

```

        strcat(Display, "Output filter cutoff frequency = ");
        strcat(Display, cell);
        strcat(Display, "Hz");
        AddRecievedData(Display);
        Display[0] = '\0';
        for (k=0; k<8; k++)
        {
            for(i=k*32+4; i<k*32+36; i++)
            {
                _itoa(coeffArray[Unit-1][i], cell, 10);
                strcat(Display, cell);
                strcat(Display, ",");
            }
            AddRecievedData(Display);
            Display[0] = '\0';
        }
        AddRecievedData(Display);
        Display[0] = '\0';
        //Acknowledge AT90USB that a new channel is selected
        packet = static_cast<char>(Unit);
        packet = packet + static_cast<char>(5);
        outArray = packet.GetBuffer(packet.GetLength());
        DYNCALL(writeData)((UCHAR*)outArray);
        packet.Empty();
    }
    else{
//        strcat(Display, "Channel entered does not exist!");
//        AddRecievedData(Display);
    }
}
/*-----
FUNCTION: OnStart
PURPOSE: Executed when Start button is pushed
COMMENTS: Created for Phantom project
-----*/
void CUsbHidDemoCodeDlg::OnStart()
{
    //UpdateData();
    DeactivateButton();
    char *outArray = 0;
    CString packet = "";
    char Display[20] = "";
    char cell[3];
    if((m_UNIT < 9)&&(m_UNIT > 0)){
        Unit = m_UNIT;
        strcat(Display, "Start Channel ");
        itoa(Unit, cell, 10); //Convert the integer to the corresponding string, ex. 13 -> "13"
        strcat(Display, cell);
        AddRecievedData(Display);
        packet = static_cast<char>(Unit);
        packet = packet + static_cast<char>(3);
        outArray = packet.GetBuffer(packet.GetLength());
        DYNCALL(writeData)((UCHAR*)outArray);
        packet.Empty();
    }
}
/*-----
FUNCTION: OnStop
PURPOSE: Executed when Stop button is pushed
COMMENTS: Created for Phantom project
-----*/
void CUsbHidDemoCodeDlg::OnStop()

```

```

{
    //UpdateData();
    DeactivateButton();
    char *outArray = 0;
    CString packet = "";
    char Display[20] = "";
    char cell[3];
    if((m_UNIT < 9)&&(m_UNIT > 0)){
        Unit = m_UNIT;
        strcat(Display,"Stop Channel ");
        itoa(Unit, cell, 10); //Convert the integer to the corresponding string, ex. 13 -> "13"
        strcat(Display, cell);
        AddRecievedData(Display);
        packet = static_cast<char>(Unit);
        packet = packet + static_cast<char>(4);
        outArray = packet.GetBuffer(packet.GetLength());
        DYNCALL(writeData)((UCHAR*)outArray);
        packet.Empty();
    }
}

```

```

/*-----
FUNCTION: OnReload
PURPOSE: Executed when Reload Data button is pushed
COMMENTS: Created for Phantom project
-----*/

```

```

void CUsbHidDemoCodeDlg::OnReload()
{
    CFile inputFile;
    inputFile.Open( "C:\\MATLAB7\\work\\testData2_Coeff.dat", CFile::modeRead);
    char totInput[totNumPoints];
    CString Element = "";
    char Display[220] = "";
    char temp[5];
    short i,j;
    short a = 0;
    short b = 0;
    short c = 0;
    bool flag = 0;
    long filePointer = 0;
    long fileSize = inputFile.GetLength();
    UINT IBytesRead;
    while(filePointer < (fileSize/totNumPoints)+1)
    {
        IBytesRead = inputFile.Read (totInput,totNumPoints);
        for(i=0; i<totNumPoints; i++)
        {
            if (a<8)
            {
                if(!(totInput[i] == ',') && !(totInput[i] == '.') && !(totInput[i] == '\n')){
                    Element = Element + totInput[i];
                }
                else{
                    if(totInput[i] == ','){
                        if (flag == 1)
                        {
                            flag = 0;
                            coeffArray[a][b] = coeffArray[a][b] +
                                _ttoi(Element);
                        }
                        else{
                            coeffArray[a][b] = _ttoi(Element);
                        }
                    }
                    //Convert the string to the corresponding integer, ex. "45" -> 45
                }
            }
        }
    }
}

```



```

        Element = "";
        b++;
    }else if(totInput[j] == '.')
    {
        coeffArray[a][b] = _ttoi(Element)*10;
        Element = "";
        flag = 1;
    }else{
        coeffArray[a][b] = _ttoi(Element);
        Element = "";
        a++;
        b = 0;
    }
}
}
}
filePointer = filePointer++;
}
inputFile.Close();
totInput[0] = '\0';
AddRecievedData("");
for(j=0; j<8; j++)
{
    strcat(Display,"Channel ");
    itoa(j+1, temp, 10); //Convert the integer to the corresponding string, ex. 13 -> "13"
    strcat(Display, temp);
    strcat(Display, " (Freq = ");
    _itoa(coeffArray[j][0], temp, 10); //char *_itoa(int value, char * string, int radix)
    strcat(Display, temp);
    strcat(Display, ", maxV = ");
    _itoa((coeffArray[j][1]/10), temp, 10);
    strcat(Display, temp);
    strcat(Display, ".");
    // _itoa((coeffArray[j][1]-((coeffArray[j][1]/10)*10)), temp, 10);
    _itoa((coeffArray[j][1] % 10), temp, 10);
    strcat(Display, temp);
    strcat(Display, ": ");
    _itoa(32*coeffArray[j][3], temp, 10);
    strcat(Display, temp);
    strcat(Display, " data points, ");
    _itoa(5*coeffArray[j][2], temp, 10);
    strcat(Display, "Output filter cutoff frequency = ");
    strcat(Display, temp);
    strcat(Display, "Hz");
    AddRecievedData(Display);
    Display[0] = '\0';
}
AddRecievedData("");
}
/*-----
FUNCTION: OnSetFreq
PURPOSE: Executed when Set Frequency button is pushed
COMMENTS: Created for Phantom project
-----*/
void CUsbHidDemoCodeDlg::OnSetFreq()
{
    // TODO: Add your control notification handler code here
    //UpdateData();
    DeactivateButton();
    char *outArray = 0;
    CString packet = "";
    char Display[40] = "";

```

```

char cell[3];

if((m_UNIT < 9)&&(m_UNIT > 0)){
    Unit = m_UNIT;
    strcat(Display,"Set Frequency for Channel ");
    itoa(Unit, cell, 10);          //Convert the integer to the corresponding string, ex. 13 -> "13"
    strcat(Display, cell);
    strcat(Display, " - ");
    itoa(coeffArray[Unit-1][0], cell, 10);
    strcat(Display, cell);
    strcat(Display, " Hz");
    AddRecievedData(Display);
    //Display[0] = '\0';
    packet = static_cast<char>(Unit);
    packet = packet + static_cast<char>(2);
    packet = packet + static_cast<char>(coeffArray[Unit-1][0]);
    //packet = packet + static_cast<char>(coeffArray[Unit-1][1]);
    packet = packet + static_cast<char>(coeffArray[Unit-1][2]);
    outArray = packet.GetBuffer(packet.GetLength());
    DYNCALL(writeData)((UCHAR*)outArray);
    packet.Empty();
}
}

```

## Appendix D: C++ Code for AT90USB1287 Microcontroller Firmware

Note: The following source code should be saved as hid\_task.c to replace the file with the same name in the USBKEY\_STK525-series6-hidio project provided by Atmel®. The compilation results in USBKEY\_STK525-series6-hidio.hex file to be loaded on AT90USB1287 microcontroller.

```
/*This file has been prepared for Doxygen automatic documentation generation.*/
//! \file *****
//!
//! \brief This file manages the generic HID IN/OUT task.
//!
//! - Compiler:      IAR EWAVR and GNU GCC for AVR
//! - Supported devices: AT90USB1287, AT90USB1286, AT90USB647, AT90USB646
//!
//! \author      Atmel Corporation: http://www.atmel.com \n
//!              Support and FAQ: http://support.atmel.no/
//!
//! *****

/* Copyright (c) 2007, Atmel Corporation All rights reserved.
 *
 * Redistribution and use in source and binary forms, with or without
 * modification, are permitted provided that the following conditions are met:
 *
 * 1. Redistributions of source code must retain the above copyright notice,
 * this list of conditions and the following disclaimer.
 *
 * 2. Redistributions in binary form must reproduce the above copyright notice,
 * this list of conditions and the following disclaimer in the documentation
 * and/or other materials provided with the distribution.
 *
 * 3. The name of ATMEL may not be used to endorse or promote products derived
 * from this software without specific prior written permission.
 *
 * THIS SOFTWARE IS PROVIDED BY ATMEL "AS IS" AND ANY EXPRESS OR IMPLIED
 * WARRANTIES, INCLUDING, BUT NOT LIMITED TO, THE IMPLIED WARRANTIES OF
 * MERCHANTABILITY AND FITNESS FOR A PARTICULAR PURPOSE ARE EXPRESSLY AND
 * SPECIFICALLY DISCLAIMED. IN NO EVENT SHALL ATMEL BE LIABLE FOR ANY DIRECT,
 * INDIRECT, INCIDENTAL, SPECIAL, EXEMPLARY, OR CONSEQUENTIAL DAMAGES
 * (INCLUDING, BUT NOT LIMITED TO, PROCUREMENT OF SUBSTITUTE GOODS OR SERVICES;
 * LOSS OF USE, DATA, OR PROFITS; OR BUSINESS INTERRUPTION) HOWEVER CAUSED AND
 * ON ANY THEORY OF LIABILITY, WHETHER IN CONTRACT, STRICT LIABILITY, OR TORT
 * (INCLUDING NEGLIGENCE OR OTHERWISE) ARISING IN ANY WAY OUT OF THE USE OF
 * THIS SOFTWARE, EVEN IF ADVISED OF THE POSSIBILITY OF SUCH DAMAGE.
 */

// This code has been modified by Jeff for the implementation of Phantom project
// _____ I N C L U D E S _____
#include "config.h"
#include "conf_usb.h"
#include "hid_task.h"
#include "lib_mcu/usb/usb_drv.h"
#include "usb_descriptors.h"
#include "modules/usb/device_chap9/usb_standard_request.h"
#include "usb_specific_request.h"
```



```

//! @brief Get data report from Host
void hid_report_out(void)
{
    Usb_select_endpoint(EP_HID_OUT);
    if(!s_usb_receive_out())
    {
        //The attempt to use loop for Usb_read_byte() here didn't result in expected functionality
        inBuf[0] = Usb_read_byte();
        inBuf[1] = Usb_read_byte();

        //inBuf[2] to inBuf[62] omitted

        inBuf[63] = Usb_read_byte();
        Usb_ack_receive_out();
        flag1 = true;
        pcktNew = true;
    }
    /** Check if we received DFU mode command from host
    if(jump_bootloader)
    {
        U32 volatile tempo;
        Leds_off();
        Usb_detach(); // Detach actual generic HID application
        for(tempo=0;tempo<70000;tempo++); // Wait some time before
        start_boot(); // Jumping to bootloader
    }
}
//=====
//! @brief Send data report to Host
void hid_report_in(void)
{
    Usb_select_endpoint(EP_HID_IN);
    if(!s_usb_write_enabled())
    return; // Not ready to send report
    if (flag1 == false)
    return;
    Usb_write_byte(coeff[0]);
    Usb_write_byte(coeff[1]);

    // Usb_write_byte(coeff[2]) to Usb_write_byte(coeff[62]) omitted

    Usb_write_byte(inBuf[63]);
    Usb_ack_in_ready(); // Send data over the USB
    flag1 = false;
}
//=====
// The following code is for taking care of multiple packets transmitted
// for a single channel by determining the total number of packets
void hid_shift(void)
{
    U8 i;
    if (pcktNew == true)
    {
        if ((packetNum == 0) && (inBuf[1] == 0x05) && (morePckt == false))
        {
            coeff[0] = inBuf[0];
            coeff[1] = inBuf[1];
        }else if ((packetNum == 0) && (inBuf[1] != 0x05) && (morePckt == false))
        {
            i = 0;
            while (i < 6)
            {

```

```

        coeff[i] = inBuf[i];
        i++;
    }
    if (coeff[1] == 0x01)
    {
        morePckt = true;
        totPcktNum = coeff[5]*32/64;
    }
} else if (morePckt == true)
{
    i = 0;
    while (i < 64)
    {
        coeff[64*packetNum+i+6] = inBuf[i];
        i++;
    }
    packetNum++;
    if (packetNum == totPcktNum)
    {
        morePckt = false;
        packetNum = 0;
    }
}
}
}

//=====
// The following code is for decoding for the channel selected from the
// packet received and issue the corresponding signal to the MUX/DeMUX
// circuit
// Depending on the command code in the packet, it also issue a sequence of
// signal change on the corresponding ports on AT90USB1287 controller
void hid_decode_command(void)
{
    attempt = 0;
    U8 com_line = 0;
    short i;
    if ((pcktNew == true) && (morePckt == false))
    {
        if (coeff[1] == 0x05)
        {
            if (coeff[0] == 0x01)
            {
                PORTC = 0x00;
            } else if (coeff[0] == 0x02)
            {
                PORTC = 0x01;
            } else if (coeff[0] == 0x03)
            {
                PORTC = 0x02;
            } else if (coeff[0] == 0x04)
            {
                PORTC = 0x03;
            } else if (coeff[0] == 0x05)
            {
                PORTC = 0x04;
            } else if (coeff[0] == 0x06)
            {
                PORTC = 0x05;
            } else if (coeff[0] == 0x07)
            {
                PORTC = 0x06;
            } else if (coeff[0] == 0x08)

```

```

        {
            PORTC = 0x07;
        }
    }else
    {
        i=0;
        PORTD = (1<<PD4)|(0<<PD2)|(0<<PD0);
        while((i==0) && (attempt<100))
        {
            com_line = PIND;
            com_line = com_line & 0b00100000;
            if (com_line == 0)
            {
                PORTD = (1<<PD4)|(1<<PD2)|(0<<PD0);
                PORTD = (1<<PD4)|(1<<PD2)|(0<<PD0);
                PORTD = (1<<PD4)|(1<<PD2)|(0<<PD0);
                PORTD = (1<<PD4)|(0<<PD2)|(0<<PD0);
                attempt++;
            } else if (com_line == 32)
            {
                i++;
            }
        }
    }
}
if ((pcktNew == true) && (morePckt == false) && (attempt < 100))
{
    if (coeff[1] == 0x01)
    {
        i = 0;
        while(i < 3)
        {
            com_line = PIND;
            com_line = com_line & 0b00000011;
            if (com_line == 0)
            {
                PORTA = coeff[i];
                PORTD = (1<<PD4)|(0<<PD2)|(1<<PD0);
            } else if (com_line == 3)
            {
                PORTD = (1<<PD4)|(0<<PD2)|(0<<PD0);
                i++;
            }
        }
        PORTD = (1<<PD4)|(0<<PD2)|(0<<PD0);

        i = 4;
        totCoeffNum = coeff[5]*32;
        while(i < (totCoeffNum+6))
        {
            com_line = PIND;
            com_line = com_line & 0b00000011;
            if (com_line == 0)
            {
                PORTA = coeff[i];
                PORTD = (1<<PD4)|(0<<PD2)|(1<<PD0);
            } else if (com_line == 3)
            {
                PORTD = (1<<PD4)|(0<<PD2)|(0<<PD0);
                i++;
            }
        }
    }
}

```

```

        PORTD = (1<<PD4)|(0<<PD2)|(0<<PD0);
    }else if ((coeff[1] == 0x02)||coeff[1] == 0x03)||coeff[1] == 0x04))
    {
        i = 0;
        while(i < 4)
        {
            com_line = PIND;
            com_line = com_line & 0b00000011;
            if (com_line == 0)
            {
                PORTA = coeff[i];
                PORTD = (1<<PD4)|(0<<PD2)|(1<<PD0);
            } else if (com_line == 3)
            {
                PORTD = (1<<PD4)|(0<<PD2)|(0<<PD0);
                i++;
            }
        }
        PORTD = (1<<PD4)|(0<<PD2)|(0<<PD0);
    }
}
i = 0;
if (attempt == 100)
{
    while (i < 64)
    {
        inBuff[i] = 0;
        i++;
    }
}
pcktNew = false;
}
//=====
/*! @brief This function increments the cpt_sof counter each times
    the USB Start Of Frame interrupt subroutine is executed (1ms)
    Usefull to manage time delays
    */
void sof_action()
{
    cpt_sof++;
}

void delay_ms(U8 ms)
{
    U8 delay_usb;
    for(;ms;ms--)
    {
        for(delay_usb=0;delay_usb<FOSC/16;delay_usb++);
    }
}

```



## Appendix E: Assembly Code for Programming ATmega32 Microcontroller

Note: The following code is to be compiled using AVR Studio developed by Atmel® and loaded to ATmega32 microcontroller.

```
;Code for ATmega32 microcontroller for the implementation of Phantom project
;See ATmega32.pdf and AVR_Insruction_Set.pdf for reference

.NOLIST ;turn listfile generation off
;Include files
.INCLUDE "C:\Program Files\Atmel\AVR Tools\AvrAssembler2\Appnotes\m32def.inc"
.LIST ;turn listfile generation on
.EQU Status=0x0060
.EQU Waveform=0x0061
.EQU Input_Amp=0x0062
.EQU Input_Freq=0x0063
.EQU Channel_In=0x0064
.EQU Current_Instr=0x0065
.EQU Dump1=0x0066
.EQU Cut_Count=0x0067
.EQU HW_Interrupt=0x0068
.EQU TotCoeffIn=0x0069
.EQU TotCoeffNumH=0x006A
.EQU TotCoeffNumL=0x006B
.EQU CutF=0x006C

.EQU Input_Val=10 ;about 100Hz
.EQU Channel=8 ;Every unit should have a unique channel number

; Definitions:
; Registers
.DEF rmp = r16 ;used as multi-purpose register
.DEF rNl = r0;
.DEF rNh = r1;
.DEF rNu = r2;
.DEF rD = r3;
.DEF rRl = r4;
.DEF rRh = r5;

;Start of main program
.CSEG;code segment
.ORG $0000

JMP MAIN
JMP SWITCH_3 ;Switch 3 IRQ Handler
JMP SWITCH_4 ;Switch 4 IRQ Handler

MAIN:
LDI r16,Input_Val
STS Input_Amp,r16
STS Input_Freq,r16
LDI r16,0
STS TotCoeffNumH,r16
LDI r16,32
STS TotCoeffNumL,r16
LDI r16,1
STS TotCoeffIn,r16
```

```

;Set up the stack pointer at the end of program memory
LDI r16,high(RAMEND)
OUT SPH,r16
LDI r16,low(RAMEND)
OUT SPL,r16
IN r16,MCUCSR           ;MCR Control and Status Register
ORI r16,0b10000000     ;Disable JTAG by setting JTD bit (bit 7) of the MCUCSR register
OUT MCUCSR,r16
OUT MCUCSR,r16         ;The JTD bit must be written twice within 4 cycles to change to
the desired value
LDI r16,$00
STS Status,r16         ;Load $00 to SwitchStatus cell in SRAM to indicate Switch 3 not
pressed initially
STS HW_Interrupt,r16
LDI r16,$00
OUT DDRA,r16          ;Set all bits in Port A to input mode
;LDI r16,$22
LDI r16,$E2           ;Set Bits 1,5,6,7 of Port D to output mode and the rest to input
mode
OUT DDRD,r16
LDI r16,$FF
OUT DDRB,r16          ;Set all bits in Port B to output mode
OUT DDRC,r16          ;Set all bits in Port C to output mode
IN r16,MCUCR           ;MCR Control Register
ORI r16,0b00001111    ;The rising edge generates an interrupt request for INT0 and INT1
OUT MCUCR,r16
IN r16,GICR           ;General Interrupt Control Register
ORI r16,0b11000000    ;Activate both INT0 and INT1
OUT GICR,r16
LDI r16,75            ;The larger the number loaded in OCR2, the longer each
countdown period, which results in a smaller frequency of the output clock signal
OUT OCR2,r16          ;Load Output Compare Register 2 with the desired number to be
counted down from
LDI r16,0b00011010    ;Clear Timer on Compare match (CTC) mode.Toggle Output Compare
pin on compare match.clkT2S/8 (From prescaler)
OUT TCCR2,r16         ;Time/Counter Control Register 2
;=====;
;PortA - 8-bit Data-in from AT90USB1287
;PortB - 8-bit Control-out, B(3..0) currently used to control DAC
;PortC - 8-bit Data-out to DAC
;PortD - 8-bit Control-in from AT90USB1287
:
:   PortB:
:       Bit 0 - Inv(RESET) to DAC
:       Bit 1 - Inv(LDAC:Load DAC) to DAC
:       Bit 2 - Inv(WR:Write) to DAC
:       Bit 3 - Inv(CS:Chip select) to DAC
:       Bit 4 to 7 - Unused
:
:   PortD:
:       Bit 0 - Communication line from AT90USB1287
:       Bit 1 - Communication line to AT90USB1287
:       Bit 2 - Interrupt signal from AT90USB1287
:       Bit 3 - Interrupt signal from AT90USB1287/External
:       Bit 4 - Reserved bit for prevent mis-sensing interrupt
:       Bit 5 - Interrupt acknowledge bit to AT90USB1287
:       Bit 6 - Unused
:       Bit 7 - Clock signal for the output switching-capacitor filter
LDI r16,(0<<PD5)
OUT PORTD,r16 ;Reset the interrupt acknowledge signal
SEI;           ;Enable all interrupts

LDI r16,0x00

```

```

OUT PORTC,r16
READ_Amp:

;-----
;For testing the EEPROM Read/Write
;Load the waveform coefficients from the Flash memory and store in the EEPROM
CLI
LDI r16,32 ;to detect end of a sinusoid period
LDI ZH,HIGH(mod_sine<<1);load high address byte
LDI ZL,LOW(mod_sine<<1);load low address byte
LDI r19,0x00
LDI r18,0x00
LOAD:
SBIC EECR,EWE
RJMP LOAD
OUT EEARH,r19
OUT EEARL,r18
LPM r17, Z
OUT EEDR,r17
SBI EECR,EEMWE
SBI EECR,EWE
INC r18 ;index the next cell in the EEPROM
INC ZL ;index the next cell in the Flash memory
DEC r16 ;countdown to end of a sinusoid period
BRNE LOAD
SEI
;-----
SINUSOID_CHECK:
; The following for checking if the present unit is selected
IN r16,PIND
ANDI r16,0b00010000
CPI r16,0
BR EQ CHECK_BUTTON

STATUS_CHECK:
LDS r16,Status
CPI r16,0x00 ;If Switch 3 pressed, then all bits in SwitchStatus are toggled to 1. If not, keep checking
BRNE CHANNEL_CHECK
NOP
NOP
NOP
NOP
CHECK_BUTTON:
LDS r16,HW_Interrupt
CPI r16,0x00
BR EQ SINUSOID_CHECK
RJMP DELAY_CALC
;-----
//RJMP SINUSOID_CHECK
;-----
;Code to decode the execution command
CHANNEL_CHECK:
LDI r16,(0<<PD5)
OUT PORTD,r16 ;Reset the interrupt acknowledge signal
LDI r16,(0<<PD1)
OUT PORTD,r16 ;Reset the communication lines
LDI r16,0x00
STS Status,r16
WAIT1a:
IN r16,PIND
ANDI r16,0x03
CPI r16,0x01

```

```

BRNE WAIT1a
;-----
CHANNEL_READ:
NOP
NOP
IN r17,PINA
LDI r16,(1<<PD1)
OUT PORTD,r16 ;Signal AT90USB1287 that the data have be received
STS Channel_In,r17
WAIT1b:
IN r16,PIND
ANDI r16,0x03
CPI r16,0x02
BRNE WAIT1b
LDI r16,(0<<PD1)
OUT PORTD,r16 ;Reset the communication lines
;-----
WAIT2a:
IN r16,PIND
ANDI r16,0x03
CPI r16,0x01
BRNE WAIT2a
;-----
COMMAND_DECODE:
NOP
NOP
IN r17,PINA
LDI r16,(1<<PD1)
OUT PORTD,r16 ;Signaling AT90USB1287 that the data have be received
STS Current_Instr,r17
WAIT2b:
IN r16,PIND
ANDI r16,0x03
CPI r16,0x02
BRNE WAIT2b
LDI r16,(0<<PD1)
OUT PORTD,r16 ;Reset the communication lines
;-----
FREQUENCY_READ:
IN r16,PIND
ANDI r16,0x03
CPI r16,0x01
BRNE FREQUENCY_READ
NOP
NOP
IN r17,PINA
LDI r16,(1<<PD1)
OUT PORTD,r16 ;Signaling AT90USB1287 that the data have be received
STS Dump1,r17
WAIT3:
IN r16,PIND
ANDI r16,0x03
CPI r16,0x02
BRNE WAIT3
LDI r16,(0<<PD1)
OUT PORTD,r16 ;Reset the communication lines
;-----
CutFreq_READ:
IN r16,PIND
ANDI r16,0x03
CPI r16,0x01
BRNE CutFreq_READ

```

```

NOP
NOP
IN r17,PINA
LDI r16,(1<<PD1)
OUT PORTD,r16 ;Signaling AT90USB1287 that the data have be received
STS CutF,r17
WAIT4:
IN r16,PIND
ANDI r16,0x03
CPI r16,0x02
BRNE WAIT4
LDI r16,(0<<PD1)
OUT PORTD,r16 ;Reset the communication lines
;-----
LDS r17,Channel_In
CPI r17,Channel ;Check if the unit intended by the data packet matches with the channel number
of the present unit
BREQ DECODE_SEQ
RJMP SINUSOID_CHECK

DECODE_SEQ:
LDS r17,Current_Instr
CPI r17,0x01
BREQ NUM_SAMPLE_READ
CPI r17,0x02
BREQ FREQ_DUMP
CPI r17,0x03
BREQ START_JMP
CPI r17,0x04
BREQ STOP_JMP
RJMP SINUSOID_CHECK

START_JMP:
RJMP DELAY_CALC
STOP_JMP:
RJMP CLEAR_OUTPUT

FREQ_DUMP:
LDS r16,Dump1
STS Input_Freq,r16
LDS r16,CutF

;Code to output sinusoid
CutF_CONV:
;Implements the frequency from 1 to 100 Hz
;Multiply 100 by 50 and store the result in R1:R0
LDI rmp,200
LDI r17,5
MUL rmp,r17 ;result stored in R1:R0
LDS rD,CutF

;Divide rNh(R1):rNI(R0) by rD(R3)
Div8CON:
CLR rNu;clear interim register
CLR rRh;clear result (the result registers are also used to count to 16 for the division steps)
CLR rRI
INC rRI

;Division loop starts
Div8CONa:
CLC ;clear carry-bit
ROL rNI ;rotate the next-upper bit of the number to the interim register (multiply by 2)

```

```

ROL rNh
ROL rNu
BRCS Div8CONb ;if the bit is a 1, then subtract.
CP rNu,rD      ;division result 1 or 0?
BRCS Div8CONc ;if smaller, then ignore subtraction step

;If the intermediate value dividable
Div8CONb:
SUB rNu,rD     ;subtract number to divide with
SEC            ;set carry-bit,result is a 1
RJMP Div8CONd ;jump to shift of the result bit

;If the intermediate value not dividable
Div8CONc:
CLC            ;clear carry-bit,resulting bit is a 0

Div8CONd:
ROL rRI       ;rotate carry-bit into result registers
ROL rRh
BRCC Div8CONa ;Zero rotating out of the result register: Division not done

STS Cut_Count,rRI

OUT OCR2,rRI      ;Load Output Compare Register 2 with the desired number to be
counted down from

RJMP SINUSOID_CHECK

NUM_SAMPLE_READ:
IN r16,PIND
ANDI r16,0x03
CPI r16,0x01
BRNE NUM_SAMPLE_READ

NOP
NOP
IN r17,PINA
LDI r16,(1<<PD1)
OUT PORTD,r16 ;Signaling AT90USB1287 that the data have be received
STS TotCoeffNumL,r17
STS TotCoeffIn,r17

WAIT5:
IN r16,PIND
ANDI r16,0x03
CPI r16,0x02
BRNE WAIT5
LDI r16,(0<<PD1)
OUT PORTD,r16 ;Reset the communication lines

CLR r19
LSL r17
ROL r19
LSL r17
ROL r19
LSL r17
ROL r19
LSL r17
ROL r19
LSL r17
ROL r19
LSL r17
ROL r19
STS TotCoeffNumL,r17

```

STS TotCoeffNumH,r19

INIT\_EEPROM:

CLI

LDS r25,TotCoeffNumH ;Set R25:R24 to the counts of waveform coefficients to be read in

LDS r24,TotCoeffNumL

LDI r27,0x00

LDI r26,0x00

OUT EEARH,r27

OUT EEARL,r26

DATA\_IN:

IN r16,PIND

ANDI r16,0x03

CPI r16,0x01

BRNE DATA\_IN

NOP

NOP

IN r17,PINA

LDI r16,(1<<PD1)

OUT PORTD,r16 ;Signaling AT90USB1287 that the data have be received

WAIT6:

IN r16,PIND

ANDI r16,0x03

CPI r16,0x02

BRNE WAIT6

LDI r16,(0<<PD1)

OUT PORTD,r16 ;Reset the communication lines

LOAD2:

SBIC EECR,EEWE

RJMP LOAD2

OUT EEARH,r27

OUT EEARL,r26

OUT EEDR,r17

SBI EECR,EEMWE

SBI EECR,EEWE

ADIW r27:r26,1

COUNT\_DOWN1:

SBIW r25:r24,1

BRNE DATA\_IN

SEI

RJMP SINUSOID\_CHECK

TEMP1:

LDI r21,0x06

RJMP SINUSOID\_CHECK

-----

;Code to output sinusoid

DELAY\_CALC:

;implements the frequency from 1 to 100 Hz

;Multiply 100 by 50 and store the result in R1:R0

LDI rmp,200

LDI r17,50

MUL rmp,r17 ;result stored in R1:R0

LDS rD,Input\_Freq

```

;Divide rNh(R1):rNI(R0) by rD(R3)
Div8:
CLR rNu;clear interim register
CLR rRh;clear result (the result registers are also used to count to 16 for the division steps)
CLR rRI
INC rRI

;Division loop starts
Div8a:
CLC ;clear carry-bit
ROL rNI ;rotate the next-upper bit of the number to the interim register (multiply by 2)
ROL rNh
ROL rNu
BRCS Div8b ;if the bit is a 1, then subtract.
CP rNu,rD ;division result 1 or 0?
BRCS Div8c ;if smaller, then ignore subtraction step

;If the intermediate value dividable
Div8b:
SUB rNu,rD ;subtract number to divide with
SEC ;set carry-bit,result is a 1
RJMP Div8d ;jump to shift of the result bit

;If the intermediate value not dividable
Div8c:
CLC ;clear carry-bit,resulting bit is a 0

Div8d:
ROL rRI ;rotate carry-bit into result registers
ROL rRh
BRCC Div8a ;Zero rotating out of the result register: Division not done

;Code for adjusting for different numbers of sample points
DELAY_ADJUST:
;Implements the frequency from 1 to 100 Hz
;Multiply 100 by 50 and store the result in R1:R0
MOV rNI,rRI
MOV rNh,rRh
;Now using 4MHz system clock. Multiply the counter by 4 before dividing it by the number of coefficient
number.
LSL rNI
ROL rNh
LSL rNI
ROL rNh

LDS rD,TotCoeffln

;Divide rNh(R1):rNI(R0) by rD(R3)
Div8M:
CLR rNu;clear interim register
CLR rRh;clear result (the result registers are also used to count to 16 for the division steps)
CLR rRI
INC rRI

;Division loop starts
Div8Ma:
CLC ;clear carry-bit
ROL rNI ;rotate the next-upper bit of the number to the interim register (multiply by 2)
ROL rNh
ROL rNu
BRCS Div8Mb ;if the bit is a 1, then subtract.

```



```

CP rNu,rD      ;division result 1 or 0?
BRCS Div8Mc   ;if smaller, then ignore subtraction step

;If the intermediate value dividable
Div8Mb:
SUB rNu,rD    ;subtract number to divide with
SEC          ;set carry-bit,result is a 1
RJMP Div8Md  ;jump to shift of the result bit

;If the intermediate value not dividable
Div8Mc:
CLC          ;clear carry-bit,resulting bit is a 0

Div8Md:
ROL rRI      ;rotate carry-bit into result registers
ROL rRh
BRCC Div8Ma  ;Zero rotating out of the result register: Division not done
;End of the division
;-----
;Start the waveform by sending a pulse with a duration greater than 50 ms
START_PULSE:
; Load PORTC with 0
LDI r16,0x00;
OUT PORTC, r16;write to DAC inputs;
;CALL output_load; output DAC load routine
;tell output DAC to load. MUST HAVE 5 us for each transition!
LDI r17, 0b00000011;input register transparent
;LDI r17, 0b00110011
OUT PORTB, r17
NOP
NOP
LDI r17, 0b00000111;input register latched
OUT PORTB, r17
NOP
NOP
LDI r17, 0b00001001;DAC register transparent
OUT PORTB, r17
NOP
NOP
LDI r17, 0b00001101;DAC register latched
OUT PORTB, r17
NOP
NOP
LDI r22,100
PULSE_DELAY1_OUT:
LDI r21,255 ;loop counter
PULSE_DELAY1_IN:
NOP          ;1 cycle
NOP          ;1 cycle
NOP          ;1 cycle
NOP          ;1 cycle
NOP          ;1 cycle
NOP          ;1 cycle
NOP          ;1 cycle
NOP          ;1 cycle
NOP          ;1 cycle
NOP          ;1 cycle
NOP          ;1 cycle
DEC r21      ;1 cycle
BRNE PULSE_DELAY1_IN ;1 cycle if false, 2 cycles if true
DEC r22
BRNE PULSE_DELAY1_OUT

```

```

; Load PORTC with the maximum voltage coefficient
LDI r16,0xFF;
OUT PORTC, r16;write to DAC inputs;
;CALL output_load; output DAC load routine
;tell output DAC to load. MUST HAVE 5 us for each transition!
LDI r17, 0b00000011;input register transparent
OUT PORTB, r17
NOP
NOP
LDI r17, 0b00000111;input register latched
OUT PORTB, r17
NOP
NOP
LDI r17, 0b00001001;DAC register transparent
OUT PORTB, r17
NOP
NOP
LDI r17, 0b00001101;DAC register latched
OUT PORTB, r17
NOP
NOP
LDI r22,100
PULSE_DELAY2_OUT:
LDI r21,255 ;loop counter
PULSE_DELAY2_IN:
NOP ;1 cycle
NOP ;1 cycle
NOP ;1 cycle
NOP ;1 cycle
NOP ;1 cycle
NOP ;1 cycle
NOP ;1 cycle
NOP ;1 cycle
NOP ;1 cycle
NOP ;1 cycle
NOP ;1 cycle
DEC r21 ;1 cycle
BRNE PULSE_DELAY2_IN ;1 cycle if false, 2 cycles if true
DEC r22
BRNE PULSE_DELAY2_OUT

; Load PORTC with 0
LDI r16,0x00;
OUT PORTC, r16;write to DAC inputs;
;CALL output_load; output DAC load routine

;tell output DAC to load. MUST HAVE 5 us for each transition!
LDI r17, 0b00000011;input register transparent
OUT PORTB, r17
NOP
NOP
LDI r17, 0b00000111;input register latched
OUT PORTB, r17
NOP
NOP
LDI r17, 0b00001001;DAC register transparent
OUT PORTB, r17
NOP
NOP
LDI r17, 0b00001101;DAC register latched
OUT PORTB, r17
NOP
NOP

```

```

LDI r22,100
PULSE_DELAY3_OUT:
LDI r21,255 ;loop counter
PULSE_DELAY3_IN:
NOP ;1 cycle
NOP ;1 cycle
NOP ;1 cycle
NOP ;1 cycle
NOP ;1 cycle
NOP ;1 cycle
NOP ;1 cycle
NOP ;1 cycle
NOP ;1 cycle
NOP ;1 cycle
DEC r21 ;1 cycle
BRNE PULSE_DELAY3_IN ;1 cycle if false, 2 cycles if true
DEC r22
BRNE PULSE_DELAY3_OUT
;The end of initiation pulse
;-----
IN r16,PIND
ANDI r16,0b00010000
CPI r16,0
BRQ SINUSOID_BEGIN
LDI r16,0x01
STS Status,r16

SINUSOID_BEGIN:
NOP
NOP
NOP
NOP
LDS r27,TotCoeffNumH
LDS r26,TotCoeffNumL ;to detect end of a sinusoid period
; Now loading from EEPROM
LDI r19,0x00
OUT EEARH,r19
LDI r18,0x00
OUT EEARL,r18

EXIT_CHECK:
;check if user wishes to stop the sinusoid
LDS r16,Status
CPI r16,0x01 ;If there is a hardware interrupt, go check if it is the STOP command
BRQ EXIT_CHECK_RETURN
LDS r16,HW_Interrupt
CPI r16,0xFF
BRQ EXIT_CHECK_RETURN
RJMP CLEAR_OUTPUT

EXIT_CHECK_RETURN:
//LPM r16, Z ;load value of DAC input into r16 from address in Z;
SBI EECR,EERE
IN r16,EEDR
; Reading the next element in EEPROM
OUT PORTC, r16;write to DAC inputs;
;CALL output_load; output DAC load routine

OUTPUT_LOAD:
;tell output DAC to load. MUST HAVE 5 us for each transition!
LDI r17, 0b00010011;input register transparent
OUT PORTB, r17

```

```

NOP
NOP
LDI r17, 0b00010111;input register latched
OUT PORTB, r17
NOP
NOP
LDI r17, 0b00011001;DAC register transparent
OUT PORTB, r17
NOP
NOP
LDI r17, 0b00011101;DAC register latched
OUT PORTB, r17
NOP
NOP

MOV r25,rRh
MOV r24,rRI
; The following divide the duration of each coefficient by 2, due to that ATmega32 is currently running at 8
MHz
LSR r25
ROR r24
; outer loop counter
LOOPY:
SBIW r25:r24,1
NOP
BRNE LOOPY

DELAY_RETURN:
SBIW r27:r26,1; countdown to end of a sinusoid period
BREQ SINUSOID_BEGIN
INC r18
OUT EEARL,r18
; Increasing the EEPROM address by 1
BRNE COUNT_UP1
INC r19
OUT EEARH,r19

COUNT_UP1:
RJMP EXIT_CHECK

CLEAR_OUTPUT:
;reset output DAC
LDI r16, $00
LDI r17, 0b00010000;input register transparent
OUT PORTB, r17
RJMP SINUSOID_CHECK

;=====
; Interrupt service subroutine wrapper
SWITCH_3: ;ISR for Switch 3
PUSH r16
IN r16,SREG
PUSH r16
//The following middle section of the ISR can be freely modified to meet the requirement of testing.
//Outside of this section of code is the routine for ISR housekeeping
IN r16,PIND
LDI r16,0xFF
STS Status,r16
LDI r16,0x00
STS HW_Interrupt,r16
;-----
;For testing

```

```

LDI r16,(1<<PD5)
OUT PORTD,r16 ;Set the interrupt acknowledge signal
;-----
//End of section for free modification
EXIT_SEQ:
POP r16
OUT SREG,r16
POP r16
RETI

SWITCH_4: ;ISR for Switch 4
PUSH r16
IN r16,SREG
PUSH r16
//The following middle section of the ISR can be freely modified to meet the requirement of testing.
//Outside of this section of code is the routine for ISR housekeeping
LDS r16,HW_Interrupt
COM r16
STS HW_Interrupt,r16
LDI r16,0x00
STS Status,r16
//End of section for free modification
POP r16
OUT SREG,r16
POP r16
RETI

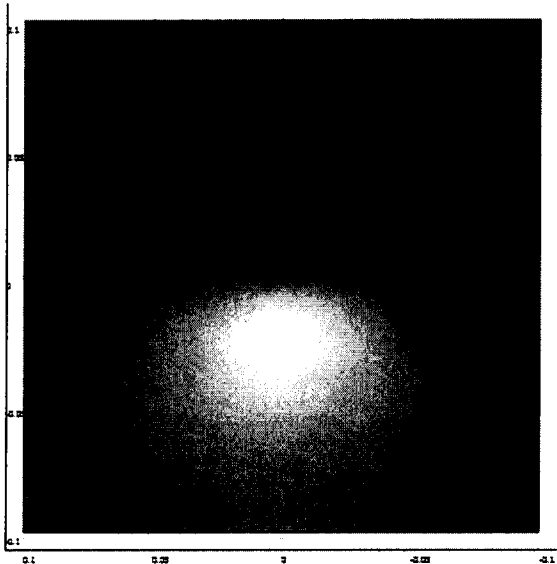
;TABLES
.CSEG
;Lookup table for sinusoid generation (8 bit DAC, DT period of 32)
;LUT:
SINUSOID:
.db 128, 153, 178, 200, 220, 236, 247, 254, 255, 251, 242, 228, 211, 189, 166, 140, 115, 89, 66, 44, 27, 13,
4, 0, 1, 8, 19, 35, 55, 77, 102, 127
TRIANGLE:
.db 0, 15, 31, 47, 63, 79, 95, 111, 127, 143, 159, 175, 191, 207, 223, 239, 255, 239, 223, 207, 191, 175,
159, 143, 127, 111, 95, 79, 63, 47, 31, 15
SQUARE:
.db 0, 0, 0, 0, 0, 0, 0, 0, 255, 255, 255, 255, 255, 255, 255, 255, 255, 255, 255, 255, 255, 255, 255, 255, 0,
0, 0, 0, 0, 0, 0
mod_sine:
.db 125, 142, 158, 172, 185, 196, 204, 208, 210, 208, 204, 196, 185, 172, 158, 142, 125, 108, 92, 78, 65,
54, 46, 42, 40, 42, 46, 54, 65, 78, 92, 108

;Value of amplitude
AMPLITUDE:
.db (5.0)/9.0*255.0; vary the value in the parenthesis from 0 to 9 only to vary reference voltage from
; 0 to 9V

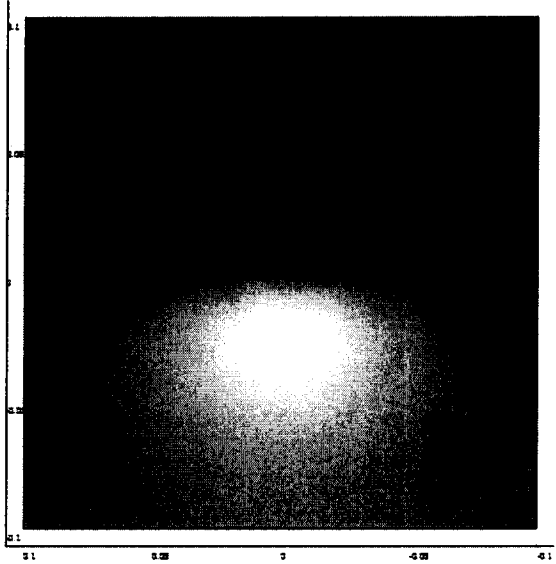
```

# Appendix F: Simulated Magnetic Field Patterns

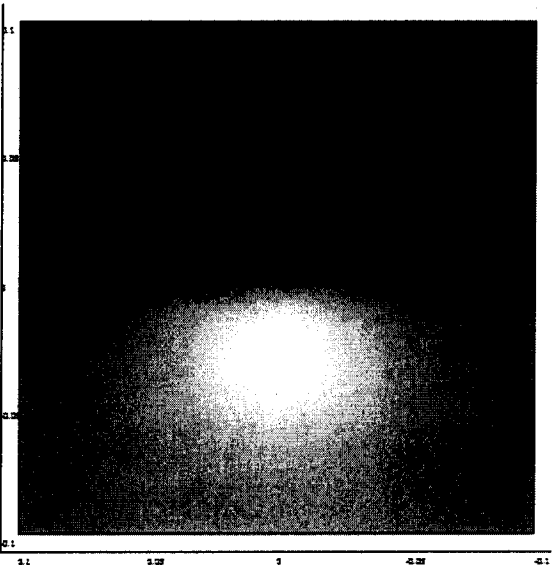
## I. Z-component with triangular coils of 5-mm base length and various leg lengths



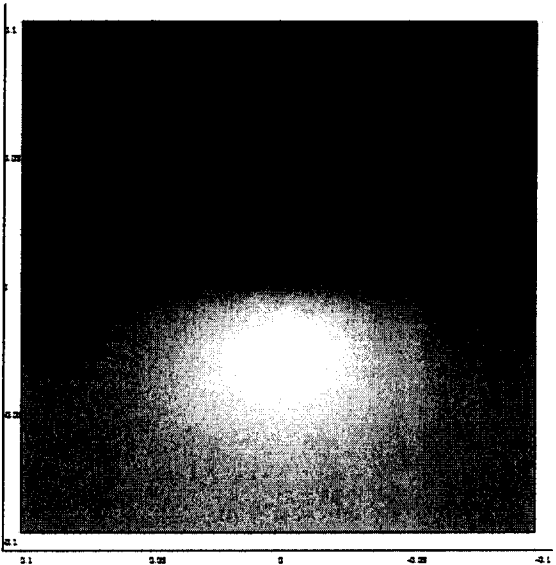
5-mm leg length



10-mm leg length

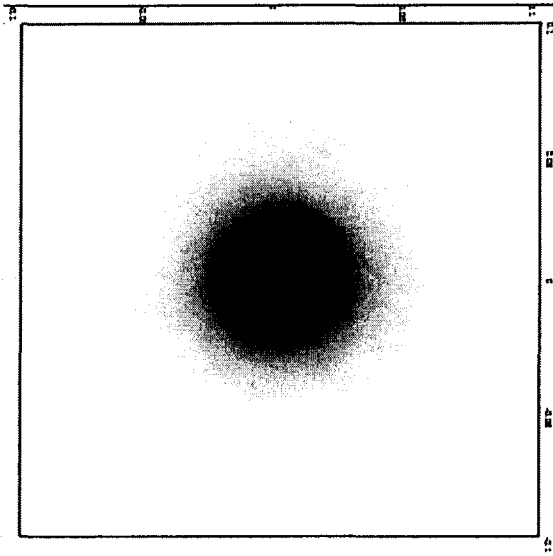


25-mm leg length

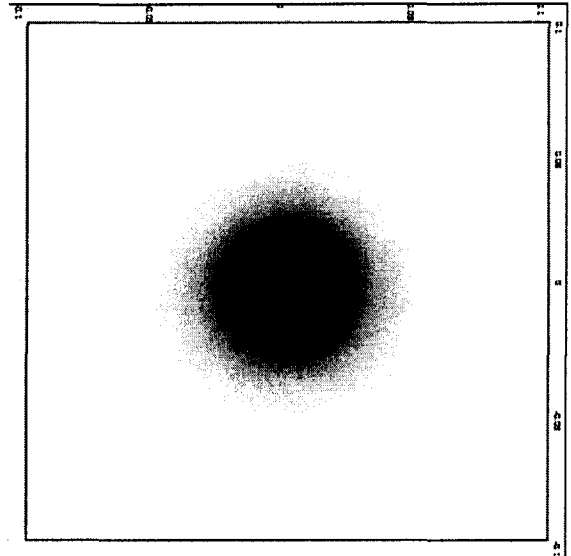


50-mm leg length

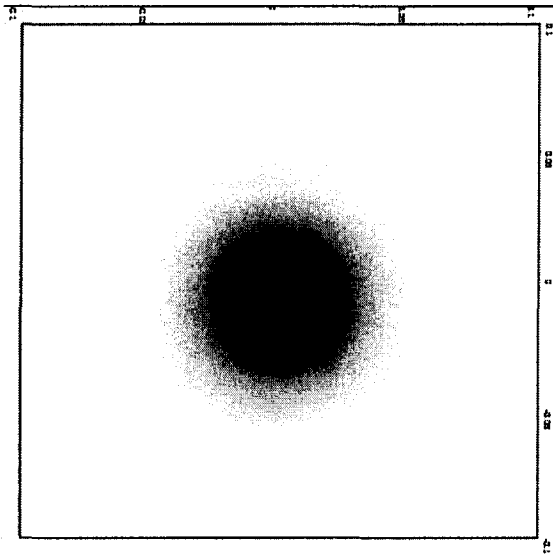
**II. Y-component with triangular coils of 5-mm base length and various leg lengths**



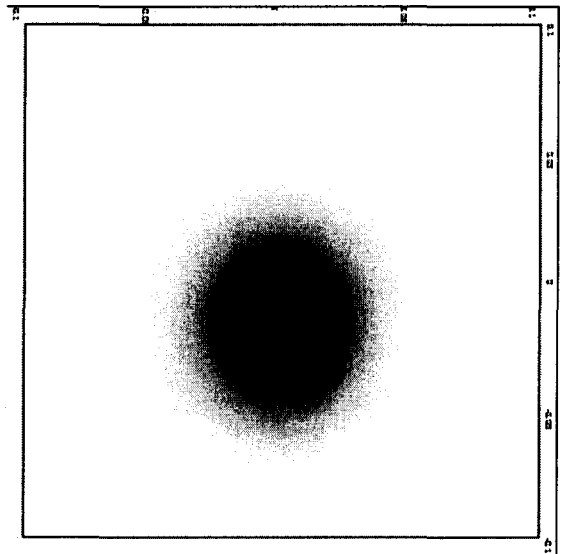
**5-mm leg length**



**10-mm leg length**

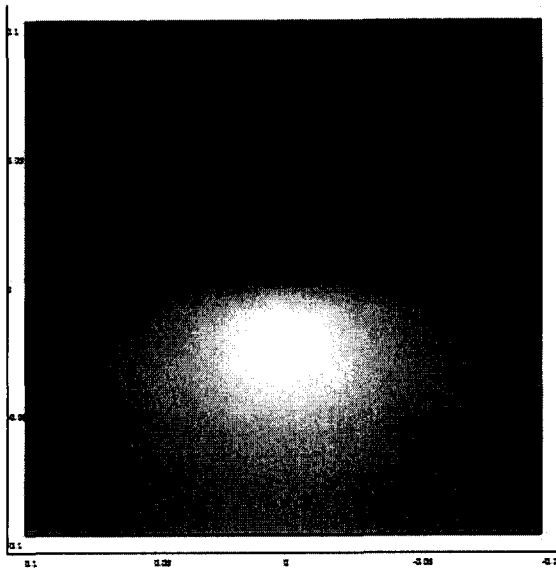


**25-mm leg length**

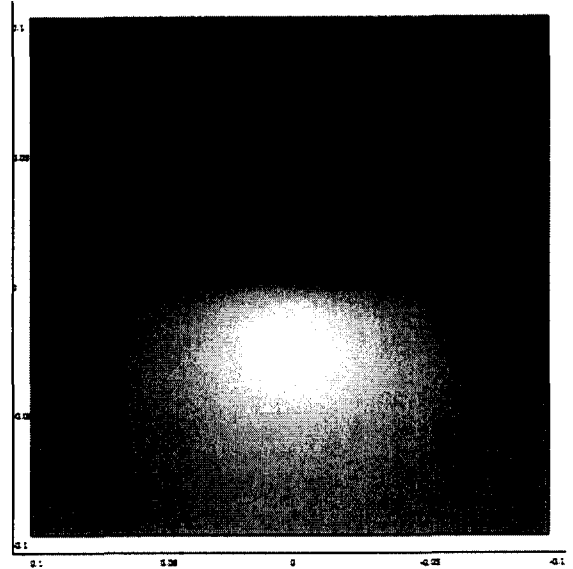


**50-mm leg length**

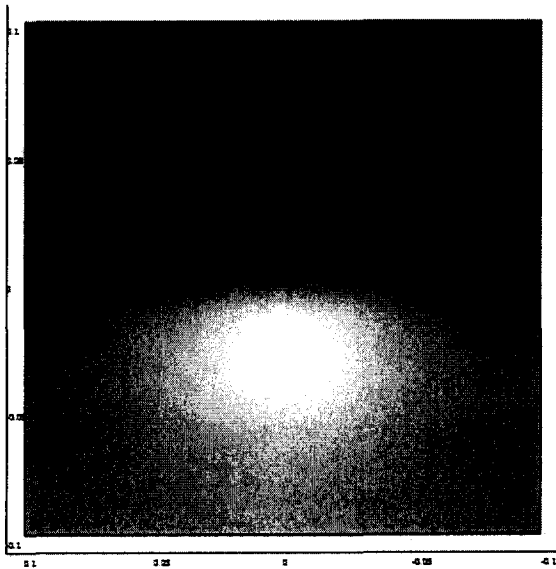
### III. Z-component with equilateral triangular coils of various side lengths



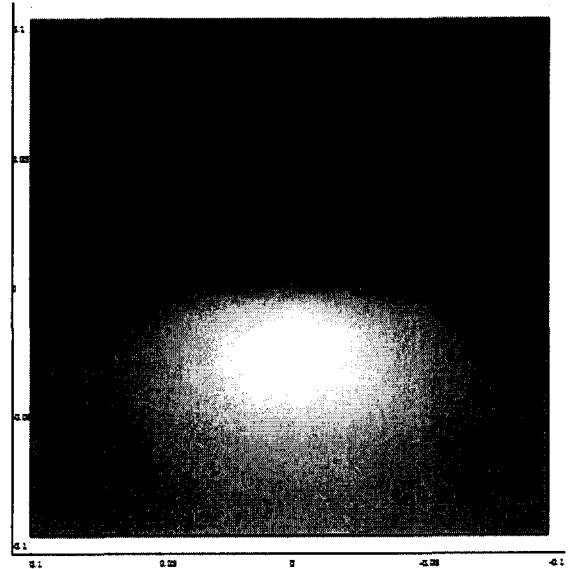
10-mm side length



20-mm side length



30-mm side length

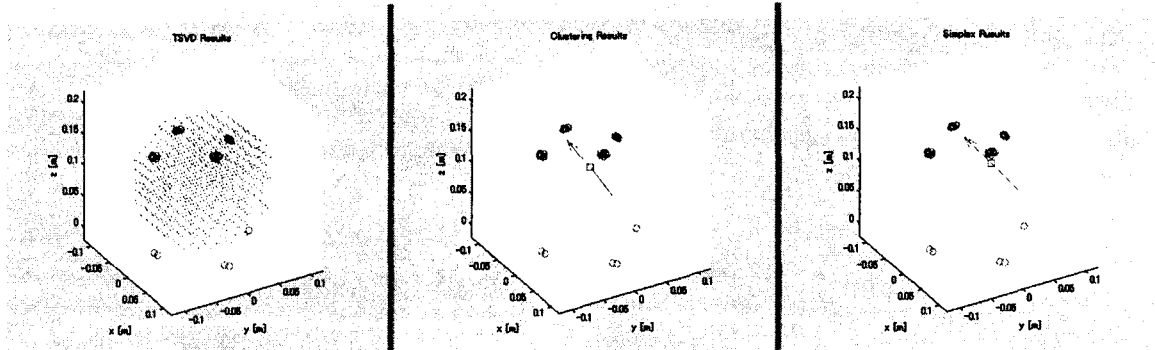


40-mm side length

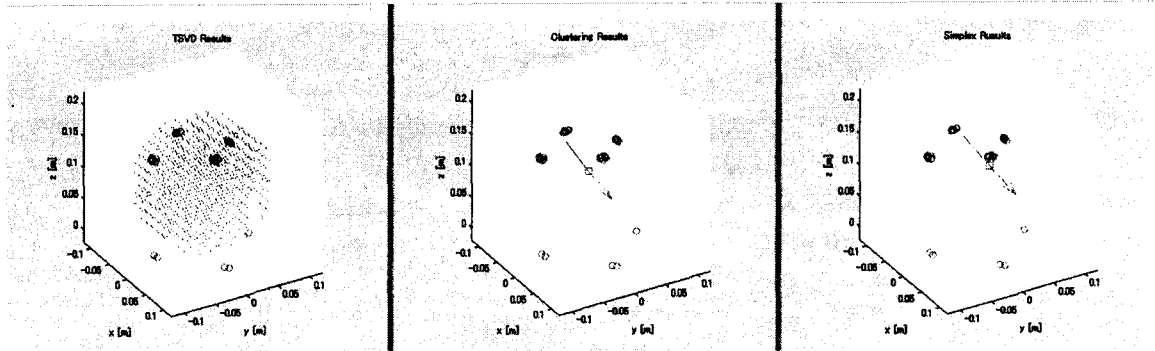


## Appendix G: Inverse Analysis Results

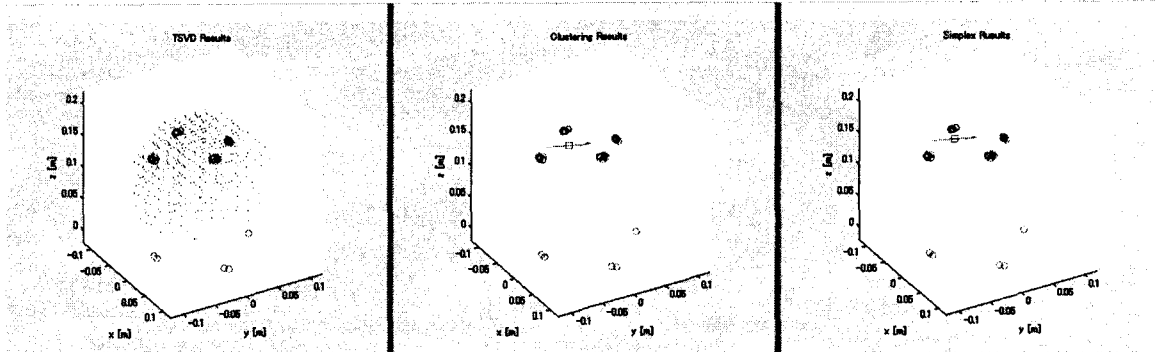
The following shows the resulting magnetic flux density distribution after TSVD (left), the resulting dipole locations after data clustering (middle), and the adjusted dipole locations after downhill simplex computation (right) of the sequential inverse analysis steps for test cases 1, 2, 3, 4, 6 and 10.



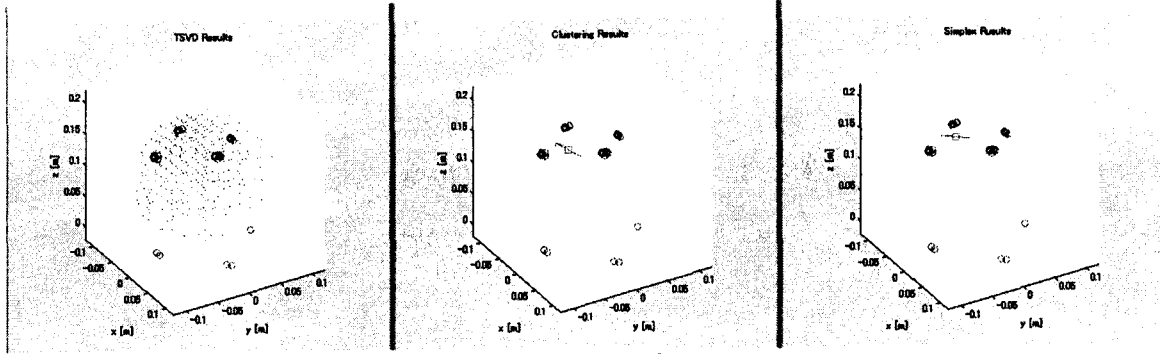
Test case 1



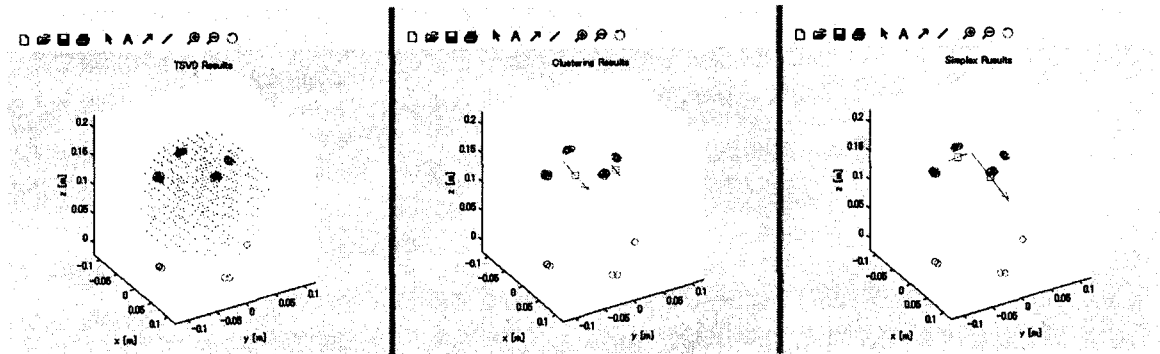
Test case 2



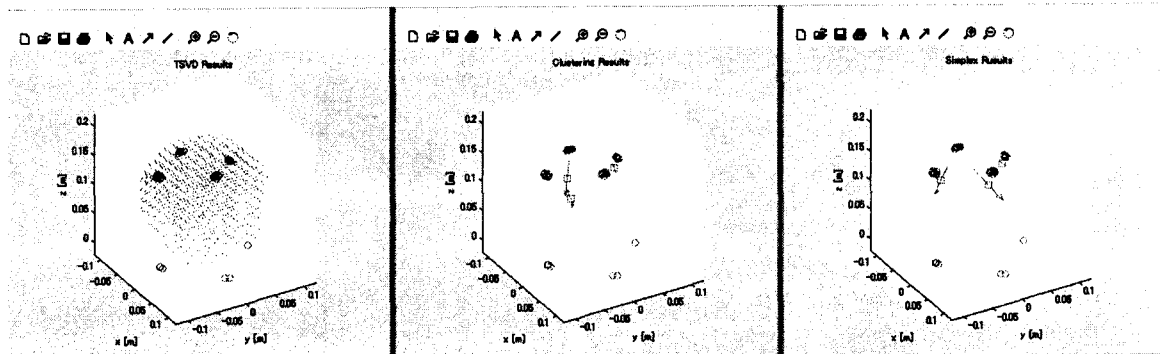
Test case 3



Test case 4



Test case 6



Test case 10

## REFERENCE LIST

- [1] N. A. Campbell and J. B. Reece. *Biology* (8th ed.) 2008.
- [2] C. Watson, M. Kirkcaldie and G. Paxinos. *The Brain : An Introduction to Functional Neuroanatomy* (1st ed.) 2010.
- [3] M. Hämäläinen, R. Hari, R. J. Ilmoniemi, J. Knuutila and O. V. Lounasmaa. Magnetoencephalography—theory, instrumentation, and applications to noninvasive studies of the working human brain. *Reviews of Modern Physics* 65(2), pp. 413. 1993.
- [4] H. Preissl. *Magnetoencephalography* 2005.
- [5] R. Rottier. The application of superconductors in medicine. 2000.
- [6] W. Haschke, E. Speckmann and A. I. RoÄtbak. *Slow Potential Changes in the Brain* 1993.
- [7] S. Baillet, J. C. Mosher and R. M. Leahy. Electromagnetic brain mapping. *Signal Processing Magazine, IEEE* 18(6), pp. 14-30. 2001.
- [8] J. C. de Munck, B. W. van Dijk and H. Spekreijse. Mathematical dipoles are adequate to describe realistic generators of human brain activity. *Biomedical Engineering, IEEE Transactions on* 35(11), pp. 960-966. 1988.
- [9] J. Sarvas. Basic mathematical and electromagnetic concepts of the biomagnetic inverse problem. *Phys. Med. Biol.* 32pp. 11. 1987.
- [10] J. Malmivuo and R. Plonsey. *Bioelectromagnetism : Principles and Applications of Bioelectric and Biomagnetic Fields* 1994.
- [11] A. Hillebrand and G. R. Barnes. A quantitative assessment of the sensitivity of whole-head MEG to activity in the adult human cortex. *Neuroimage* 16(3, Part A), pp. 638-650. 2002.
- [12] S. S. Nagarajan. Advances in electromagnetic brain imaging. Presented at Human Vision and Electronic Imaging XV. 2010, Available: <http://dx.doi.org/10.1117/12.849117>.

- [13] M. S. Hämäläinen and R. Ilmoniemi. Interpreting magnetic fields of the brain: Minimum norm estimates. *Medical and Biological Engineering and Computing* 32(1), pp. 35-42. 1994.
- [14] R. J. Ilmoniemi. Estimates of neuronal current distributions. *Acta Otolaryngol.* 111(S491), pp. 80-87. 1991.
- [15] S. Baillet, J. Riera, G. Marin, J. Mangin, J. Aubert and L. Garnero. Evaluation of inverse methods and head models for EEG source localization using a human skull phantom. *Phys. Med. Biol.* 46pp. 77. 2001.
- [16] R. M. Leahy, J. C. Mosher, M. E. Spencer, M. X. Huang and J. D. Lewine. A study of dipole localization accuracy for MEG and EEG using a human skull phantom. *Electroencephalogr. Clin. Neurophysiol.* 107(2), pp. 159-173. 1998.
- [17] P. McVeigh, A. Bostan and D. Cheyne. Study of conducting volume boundary influence on source localization using a realistic MEG phantom. *Int. Congr. Ser.* 1300(0), pp. 153-156. 2007.
- [18] M. Spencer, R. Leahy and J. Mosher. A skull-based multiple dipole phantom for EEG and MEG studies. Presented at Biomag 96: Proceedings of the Tenth International Conference on Biomagnetism. 2000, .
- [19] P. C. Hansen, M. L. Kringelbach and R. Salmelin. *MEG : An Introduction to Methods* 2010.
- [20] J. Clarke and A. I. Braginski. *The SQUID Handbook* 2003.
- [21] NATO Advanced Study Institute on Biomagnetism and S. J. Williamson. *Biomagnetism : An Interdisciplinary Approach* 1983.
- [22] VSM MedTech Ltd., *Data Acquisition Guide CTF MEG Software Release 5.4*. VSM MedTech Ltd., 2006.
- [23] Y. Kishimoto, "Studies of Real-Time Monitoring Techniques by Inverse Analysis of Electromagnetic Field: Applications to LSI Electroplating Control and Brain Function Diagnostics," pp. 117-145, 2010.
- [24] J. Liu, Y. Kishimoto, T. Cheung, A. M. Parameswaran and K. Amaya. Development of human brainwave simulating device for magnetoencephalography and the corresponding dipole localization study. Presented at 17th International Conference on Biomagnetism Advances in Biomagnetism–Biomag2010. 2010, .

- [25] G. Uehara, M. Miyamoto, Y. Adachi, Y. Haruta, J. Kawai, T. Shimozu and M. Kawabata. An effect of electrical double layer on MEG phantom with saline water. Presented at International Congress Series. 2007, .
- [26] Y. Kishimoto, J. Liu, T. Cheung, A. M. Parameswaran and K. Amaya. Magnetic dipole localization studies for magnetoencephalography using multiple phase inverse analysis and the experimental verification. *Canadian Medical and Biological Engineering Conference* 2009.
- [27] D. Halliday, R. Resnick and J. Walker. *Fundamentals of Physics* (5th ed.) 1997.
- [28] G. Uehara, M. Higuchi, Y. Adachi, J. Kawai, H. Tanaka, Y. Haruta, M. Miyamoto, T. Shimozu and M. Kawabata. An error in magnetic field of isosceles-triangle coil as a representation of equivalent current dipole. Presented at International Congress Series. 2007, .
- [29] A. V. Oppenheim, A. S. Willsky and S. H. Nawab. *Signals & Systems* (2nd ed.) 1997.
- [30] COMSOL AB, *COMSOL Multiphysics User's Guide Version 3.3*. COMSOL AB, 2006.